



University of Évora

ARCHMAT

(ERASMUS MUNDUS MASTER IN ARCHaeological MATerials Science)

Mestrado em Arqueologia e Ambiente (Erasmus Mundus –ARCHMAT)

## Analytical evaluation of paper degradation

Drita Abazi m34315

Professor Doctor Teresa Ferreira  
(Supervisor – University of Évora)



Professor Doctor Cristina Barrocas Dias  
(Co-Supervisor – University of Évora)



Doctor Ana Manhita  
(Co-Supervisor – University of Évora)



Évora, October 2016

"A Tese não inclui as Críticas e sugestões do Juri"



## **Acknowledgments**

I would like to express my sincere gratitude to Professor Professor Teresa Ferreira, supervisor of this thesis, Professor Cristina Dias, and Doctor Ana Manhita, co supervisor of the thesis, for their systematic guidance, their patience, motivation and immense knowledge, advice and assistance in correcting the imperfections in this thesis.

I would like to acknowledge Professor Francisca Figueira from the Laboratório José de Figueredo in Lisbon, for her help and advices.

I would also like to reflect on the people who have supported and helped me during this period, Margarida Nunes for assisting with the operation of AT-FT-IR, SEM-EDS and micro-XRD instrumentation and data analysis as well as cross checking the many thesis drafts.

Sérgio Martins for help with operations in Py-GC/MC and the patience that he has shown during the work.

The Erasmus mundus master project (2014-2016) for funding the project, and HERCULES laboratory staff.

# Contents

Acknowledgement.....	i
Table of contents.....	ii
List of figures.....	iii
List of tables.....	iv
Abstract.....	v
Resumo.....	vi
1.INTRODUCTION .....	i
1.1 The invention of paper and evolution .....	1
1.2. Paper production and paper components .....	3
1.2.1. Cellulose .....	4
1.2.2. Hemicellulose .....	5
1.2.3. Lignin .....	6
1.3. Paper degradation.....	8
1.4. Discoloration of the paper .....	10
1.5. Sizing of the paper .....	12
1.6. Analytical techniques used to analyses papers samples and the description of their methodology .....	14
i. Technical photography .....	14
ii. Optical microscopy.....	15
iii. Scanning electron microscopy/energy dispersive X-ray spectroscopy- SEM/EDS.....	16
iv. Fourier transform infrared spectroscopy (FT-IR) .....	16
v. Micro X-ray diffraction .....	18
vi. Pyrolysis-Gas Chromatography/Mass Spectrometry (Py-GC/MS) .....	19
2.METHODS AND MATERIALS .....	20
2.1. Selection of the samples.....	21
2.2. Technical photography .....	23
2.3. Optical microscopy .....	23
2.4. Scanning electron microscopy-energy dispersive X-ray spectroscopy (SEM-EDS) .....	23
2.5. Fourier transform infrared spectroscopy (FT-IR) .....	24
2.6. Micro -X-ray Diffraction- ( $\mu$ -XRD) .....	24
2.7. Pyrolysis-Gas Chromatography/Mass Spectrometry (Py-GC/MS) .....	25
2.7.1. Sample preparation.....	25
2.7.2. Analysis by Py-GC / MS .....	25
3.RESULT AND DISCUSSION .....	26
3.1 Morphological characterization of paper samples.....	27
3.1.1 Description of paper samples and foxing stains (second group of samples) .....	27
3.2 Photographic imaging .....	28
3.3 Optical microscopy .....	30
3.4 Scanning electron microscopy coupled with energy dispersive X-ray spectroscopy – SEM-EDS	32

<b>3.5 Fourier transform infrared spectroscopy (FT-IR)</b> .....	44
<b>3.6 Micro X-ray diffraction (<math>\mu</math>-XRD)</b> .....	49
<b>3.7 Pyrolysis-Gas Chromatography/Mass Spectrometry (Py-GC/MS)</b> .....	51
<b>3.7.1 Evaluation of Py-GC/MS to access paper foxing</b> .....	51
<b>3.7.2 Composition of papers using Py-GC/MS</b> .....	60
<b>4.CONCLUSIONS</b> .....	65
<b>BIBLIOGRAPHY</b> .....	68
<b>APPENDIX</b> .....	76

## List of figures

### 1.INTRODUCTION

Figure 1.1 Molecular structure of cellulose (n=DP, degree of polymerization) .....	5
Figure 1.2. Schematic representation of the structure of lignin .....	7
Figure 1.3. Substituents of lignin .....	7
Figure 1.4. Scheme of Fourier transform infrared spectrometer .....	17
Figure 1.5. Diffraction of the x-rays from the parallel planes .....	18

### 2.METHODS AND MATERIALS

Figure 2.1 Photographic images of paper samples S1, S2, S3 and P, NB, OB obtained under standard light; Notes: a)S1, b)S2, c)S3, d)P, e)NB and f)OB.....	22
--	----

### 3.RESULTS AND DISCUSSION

Figure 3.1. Areas of analysis selected for the SEM-EDS study; Legend: 1- area containing darker stains, 2- area from the whitish stains, 3-unfoxed area.....	33
Figure 3.2. Point analysis of unfoxed area in paper sample P.....	36
Figure 3.3. Point analyses of foxed area (darker stains, area 1) in paper sample P.....	37
Figure 3.4. Area analyses of foxed area (darker stains, area 1) in paper sample P.....	38
Figure 3.5. Point analysis of foxed area (whitish stains, area 2) in paper sample P.....	39
Figure 3.6. Point analysis of unfoxed area in sample NB.....	40
Figure 3.7. Point (top) and area (bottom) analysis of foxed area in sample NB.....	41
Figure 3.8. Point (top) and area (bottom) analysis for the unfoxed area in sample OB.....	43
Figure 3.9. Point analysis of foxed area in sample OB.....	44
Figure 3.10. Area analysis of foxed area in sample OB.....	44
Figure 3.11. Attenuated total reflection Fourier transform infrared spectra of unfoxed (red line) and foxed darker areas (blue line) of paper sample P .....	46
Figure 3.12. Attenuated total reflection Fourier transform infrared spectra of foxed dark stains (blue line) and foxed whitish stains (red line) of paper sample P.....	46
Figure 3.13. Attenuated total reflection Fourier transform infrared spectra of unfoxed (red line) and foxed areas (blue line) of paper sample NB.....	47

Figure 3.14. Attenuated total reflection Fourier transform infrared spectra of unfoxed (red line) and foxed areas (blue line) of paper sample OB.....	48
Figure 3.15. Micro-XRD diffractogram of paper sample P; C-cellulose.....	50
Figure 3.16. Micro-XRD diffractogram of paper sample NB; M-muscovite, K-kaolinite, C-cellulose.....	51
Figure 3.17. Micro-XRD diffractogram of paper sample OB; M-muscovite, K-kaolinite, Al- Aluminium Magnesium Hydroxide Silicate, C-cellulose.....	51
Figure 3.18. Py-GC/MS pyrogram of sample S1, Legend: S1F-01 sample from a foxing stain; S1-01, sample from the unfoxed area of the sample.....	52
Figure 3.19. Py-GC/MS pyrogram of sample S2, Legend: S2-F01, sample from a foxing stain; S2-01, sample from the unfoxed area of the sample.....	53
Figure 3.20. Py-GC/MS pyrogram of sample S2, Legend: S2-01 and S2-02, sample from the unfoxed area from two different areas of the sample.....	59
Figure 3.21. Py-GC/MS pyrogram of sample S3-powder, Legend: S3-Powder-01 and S3-Powder-02, samples from different unfoxed areas of the paper.....	60
Figure 3.22. Possible pathways of pyrolysis mechanism of cellulose, hemicellulose and lignin.....	62
Figure 3.23. Py-GC/MS pyrogram of sample P.....	64
Figure 3.24. Py-GC/MS pyrogram of sample NB.....	65
Figure 3.25. Py-GC/MS pyrogram of sample OB.....	65

## List of tables

### 3.RESULT AND DISCUSSION

Table 3.1. Optical microscopy observation .....	28
Table 3.2. Photographic Images of the Paper Samples under different illuminations.....	29
Table 3.3 Optical microscopy observation.....	31
Table 3.5 Scanning electron microscopy micrographs of foxed and unfoxed areas in paper sample P, NB and OB.....	34
Table 3.6 EDS elemental mapping for the unfoxed area of paper sample P.....	36
Table 3.7. EDS elemental mapping for the foxed area (darker stains, area 1) in paper sample P.....	37
Table 3.8. EDS elemental mapping for the foxed area (whitish stains, area2) in paper sample P.....	38
Table 3.9. EDS elemental mapping for the unfoxed area in paper sample NB.....	39
Table 3.10. EDS elemental mapping for the foxed area in paper sample NB.....	40
Table 3.11. EDS elemental mapping for the unfoxed area in paper sample OB.....	42
Table 3.12. EDS elemental mapping for the foxed area in paper sample OB.....	44
Table 3.13 Peak Wave numbers (cm <sup>-1</sup> ), Tentative Assignment, and Interpretation of ATR-FTIR spectra of sample NB, P and OB.....	49
Table 3.14. Compound obtained from the Py-GC/MS from the foxed and unfoxed area of the sample S1.....	54

## **Abstract**

The aim of this work was in first place to define a methodology for the use of Py-GC/MS as a characterization technique for the organic compounds present in paper samples containing foxing stains, paper have a complex structure and mostly consist with cellulose fibers. Additionally, it was intent to characterize paper samples containing foxing stains with a batch of non-destructive analytical techniques. The work intent to deepen our knowledge on foxing stains, its chemical nature and morphological aspects. For characterization of the morphology of paper samples and foxing stains was used photography under different illuminations and optical microscopy. The presence of fibers disruption was observed with scanning electron microscopy coupled with energy dispersive spectroscopy (SEM-EDS), and also the nature of the fillers that is present in different areas. Attenuated total reflection Fourier transform infrared spectroscopy (ATR-FTIR) was used for identification of the sizing agents, determination of the chemical composition of additives that were used for production of paper, and comparison between foxing stains and unfoxed areas was allowed. Micro X-ray diffraction was used to evaluate the crystalline fillers in the sample. Pyrolysis-Gas Chromatography/Mass Spectrometry (Py-GC/MS) was used for chemical analysis to identify the organic components and different classes of organic compounds.

## **Resumo**

O objetivo deste trabalho foi definir, em primeiro lugar, uma metodologia para o uso de Py-GC / MS como técnica de caracterização dos compostos orgânicos presentes em amostras de papel contendo manchas de foxing, o papel tem uma estrutura complexa e consiste principalmente com fibras de celulose. Além disso, pretendia caracterizar amostras de papel contendo manchas de raposas com técnicas analíticas não destrutivas. Para a caracterização da morfologia das amostras de papel e das manchas de foxing foi usada fotografia sob diferentes iluminações e microscopia óptica. A presença de fibras de ruptura foi observada por microscopia electrónica de varrimento juntamente com espectroscopia dispersiva de energia (EDS-SEM), assim como a natureza dos materiais de enchimento que está presente em diferentes áreas. Espectroscopia de infravermelho com transformada de Fourier em modo de reflexão total atenuada (ATR-FTIR) foi utilizada na identificação dos agentes de colagem, e na determinação da composição química de aditivos usados na produção de papel, e a comparação entre foxing manchas e áreas unfoxed foi deixada. Micro difracção de raios X foi usada para avaliar o enchimentos cristalinos na amostra. Cromatografia pirólise-gasosa / espectrometria de massa (Py-GC / MS) foi utilizada para análise química para identificar os componentes orgânicos e diferentes classes de compostos orgânicos.

## **1.INTRODUCTION**



## 1.1 The invention of paper and evolution

People had always tried to find out something easier to write on than papyrus or parchment, that at the same time, should be easier and cheaper to make. People used various ways to express through writing in particular palm leaves, whale bone, seal teeth, shells, turtle shell, and more subsequently, silk and bamboo. It was also common to use stone, clay and even tree bark (Reis 2009). It required long time to come up with paper. The mankind has used different writing material for a long time, but paper has become one of the most used materials of all times. From the earliest time, paper has retained the main characteristic and today offering different usages. The process of papermaking spread all over the world and originally intended purely for writing and printing purposes.

Paper is an essential element to everyday life; it is the basic material written communication most used and has a rich and colorful history and has been playing essential role in the development of cultures all over the world (Manso *et al.*, 2009).

105 A.D. is often cited as the year in which papermaking was invented by Ts'ai Lun and was reported to the Chinese Emperor the process for papermaking with specific reference to its use for writing and record keeping. Nevertheless, the manufacture of paper seemed to have occurred in China before the date, around the second century BC, during the ancient Han Dynasty, 200 years before the official historic records (Manso *et al.*, 2008, 2009 & 2011; Enami *et al.*, 2010).

Originally, paper seemed to be made with a wide variety of materials by mixing plants and trees, as hemp and bamboo, old fish nets and textile waste, and also other sources of fiber were used to assist in refining (Williams 2006). The procedure consisted of disintegrating the fibers by fractionation and removal of the water; the operation was repeated with the new leaves and then pressed and placed in the heated drying walls.

Progressive improvements were made for obtaining better paper quality with the use of soft material on wooden mold coating, rice straw, seaweed, and starch as a sizing agent (Williams 2006).

The Chinese have guarded the secret of the production process for a long time and tried to eliminate other centers for manufacturing of paper. From China the manufacturing process was later taken to Korea in the year 600 and in 610 a Korean monk named Don-Cho shared his knowledge about this technique in Japan (Williams 2006) and they quickly introduced innovations for manufacturing of the paper.

The techniques that were used in China and Japan were similarly, the technique used for the pulping process was giving a characteristic appearance and excellent quality to the produced paper, because the long fibers were not cut but simply prepared by beating.

In the year 751 the Chinese were at war with the Arabs and were defeated, the secret spread quickly through different places in the world. Some Chinese prisoners who fell into Arab hands, were artisan knowledgeable in papermaking technique, they were taken to Samarkand and transmitted their knowledge of papermaking. From there, this secret spread rapidly in Baghdad about forty years later and in Egypt in the year 900 (Enami *et al.*, 2010).

The techniques for producing paper changed depending what kind of materials they were adding for making paper. In Europe the process of papermaking arrived 12<sup>th</sup> century, it had become the most common writing material in Europe, since Europeans learned this art from the Arabs (Manso *et al.*, 2008; Williams 2006).

In Europe, rag fibers used as raw materials were flax, hemp and jute. The rags were subjected to a fermentation process, essential for obtaining paper with good quality. The process was so long and difficult, others techniques were performed and the technology has improved over time. With the improving of the techniques, there was a large increase for paper demand, which led to a considerable shortage of raw materials, rags, thus beginning to be used plant fibers (Enami 2010).

Major changes in paper production were made in the second half of the 19<sup>th</sup> century, when rags were replaced by wood. The production became fully automated in all its stages from the preparation of pulp, the formation of the paper sheet, to the use of additives and finishes (Celpa, 1993).

Paper production consists of three main steps: preparation of pulp, sheet formation and drying. During the production process it is important to consider some factors such as dyeing, sizing, pH correction and additives. The first phase of production consists in defibrations of fibers, intended to keep pulp free of impurities that will provide the required qualities to the paper by milling the fibers.

The second production stage is the formation of the sheet. The cellulose fibers are suspended in water and placed on a wire screen. The water flowing through this and the fibers are retained, forming a sort of fabric, with small yarns and drawn slightly each other. The third and final step is drying, in which the sheet is pressed to remove all the water and then passed through heated iron cylinders, occurring water evaporation.

## **1.2. Paper production and paper components**

For many centuries paper has been used for documenting different historical events that are important for our history and recording the cultural achievements all over the world. The decomposition of paper is one inevitable process. The time that takes to paper decompose depends from several factors, still under study, namely, the production technology and environment factors (Strlič *et al.*, 2008).

Protection and preservation are important issues for the cultural heritage safeguard. Documents with different information as books, manuscripts, prints, and paintings are archives and museums' responsibility, and they need to have safe storage, care and conservation treatment for long life. Degradation process and factors that have effect in duration and stability of paper are important factors (Strlič *et al.*, 2005). For better protection of the paper is good to know the nature and production process of the paper.

When wood pulp entered in the papermaking process the quality of the paper has been reduced. Depending from the mechanical or chemical process, paper made with wood pulp was more or less well purified. Depend from process, the difference with the papers that are produced previously is that the wood pulp is sized with rosin in an acidic medium and the paper will be yellowed and loses its original flexibility. During the process of papermaking, gelatin as an external sizing agent and very stable agent was used before the internal sizing with rosin and later this was replaced with the process of alkaline neutral sizing (Song *et al.*, 2011).

Different papers documents that are printed in 19<sup>th</sup> and 20<sup>th</sup> century are in bad condition and not possible to read them. With the increased production of the paper there were also changes in the machinery, and new pulping processes were introduced, and as well new fillers, dyes, coatings, and sizing products. The paper that was produced in this period was with low stability. With an increased concern for the environment, the use of neutral sizing became a norm only in the 1990s (Strlič *et al.*, 2005; Proniewicz *et al.*, 2002). In the second half of the 20<sup>th</sup> century, the different fillers and china clay that was one of the most usual fillers were replaced with the use of calcium carbonate, that is consistent with the alkaline neutral sizing (Bazley *et al.*, 1991).

Paper is made from cellulose fibers, and in medieval times, the production of paper was from linen, hemp and cotton rags and at that time the cellulose material was of high quality, but the papermaking fiber depend also from the technique that is used. The pulping process has developed in different way in different countries, different changes were made on fibrous and non-fibrous materials as cellulose (Udriștioiu 2012), hemicelluloses and lignin, wood pulp, sizing agents, fillers and coatings.

The composition of paper changed from almost pure cellulose to cellulose and significant amounts of hemicellulose and lignin. Paper made with wood pulp was well purified, according to chemical or mechanical processes (Manso *et al.*, 2005). These fibers can be hold together in the plant from the bonding material that is called lignin, which is a complex natural organic polymer.

### **1.2.1. Cellulose**

Cellulose is the most abundant biopolymer on Earth and people have used it for thousands of years in various forms as an indispensable material for human civilization, such as clothing, housing and application in building materials and as writing medium, textile, paper (Corsaro *et al.*, 2013; Watkins, 2015). Figure 1.1 shows the molecular structure of cellulose as a carbohydrate polymer of glucose generated from repeating  $\beta$ -D-glucopyranose molecules that are covalently linked through acetal functions between the equatorials OH group of C4 and C1 carbon atom of  $\beta$ -1,4-glucan (Klemm *et al.*, 2005; Park *et al.*, 2010; Cristina 2011). Hydroxyl groups forms hydrogen bonding between cellulose chains holding them together to form fibrils, from which the cellulose fibers will be formed. The structure of cellulose is mainly due to the presence of covalent bonds, hydrogen bonds (Ratanakhanokchai 2013). The molecule of cellulose has many hydroxyl groups that interact strongly with water. Through drying and pressing the remaining water is removed, which bonds the fibers together into a sheet (Daniels 1996). The rest consist from amorphous form.

Mechanical properties of the cellulose have strong influence from the physical properties of cellulose, including solubility, hydroxyl reactivity and crystallinity that comes from the formation of intra- and inter-molecular hydrogen bonds in the cellulose (Fan 2012). The length of cellulose chain can vary from between 2,000 to 12,000 glucose units, this depend on the source, however the majority of cellulose molecules are from 8,000 to 12,000 units in length (Carr 2012). The polymerization degree of cellulose from the wood is up to 10,000, while the polymerization degree of cellulose from cotton reaches up to 15,000.

The ability of strong intramolecular hydrogen bonds held the cellulose chains together into fiber that give strength to mechanical properties and chemical stability to cellulose (Laguardia 2005). The strength of cellulose depends from the degree of polymerisation, so chemical and physical factors are the major contributors to paper deterioration.

Cellulose fibers have weak points for chemical attack and mechanical forces; they contain various defect such as pores, crack, nodes, compression, failure and other site of damage (Ioelovich 2008). Cellulose is found also in cotton plants or as combination of lignin and with other polysaccharides, so-called hemicelluloses in the cell wall of woody plants (Corsaro 2013). Other source of fibers are rags and silk, even hemp rope, old sails, old fishing, and certain amounts of additives, e.g., fillers, pigments and metal ions (Laguardia 2005).

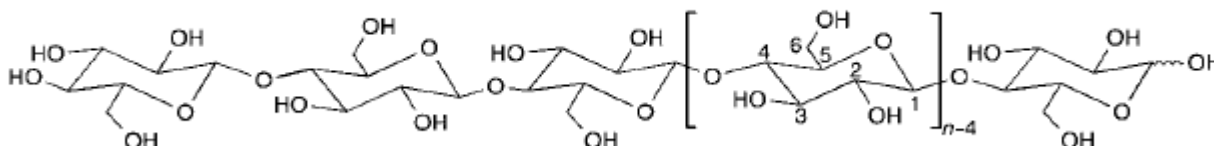


Figure 1.1 Molecular structure of cellulose ( $n=DP$ , degree of polymerization) (Klemm et. al., 2005)

### 1.2.2. Hemicellulose

Hemicellulose is a group of complex carbohydrates and is the second most abundant renewable organic material and with cellulose they are not chemically homogeneous. Hemicellulose makes up 25–30% of total wood dry weight. It is a polysaccharide which can be made from different monosaccharides, with a lower molecular weight than cellulose (Ratanakhanokchai 2013).

Hemicelluloses includes different polysaccharides that contain many of sugars monomers like: D-xylose, L-arabinose, D-mannose, D-glucose, D-galactose, L-rhamnose, and acetyled sugars. The type of hemicellulose varies depending on monomer composition (Xiaoa 2001). Hemicellulose consist of shorter chains sugars units that are linked together by  $\beta$ -1,4- and occasionally by  $\beta$ -1,3-glycosidic bonds.

The main component of hardwood trees that is found in hemicellulose is glucuronoxylan, while glucomannan is predominant in softwood. In contrast to cellulose, hemicellulose it is easily hydrolyzed. Hemicelluloses are bound in the plant cell walls, sometimes with different chains to cellulose to form a network of cross-linked fibers. They do not form aggregates; they have amorphous structure (Pe´rez 2002).

Hemicelluloses are also covalently united to lignin, together with cellulose they are forming a highly complex structure (Ratanakhanokchai 2013).

### 1.2.3. Lignin

Lignin is class of complex polymer that is present in plant cell walls and wood tissues, they are particularly important in the cell walls, especially in wood and bark and is one of less characterized molecular group between the wood components (Ratanakhanokchai *et al.*, 2013; Derkacheva 2008; Xiaoa 2001).

After cellulose, is one of the most abundant natural polymer that is found and it is covalently linked to cellulose and hemicellulose in the cell wall of almost all plants used in paper industry, is insoluble in water and stable in nature (Heldt *et al.*, 2005). Lignin show a certain variation in the chemical composition because of its complex macromolecule (Figure 1.2) and it is widely accepted that are different pathway for the biosynthesis of lignin that begin with the reaction of the cytosol with the synthesis of glycosylated monolignols from the amino acid phenylalanine -this is phenylpropanoid pathway- and the enzymatic polymerization of three types of phenols (Figure 1.3), which include coniferyl, sinapyl, and p-coumaryl alcohols joined together by different types of functional groups and linkages (Lisperguer *et al.*, 2009; Watkins 2015).

Lignin is composed from three monomers that are derived from phenylpropanoid units, *p*-coumaryl alcohol, coniferyl alcohol and sinapyl alcohol, they are joined through alkyl–aryl, alkyl–alkyl and aryl–aryl ether bonds. The primary purpose is to give strength and water permeability to plants, but also to protect plants from pathogen infections (Ratanakhanokchai *et al.*, 2013; Xiaoa 2001).

The main component of softwood lignin is coniferyl alcohol, while guaiacyl and syringyl alcohols are the main components of hardwood lignin (Pérez *et al.*, 2002; Derkacheva 2008). They are numerous sources available of lignin and cellulose: hemp, cotton, jute, silk and wood pulp. The areas in which lignin is applicable include: emulsifiers, dyes, synthetic floorings, sequestering, binding, thermosets, dispersal agents, paints and fuels (Watkins 2015).

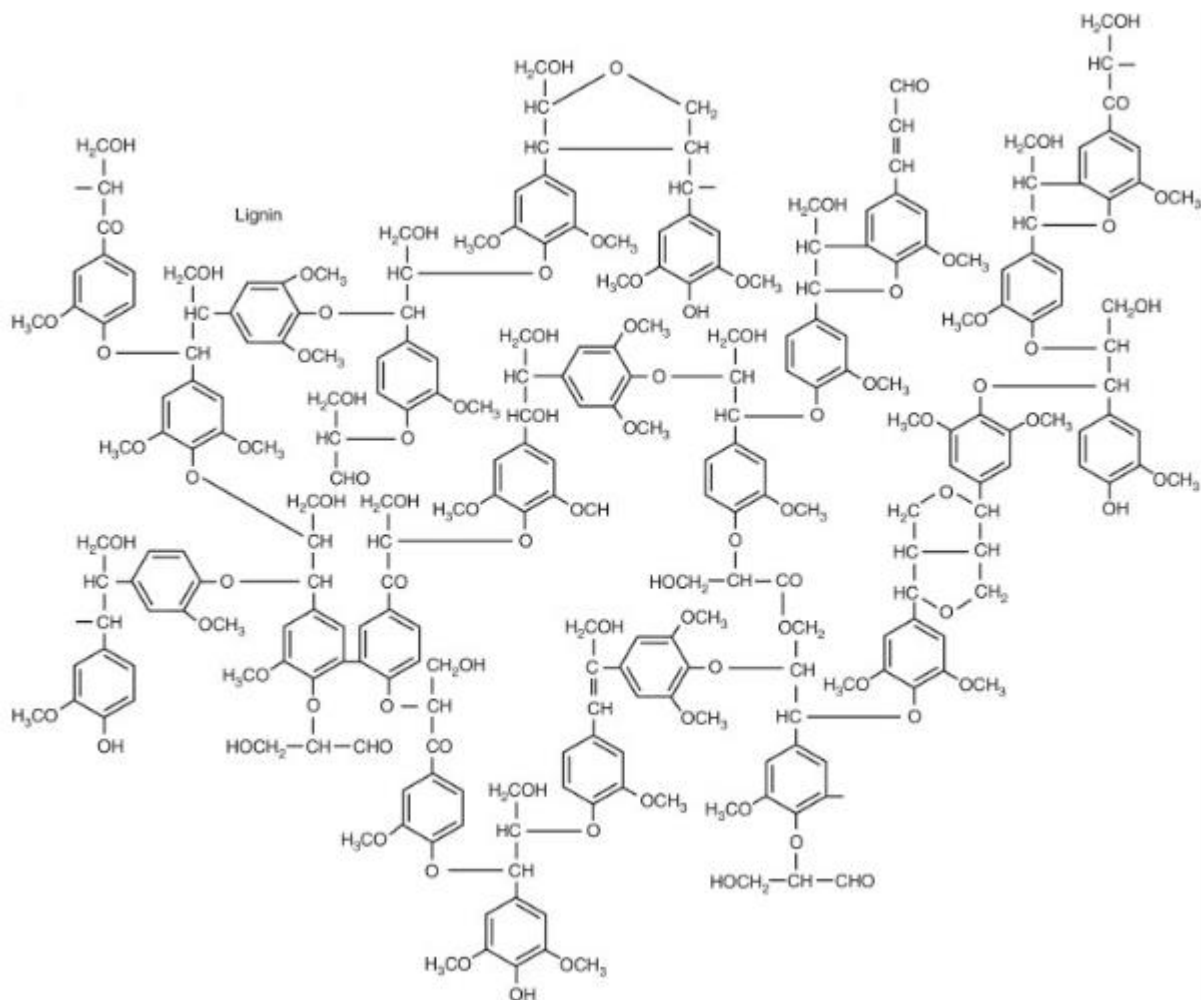


Figure 1.2. Schematic representation of the structure of lignin (Watkins *et. al.*, 2015)

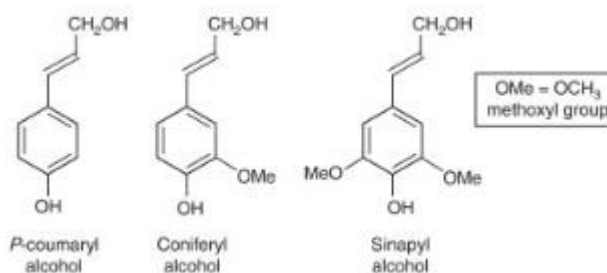


Figure 1.3. Precursors of lignin (Watkins *et. al.*, 2015)

### 1.3. Paper degradation

The deterioration of paper in books and archival materials because of the degradation of its cellulosic substrate has been recognized for many years. It is alarming that many materials in libraries are prone to rapid degradation, also most of the materials that are produced between 1850 and 1950 are now fragile. The major changes in paper degradation include, biological, physical and chemical changes. When paper degradation is at the beginning is more easy to control than when the changes are more developed (Bronzato *et al.*, 2013; Lin 2006).

The paper degradation is a process of physical and chemical changes, conditioned by internal and external agents. Internal agents are directly related to the composition of paper, the type of fibers, chemical residues and metal ions present. External agents are physical and biological agents, in particular, temperature, relative humidity, ultraviolet radiation, atmospheric pollution and microorganisms (Pinzari *et al.*, 2006).

Within the external factors can be considered as more harmful, light source (natural or artificial), temperature and relative humidity, presence of microorganisms, packaging and inappropriate handling. The high temperature combined with high humidity lead to contraction and elongation of paper fibers and favor the proliferation of biological agents. The brightness is another source of paper degradation. Natural or artificial radiation is harmful for the paper, therefore the action of ultraviolet radiation is irreversible and extends even after the irradiation period has ended, thus contributing to the oxidation of cellulose (Manso *et al.*, 2006; Proniewicz *et al.*, 2001; Porck 2000; Zou 1994).

One external or environmental factor is, among others, the effect of moisture in paper, leading to the subsequent growth of fungi and bacteria. The growth of fungi will destroy the paper sizing and cause stains, and can be responsible for the loss of paper strength (Vohrer *et al.*, 2001).

Paper often contains traces of ions metal, in particular transition metals from the production process or contamination. These metal ions may be responsible for other process of deterioration of paper: the oxidative degradation of cellulose. Among the transition metal ions, copper appears to be catalytically active, followed by iron, cobalt and chromium (Šelih *et al.*, 2007; Malešič *et al.*, 2012; Laguardia *et al.*, 2005).



The presence of oxide groups is one of the reasons for the degradation of the cellulose macromolecules. The degree of polymerization of the cellulose is reduced and reducing free end-groups that are formed, which can easily be oxidized to carboxyl groups which induce autohydrolytic breakdown of cellulose (Fellers *et al.*, 1989). Internal components of acidic hydrolysis can form hydronium cations ( $H_3O^+$ ) that can catalyze the cleavage of the glycosidic bond or by the action of cellulolytic enzymes (Corsaro *et al.*, 2013).

A decrease in the degree of polymerization directly affects mechanical properties of paper, such as tensile, tear, bursting strength and folding endurance (Jong *et al.*, 2012). Long storage of different documents in archives will cause acidic paper to become delicate and brittle until it finally disintegrates, and because of this the writing in the documents also will be destroyed (Dabrowski 2003).

Several millions of books in the world suffer from the effects of acid degradation, i.e. the atmospheric hydrolysis of the inorganic salts resulting in the formation of acids, which attack cellulose fibers of paper. Paper conservators have difficult job and they are making a lot of studies to find solutions about the deacidification but the chemical agents that are applied are in small amounts. They try to find appropriate method that would protect the documents that are in archives, museums and those with historical value (Kiuberis 2005).

Deacidification is performed as a basic paper conservation technique, either manually or as a mass treatment. In manual techniques, water solutions of calcium or magnesium bicarbonate or of calcium hydroxide are most often used. Mass deacidification is carried out in batches with organic solvents and several procedures are available (Strlič *et al.*, 2005).

Oxidation process, the degree of polymerization of the cellulose is reduced and carboxyl groups (aldehydes and ketones) are formed (Fellers *et al.*, 1989). Oxidation of cellulose, is process that usually run through the radical mechanism initiated by active oxygen species, with this process, the steps of the reactions are consecutive and numerous. The units of  $\beta$ -D-glucopyranose can be converted to an unstable oxidized derivative, with this the ring will open and in this way start the oxidative degradation (Corsaro 2013).

During the oxidation of paper can occur different phenomenon, the tideline phenomenon is one of the phenomenon and is of relevance to the conservation of paper, they are brown lines in paper and can affect the degradation of cellulose in the brown area itself and in neighboring areas (Jong *et al.*, 2012). This phenomenon can occur when the paper is exposed to moisture.

Possibly, hydrogen peroxide, water-soluble alkyl hydroperoxides and free radical species, such as peroxy, alkoxy, and hydroxyl radicals, present in the sheet, accumulate in the tideline area, where they meet with oxygen and rapidly multiply as a result of free radical chain reactions, leading to colored and other degradation products (Souguir *et al.*, 2008).

The phenomenon of discoloration that occur in different papers, including foxing stains, is associated with the oxidation of cellulose, it can occur as a result of reactions at the wet-dry interface (Souguir 2008).

#### **1.4. Discoloration of the paper**

The discoloration and weakness of paper over time can be as result of the spontaneous phenomena of cellulose degradation. To understand deterioration pathways and improving stability of papers and documents in cultural heritage, is essential to have detailed knowledge of products arising from cellulose degradation (Corsaro 2013).

For paper, a common symptom of natural ageing is yellowing. Yellowing of paper has been attributed to photochemical reactions, which can be especially problematic for paper containing lignin. Discoloration of paper is effect used in historical documents that can also be due to a type of stain known as foxing. The foxing has been studied since 1930 by scientists and conservationists to elucidate the causes and establish protocols for the detection, prevention and treatment (Choi, 2007). Foxing stains can be seen on different types of documents dating from the early sixteenth to the twentieth century (Manso *et al.*, 2009; Buzio 2004). Foxing stains are considered to be damage for historical documents, newsprint, old books and manuscripts (Peters 2000).

Foxing is a term that is used to describe stains that occur in form of small isolated patches of discoloration, stains often have an orange coloration or shades between yellow and dark brown (Manso *et al.*, 2009; Bukova, 2008), usually they are limited in size, which are generally of small dimensions to relatively large stains and shape (Missori *et al.*, 2004; Peters 2000). Paper that have high quality usually have dark foxing stains. Paper with low quality like newsprint, stains are with light color and having a critic shade.

To determine if certain stain need to be considered as foxing stain is hard because of the absence of specific criteria for definition of foxing stains (Goltz *et al.*, 2010; Choi 2007). Foxing is a complex phenomenon and a lot of researchers working to understand the cause of foxing, because is not yet completely understood (Buzio *et al.*, 2004).

The presence of metal ions has been considered as a major cause of foxing. Metal contamination can result from the papermaking process or dust in the air. The dust in the air can contain up to 15% iron (Rebrikova and Manturovskaya 2000). Cellulose is directly oxidized catalytically in the presence of iron, copper and cobalt compounds and the reaction is faster at high relative humidity values (Katherine 1992). Iron plays an important role in accelerating the foxing and may lead to its appearance in a short time because its acidity is very high (Katherine, 2013). Bicchieri (2002) also states that the iron ion displaces calcium ions causing the weakening of the cellulose polymer. Copper is also responsible for stains that have a dark brown color and may have sometimes a bluish green ring to delimit the spot. It was found that copper is corroded by the presence of chloride and this corrosion migrate to surrounding areas, which may form stains (Choi, 2007). Besides these metallic ions, other species may be related to the appearance of foxing. For example, hydrogen sulfide emitted from environmental pollution induces black spots (Choi, 2007). Another very important factor in the appearance of foxing is the relative humidity (RH).

Nevertheless, foxing stains are characterized by a three-dimensional structure considering that foxing stains can penetrate into paper, and even move through successive pages, when increases the distance from the center of infestation their intensity decreases (Buzio *et al.*, 2004). The foxing appearance depends on: technology of the paper production, level of dust and dirt on books, level of light exposure and the microclimate conditions during storage (Rebrikova and Manturovskaya 2000).

## 1.5. Sizing of the paper

The process of sizing is applied to the paper to act as a protective filler. Early oriental paper was unsized, soft, pliant, and absorbent. The Chinese have used a procedure similar to the coating, they apply in the surface of the paper gypsum and after a period they start to use an adhesive made from lichen. The Arabic papers were familiar to parchment, they were glazed to produce a highly polished surface, this process was after they were sized with starch (Garlick *et al.*, 2013).

In the 13<sup>th</sup> century gelatin was introduced as sizing agent in replacement of the starch paste, this method was used until 18<sup>th</sup> century, different additives such as alum were added to the gelatin and started to become more widespread (Missori *et al.*, 2006). The use of this protein has additional advantages such as to improve their surface in terms of writing, to increase the physical and chemical strength of paper by decreasing the degradation of cellulose, to avoid discoloration of paper, to protect from environmental contaminants and may promote paper stability (Ormsby *et al.*, 2011; Barrett, 2011). The main problem with the generated sizing gelatin was their rapid deterioration in liquid medium during the manufacturing process, especially when weather was hot (Barrett *et al.*, 2011; Garlick, 1986).

Gelatin is the outcome of the somewhat random breakage of chemical bonds in collagen to form shorter chains of amino acids, the length of these peptide chains can vary, which affects properties of gelatin (Missori *et al.*, 2006; Kolbe, 2004).

In the 19<sup>th</sup> century for production of the papers animal glue was used for sizing, and it was substituted by rosin and alum, and more lately by others synthetic products (Laguardia 2005).

The deterioration of the physicochemical properties of paper continued into the 20<sup>th</sup> century with the invention of the chemical wood pulp and the introduction of calcium carbonate as a filler (Adams *et al.*, 2011).

The process of sizing can be realized in two main ways: internal sizing and surface sizing. With internal sizing, very small amounts of sizing compounds are needed and it depends heavily on fiber hydrophobicity (Bajapi *et al.*, 2005), in this way the sizing is possible at very low levels of added chemicals (Lindström 2008). Internal sizing agents are used in the paper industry to accomplish resistance against fluids, improving paper properties like wet strength and printability (Hundhausen *et al.*, 2009).

Different compounds are available to make the sizing of paper to be more effective, but three chemical compounds dominate internal sizing commercially: alkyl ketene dimer (AKD), alkenyl succinic anhydride (ASA) and rosin.

Alkyl ketene dimer (AKD) is one of paper sizing agent that is most widely used in natural papermaking (Song *et al.*, 2012) and theoretically esterify wood compounds and result in a surface modification (Hundhausen *et al.*, 2009). Alkyl ketene dimer (AKD) is a wax-like solid that produces extreme degrees of sizing, and is thought to bond in cellulose covalently (Bajapi *et al.*, 2005).

Alkenyl succinic anhydride (ASA), is not so hydrophobic as AKDs, is in liquid form, oily material, and forms unstable emulsions in water. Alkyl ketene dimer (AKD) are less reactive types of sizing agents and enough stable toward hydrolysis, while alkenyl succinic anhydride (ASA) are very reactive sizing agents towards cellulose, but also very sensitive to hydrolysis, from this is concluded that these sizing agents are at the opposite in terms of stability of hydrolysis and reactivity toward cellulose (Lindström 2008).

Internal sizing can be categorized into three types regarding the pH: acid sizing, neutral sizing, alkaline sizing.

Surface sizing is old operation that includes the application of some hydrophobic chemicals to the areas of already formed paper at the convenient place at the dry end of the paper machine. The main surface sizing solutions consist of mainly modified starch. To have special effects sometimes others agent may include, such as polyvinyl alcohol, animal glue, wax chemicals, methylcellulose and carboxymethyl cellulose (Bajpai *et al.*, 2005).

## **1.6. Analytical techniques used to analyses papers samples and the description of their methodology**

The characterization of papers with analytical techniques are an essential prerequisite in this field and can provide different information about the paper samples that are under investigation. Spectroscopy and optical based techniques were used to study paper degradation, some of its special characteristics make it an excellent tool for studying paper in a simple and non-destructive way (Missori *et al.*, 2005).

In this thesis, samples were analyzed by various analytical techniques for their characterization. The purpose of the examination with in-situ and non-destructive techniques is to get as much as possible information about the characteristic of paper without destroying the original sample.

We will do short review of the techniques that were used to characterize and analyzed the paper samples. With these techniques we manage to have different information, by examining the paper under various illuminations and with different magnifications. More informative techniques were used like X-ray diffraction, ATR-Fourier transform infrared spectroscopy, scanning electron microscopy/energy dispersive X-Ray spectroscopy (SEM/EDS) and pyrolysis gas chromatography (Py-GC/MS).

### **i. Technical photography**

Imaging is an important technique and its main use has been for visual documentation. This method is use for direct observation and is considered to be starting point of every visual and scientific examination. Images have been used to document condition of the objects and microscopic examinations. Images are used rarely as an analytical tool to relate the physical properties of one art object (Berns *et al.*, 2005).

From the photography a lot of information can be obtained and those information, can give deep knowledge about the history of display and storage, its condition, color of paper, presence and degree of deterioration. With this technique is possible to have large field of view and complete depth of focus. Different examination can be performed using different types of illumination as standard, transmitted, and raking light and ultraviolet (UV) radiation.

## **ii. Optical microscopy**

Optical microscopy is fast method that has been used for many years to identify historical objects and a broad range of materials, including minerals, metals, ceramics, fibers and paints. With optical microscopy is possible to magnify small objects or particular areas, optical microscopy provides information on the structure and morphology of the object that with naked eye is not possible to have that information (Stuart *et al.*, 2007; Murphy, 2012). Some of its special characteristics make it an excellent tool for studying paper in a simple and non-destructive way.

This technique involves the variety of the light from the microscope to examine the materials. In fact, samples can be examined by transmitted or reflected light, where a single three-dimensional image is obtained. The microscope can be also in different mode, normal mode operation in optical microscopy is bright field, and in the dark field mode is possible to have phase contrast, fluorescence and ultraviolet (Stuart *et al.*, 2007; Leng, 2008).

The microscope basically consists of two optical systems, the optical part, and mechanical part that have two objectives. The focus of the microscope systems is in the same area of the object but at an angle from each other. The lens has an essential optical characteristic that is expansion and is determined from the magnification of the objective and eyepiece.

The stereomicroscope can work with different range of magnification, in low and high magnification, but also changes the quality and complexity. Maximum significant magnification is about x 140 (Stuart *et al.*, 2007; Murphy *et al.*, 2012).

### **iii. Scanning electron microscopy/energy dispersive X-ray spectroscopy- SEM/EDS**

Scanning electron microscopy is a powerful technique for the examinations of materials. SEM uses a beam of electrons and through this is possible to obtain images with high magnification and good depth of the field (Stuart *et al.*, 2005). SEM equipment involve backscattered electrons (BSE) that provide information about elemental distribution and secondary electrons (SE) that produce an image that shows the morphology and the characteristic of the sample (Stuart *et al.*, 2005; Leng, 2008). SEM analysis allows to investigate and magnify the typical paper morphology, microstructure examination and characterization of fibers, also comparison of physical differences on paper artifacts (Ferreira *et al.*, 2010), whereas information on the nature of the inorganic fillers (Castro *et al.*, 2008) may be obtained from several analytical techniques, matching the qualitative results of EDS with those coming from the infrared studies (Castro *et al.*, 2008; Kiuberis, 2005). The results of the elemental composition and the nature of fillers that is present in different areas are determined and spectra generated when SEM is coupled with energy dispersive X-ray spectrometer (EDS) (Manso *et al.*, 2011). The scanning electron microscope operates in high vacuum, while recent studies have development that for biological samples is possible low pressure (Stuart *et al.*, 2005).

### **iv. Fourier transform infrared spectroscopy (FT-IR)**

Infrared spectroscopy is suitable technique for analysis of historical artefacts, taking into consideration the huge number of objects surveyed to establish the state of preservation (Manso *et al.*, 2009). Shows big capacity to study material surface in conservation and restoration. Infrared spectroscopy offers a potential for the assignment of absorbance bands to specific molecular structures and to determine a variety of chemical and mechanical properties, also is used for characterization of the morphology (Weinstock 1993).

Infrared spectroscopy has great importance for the characterization of the paper, and is possible to analyses paper in different fields of application, yields information about paper deterioration and ageing products in paper samples (Johansson 2000). This spectroscopic method was applied for identification of the origin of cellulosic fiber structure, and the degradation process, also the determination of the chemical composition of additives used in the process of papermaking, in order to identify the primary components of paper and to estimate the presence of other compounds (Udriștioiu 2012).



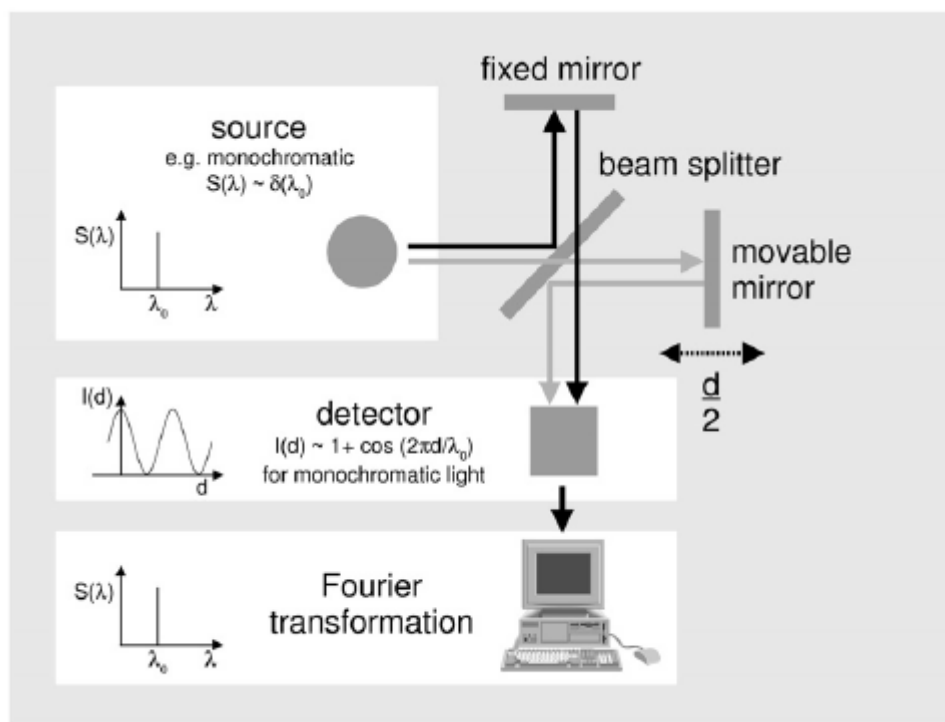


Figure 1.4. Scheme of Fourier transform infrared spectrometer (Barth *et al.*, 2007)

Considering that the instrument is portable, it can safely be used in an archival, library or museum and the application of analytical techniques free of chemicals or solvents is mandatory (Strlič *et al.*, 2008; Manso, 2009; Kavkler, 2012).

Attenuated total reflection Fourier transform infrared spectrometry (ATR-FT-IR) was used to differentiate the foxing stains from the unfoxed areas of the samples, this technique uses the internal reflectance of an infrared beam within ATR crystal (Skoog 1998).

An infrared spectrometer can be operated in different ways, with attenuated total reflection (ATR) spectroscopy being the most adequate for the analysis of paper sheets. During reflection, the infrared radiation penetrates a short distance into the sample before being reflected back. The intensity of the radiation that penetrates the sample decays exponentially with the distance from the surface, giving the analysis a very short ability of penetration. Therefore, ATR is particularly effective for the analysis of surfaces and most suited for the purposes of this study (Ferreira *et al.*, 2009).

## v. Micro X-ray diffraction

X-ray diffraction technique is a good tool for the non-destructive characterization of crystalline and non-crystalline materials and is perhaps one of the most widely used analytical techniques (Pandian 2014). The X-rays are generated by a cathode ray tube, filtered to produce monochromatic radiation, collimated to concentrate, and directed toward the sample (Dutrow *et al.*, 2016).

X-ray diffraction (XRD), is used for the determination of the structure of crystalline materials. The distance between the crystalline plans satisfies Brag's law, equation 1:

$$d\sin\theta = \lambda m$$

the atoms can be hit from the X-ray beam of the wavelength ( $\lambda$ ), where d present the distance between the crystal planes from the rays that are reflected from the atoms that are located in two parallel planes,  $\theta$  present the angle between the plane and the diffracted beam (Figure 1.5) (Howell 2007).

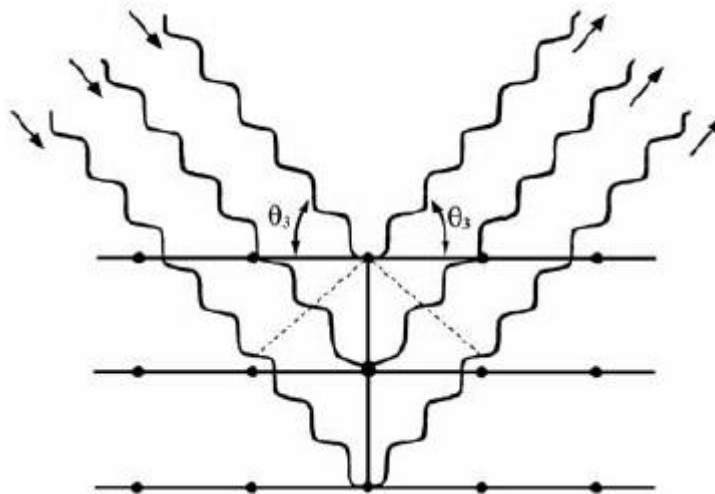


Figure 1.5. Diffraction of the x-rays from the parallel planes (Howel *et al.*, 2007)

The XRD provides information about the arrangement of the atoms and composition of the crystalline materials. Paper is composed of a matrix of cellulose, and to confer to paper the desired physical-mechanical properties, cellulose is added with a variety of inorganic fillers, the quantity and nature of which are characteristic of each manufacturer. The analysis with the X-ray diffraction allows to investigate the polymeric matrix and the inorganic formulation of paper composition (Causin *et al.*, 2010).

## **vi. Pyrolysis-Gas Chromatography/Mass Spectrometry (Py-GC/MS)**

Pyrolysis-Gas Chromatography/Mass Spectrometry (Py-GC/MS) is destructive method and is used for chemical analysis to identify the organic components. The samples that can be analyzed with this method are in very small amounts (Keheyen *et al.*, 2009), some of the samples were analyzed without any manipulation, but with one part of the samples we did some manipulation. With this method samples are thermally decomposed in the absence of oxygen (in an inert atmosphere) into volatile and semi volatile molecules, separated by gas chromatography and detected using mass spectrometry, so with the combination of gas chromatography and mass spectrometry (GC/MS) those molecules can be analyzed (Keheyen *et al.*, 2008; Adams 2011). For identifying the individual peaks in pyrogram, mass spectroscopy is used. During the process of decomposition of the samples in high temperature the chemical bonds will break in a reproducible way, which depends on the structure of the molecule and the thermal energy available at a given pyrolysis temperature (Keheyen *et al.*, 2008).

Different review articles deal with the application of Py-GC/MS for analyses of historical papers and various wood type (Keheyen *et al.*, 2008; Gao *et al.*, 2013; Lin *et al.*, 2009; Gu *et al.*, 2013; Schwarzingen *et al.*, 2010).

Pyrolysis of the samples has been done also in presence of tetramethylammonium hydroxide (TMAH) and the aim of this study is to characterize the organic components, as well to identify different classes of organic substances (Keheyen *et al.*, 2009; Río *et al.*, 2005).

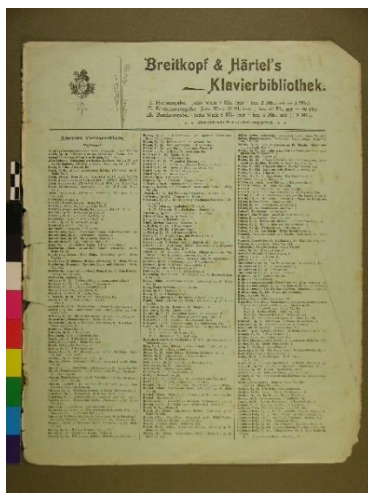
## **2.METHODS AND MATERIALS**

## 2.1. Selection of the samples

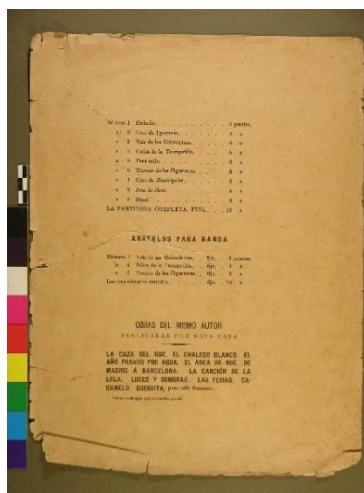
For this study two groups of samples were used: samples S1, S2 and S3 are presented in figure 2.1, already characterized by non-destructive techniques in a previous work (Relvas *et al.*, 2015). S1 and S2 are music papers and sample S3 is a manuscript dating from 1862. Evaluation of fillers in sample S1 and S2, showed the presence of Al and Si, suggesting the use of an aluminum silicate. On sample S2 were found particles rich in Ca and S, pointing out the presence of calcium sulphate. In sample S3, particles rich in Ca in a much lesser extent than in the samples S1 and S2.  $\mu$ -XRD showed the presence of kaolinite on both samples S1 and S2, while the presence of muscovite, was detected particularly on sample S2. The presence of kaolinite and muscovite was confirmed also by FT-IR analysis. Sample S2 showed the presence of lignin, suggesting that paper is composed from mechanical wood, while sample S1 suggest the use of resinaceous sizing, and sample S3 the presence of amide I and II, suggesting the use of proteinaceous sizing (Relvas *et al.*, 2015). These samples were used in this study for development of a methodology to analyze organic compounds by Py-GC/MS used in paper production. Additionally, this group of samples was used for the evaluation of the organic nature of foxing stains.

The second group of samples was collected from stationary shops in Lisbon, from different manufactures. Paper conservator selected the samples by visual observation, based on the color of the foxing stains, and morphology of the papers. Samples were labeled as NB (new book) dating from 1931, OB (old book) dating from 1951 and P (print).

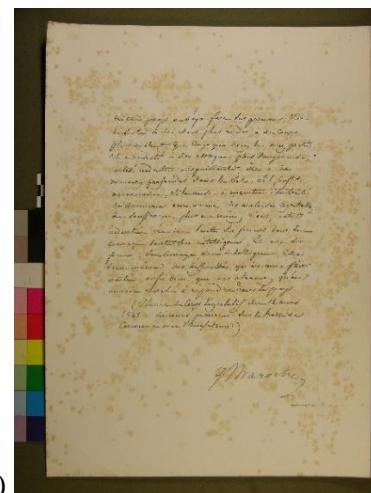
Samples that were analyzed in this study does not have historical value and they have a variations of composition.



a)



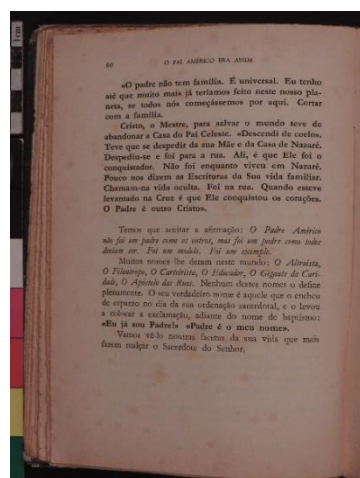
b)



c)



d)



e)



f)

Figure 2.1 Photographic images of paper samples S1, S2, S3 and P, NB, OB obtained under standard light; Legend: a)S1, b)S2, c)S3, d)P, e)NB and f)OB

## **2.2. Technical photography**

Photographic imaging was used as a first step for the visual characterization of the samples. It is frequently used in documentation and evaluation of the surface morphology and chromatic description of the paper samples. Ultraviolet radiation was used to define details of the paper samples which may not be observed under standard light as fluorescence. In fact, some foxed stains present fluorescence under UV radiation.

The images of the paper samples were obtained using a Nikon Coolpix P520 camera located on a column stand under different types of illumination as standard, raking, and transmitted light. The images captured in macro mode with film sensitivity (ISO 400) and using the same focal distance. The same conditions were used to capture the images under UV radiation, except for the film sensitivity (ISO 800), using an Waldmann W portable lamp with two TL4W/08 F4T5/BLB Philips lamps.

For the photographic imaging under different illuminations different conditions were used: under standard light two sources of equal intensity equidistant from the object were used, while in the raking light mode, the light source was positioned at a low angle, located in one side of the paper sample and the light was projected across the surface. Under transmitted light a light box was used for the study.

## **2.3. Optical microscopy**

The samples were observed by optical microscopy to obtain morphological information. Optical microscopy is a rapid method that provides information that is not visible to the naked eye. A Leica M205C microscope lens (maximum numerical aperture of 0.075 with 1.0× achromatic objective) was used for the analyses coupled to a Leica CLS × 100 light spot (Leica Microsystems). The incorporated digital camera Leica DFC 295 (Leica Microsystems) was used for image capturing.

## **2.4. Scanning electron microscopy-energy dispersive X-ray spectroscopy (SEM-EDS)**

Scanning electron microscopy (SEM) was used to observe the surface of the paper samples in high resolution, on the foxed and unfoxed areas. SEM-EDS is a technique frequently used for determination of elemental composition of different types of materials. SEM-EDS enabled detailed profiling of the elements present on the surface of the samples, elemental composition mapping, element point analysis and semi-quantitative analysis beside from morphological information.

Samples were cut in small pieces from the foxed and unfoxed areas and placed face-up on two-sided sticky tapes on aluminum SEM specimen holders.

Analyses were performed using a Hitachi S-3700N SEM coupled with a Bruker XFlash 5010 Silicon Drift Detector-SDD energy dispersive X-ray-EDX spectrometer.

The analyses were done in the variable pressure mode under a pressure of 20 Pa, avoiding coating the samples. Accelerating voltages of 20 kV was used for chemical analyses, while SEM imaging in the backscattered mode was used with accelerating voltages of 15 kV or 10 kV. The EDS detector have resolution of 123 eV at the Mn K $\alpha$  line energy. The system allows reliable chemical mapping and point analysis from Na K $\alpha$  X-ray emission energy up to the L emissions of the heaviest elements. Data was analyzed with Esprit1.9 software from Bruker Corporation.

## **2.5. Fourier transform infrared spectroscopy (FT-IR)**

The samples were analyzed in ATR mode which allowed in-situ and non-destructive analysis. To reduce the effect of carbon dioxide and water vapor, background measurements were performed before sample analysis.

The samples were in direct contact with the diamond crystal, positioned on the surface of the sample holder and pressure was subjected to the samples. The analyses were carried at room temperature and ambient humidity. The FT-IR spectra were obtained in ATR mode with a single-reflection diamond ATR module using a Bruker Alpha spectrometer.

The spectra were acquired in the absorbance mode, in the range of 4000 to 375 cm<sup>-1</sup> with 128 scans and spectral resolution of 4 cm<sup>-1</sup>. They were recorded and analyzed using OPUS/Mentor software (version 6.5).

The components of the paper were identified by comparing the main features of the obtained spectra with articles that have work in similar method and samples.

## **2.6. Micro -X-ray Diffraction- ( $\mu$ -XRD)**

X-ray diffraction is a technique used to identify and study materials with crystalline structure. The analyses were performed direct on the samples using a Bruker AXS D8 Advance diffractometer with a DAVINCI design, equipped with a Cu K $\alpha$  radiation source, a Göbel mirror assembly and a LynxEye 1D detector, and operating with a DIFFRAC.SUITE software package. The analyses were carried out with a 0.3 mm diameter pinhole collimator. The diffraction patterns were collected from 3° to 75° 2 $\theta$  at a step size of 0.05° 2 $\theta$ , with a time per step of 1s and a working voltage and current of 40 kV and 40 mA, respectively. The identification was performed with DIFFRAC.EVA software package using the ICDD PDF X ray pattern database.



## **2.7. Pyrolysis-Gas Chromatography/Mass Spectrometry (Py-GC/MS)**

### *2.7.1. Sample preparation*

For better sample homogenization, paper samples were finely grounded using liquid nitrogen. Samples of approximately -200 µg were weighted in stainless steel Eco-cup capsules and 3 µL of derivatizing agent, tetramethylammonium hydroxide (TMAH, 25% in methanol), were added. Samples were left to dry for a while and then pyrolysed. Several replicates were made for each type of paper, foxing and non-foxing areas.

### *2.7.2. Analysis by Py-GC / MS*

The pyrolyzer- system used was a double-shot PY-3030D from Frontier Lab. The interface was maintained at a temperature of 280 ° C. The pyrolyzer was coupled to a Shimadzu GC2010 gas chromatograph, also coupled to a GCMS-QP2010 Plus mass spectrometer. A capillary column Phenomenex Zebron ZB-5HT (30 m length, 0.25 mm internal diameter, 0.50 µm film thickness) was used for separation, with helium as carrier gas, and adjusted to a flow rate of 1.5 mL/- min. The splitless injector operated at a temperature of 250 ° -C. The GC temperature program was: 40 ° -C for 5 minutes, then ramp until 300 ° -C at 5 ° -C -/- minute, followed by an isothermal period of 13 minutes. Source temperature was set at 240 ° -C and the temperature of the interface was kept at 280 ° -C. The mass spectrometer was programmed to acquire data between 40 and 850 m -/- z. Sample were placed in a 50 uL Eco-cup capsule, and transferred to the double-shot pyrolyzer with the aid of an Eco-stick. The capsule was placed in the pyrolysis interface, where it was purged with helium for 2 minutes. Sample were pyrolyzed using a single-shot method with a temperature of 500 ° -C for 12 seconds and then analyzed on the GC/MS system. Identification of compounds was performed using the software AMDIS and NIST database. To avoid contamination between samples, blank runs were inserted between each Py-GC/MS analysis.

### **3.RESULT AND DISCUSSION**

### 3.1 Morphological characterization of paper samples

In this section the results of the second group of samples, *NB* (new book), *OB* (old book) and *P* (print) are presented in the first place since they included the analytical characterization of the paper samples by different techniques. After that, the Py-GC/MS results from the first group of samples S1, S2 and S3 which include the methodology designed for the analysis with this technique will be presented followed by Py-GC/MS the results from the second group of samples.

Paper is a complex matrix, being the main components cellulose, hemicellulose and lignin, eventually in significant amounts. It also contains others components such as non-fibrous materials, like fillers, coatings and sizing materials. Material characterization was done to evaluate the morphology and chemical composition of the paper samples under study and compare degraded areas due to foxing stains with non-degraded areas to contribute to a better understanding of this specific degradation process.

#### 3.1.1 Description of paper samples and foxing stains (second group of samples)

Paper samples photographed under different illumination are presented in the table 3.1. Sample that is labeled with *P* is a lithography, with white color and very smooth surface, without gloss on the surface, printed on medium thickness. It is a translucent paper and it contains rag fibers. The foxing stains are agglomerated, with irregular shape, and colored with is brown/grey hues. They present, fluorescence under UV radiation. The back of the paper samples present larger intensity of the foxing stains.

The paper sample *NB* (page 63) is paper with crema color, velino, roofless, slight surface texture, the paper is printed in medium thickness. The paper and the foxing stains are translucent. The paper sample contains mainly mechanical soft-wood (70%) and chemical soft-wood. The foxing stains have an orange coloration, with irregular shape and diffuse contour.

The paper sample *OB* is a paper with off white color, the texture is very smooth like coucheé, and it is a translucent paper. The paper is printed in a medium thickness. Foxing stains in the page that is analyzed are not visible to the naked eye but visible under UV radiation. The paper sample contains a mixture of rag fibers (20%) and chemical soft-wood (70%) fibers and a little bit of mechanical wood (10%).

Table 3.1 present a descriptive summary of each sample.

Table 3.1 General description of the paper samples

Samples	Texture	Color	Presence of foxing
<i>P</i>	Smooth	White/without gloss	Irregular spots and high concentration on its entire structure, particularly the verso part
<i>NB</i>	Slight surface texture	Crema	Uniform spots on the entire surface
<i>OB</i>	Very smooth like coucheé	Off white	not visible to the naked eye but visible under UV radiation

### 3.2 Photographic imaging

The first evaluation of morphological characterization of the paper samples was done by photographic imaging under different illuminations.





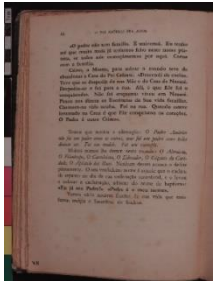

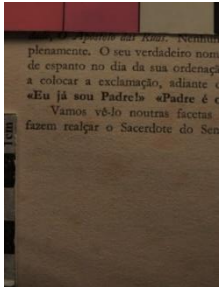


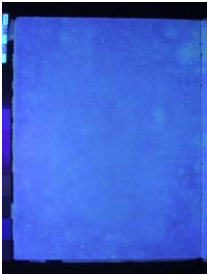

Photographic images (Table 3.2) were used to record the natural tones of the paper samples, the foxing stains and the conservation state of the samples. The paper samples have different characteristics such as texture, thickness and color. The foxing stains have different morphological aspects. Images with raking light were done in macro mode. Standard light was used to obtain information about color, deformations, and damages on the paper, while transmitted light was used for better visualization of the foxing stains and paper structure. Transmitted light can give information about the paper structure, thickness and opacity. The verso of the samples was also evaluated and the gathered information showed that the paper sample *P* presented more foxing stains on it. Sample *NB* showed the presence of foxing stains also on the back of the page, while sample *OB* do not present foxing stains because they are not visible to naked eye.

The samples were also observed under UV radiation (Table 3.2) that according to Rakotonirainy *et al.*, 2015 is the adequate method to analyze the ultraviolet induced visible fluorescence of the paper. Fluorescence is not observed when the discoloration of the foxing stains has developed into dark-brown but can be observed before discoloration. UV fluorescence, in the early stage of the foxing stains is more easily detected than in the colored stains.

Some studies (Manso *et al.*, 2009; Rakotonirainy *et al.*, 2015) reported that some foxing stains fluoresce under UV radiation. That is the case with the paper samples *P*, *NB* and *OB* that under UV radiation, the foxing stains are fluorescent, also fluorescence can occur in some clear areas. The foxing stains on the paper sample *OB* with naked eye were not visible but when the paper was under UV radiation the foxing stains were visible. Some studies (Bicchieri *et al.*, 2002) suggested that fluorescence can occur in intermediate stage of degradation process of paper.

The use of raking light reveals detailed characteristic and topography of the paper, including surface texture like irregularities and planar deformations.

*Table 3.2. Photographic Images of the Paper Samples under different illuminations*

Sample	Standard light	Transmitted light	UV radiation	Raking light
<i>P</i>				
<i>NB</i>				
<i>OB</i>				
















### 3.3 Optical microscopy

For a more detailed view, the paper samples were observed by optical microscopy with different magnifications (Table 3.3) which allowed a better morphological description of the foxing stains. In the table 3.3 is presented also the paper sample *OB* only for the unfoxed areas because foxing stains in the page that is analyzed are not visible to the naked eye but visible under UV radiation.

Through the observation it becomes easier to differentiate the texture of paper samples and it was possible to see the color of the foxing stains. The observation under a stereomicroscope showed differences in the morphology between the different paper samples.

The magnification of 7.8x is the lowest and is possible to distinguish the spots, color and vary in size. The paper sample *P* has a high concentration of foxing stains in one place, with irregular shape and with brown/grey color, while the paper sample *NB* has a cream color and the foxing stains are uniform, foxing stains are not visible with naked eye in the paper sample *OB*. The 20x magnification can distinguish better the shape and size of the foxing stains, while the 63x magnification becomes quite useful in order to differentiate the roles for texture and themselves spots of foxing.

Table 3.3. Optical microscopy observation

Sample	Magnification		
	7.8x	20x	63x
<i>P-foxed areas</i>			
<i>P-unfoxed areas</i>			
<i>NB-foxed areas</i>			
<i>NB-unfoxed area</i>			
<i>OB</i>			

### 3.4 Scanning electron microscopy coupled with energy dispersive X-ray spectroscopy – SEM-EDS

The scanning electron microscopy (SEM) analysis allowed to observe the surfaces of paper samples in the foxed and unfoxed areas at high resolution in the backscattered electron imaging mode and also to determine the main elemental components by EDS analysis.

Three different areas of analysis were selected in the paper sample *P* (Figure 3.1) for morphological examination and elemental analysis: an area containing darker stains (1), an area from the whitish stains (2) and an unfoxed area (3).



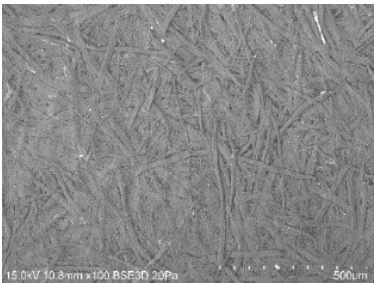
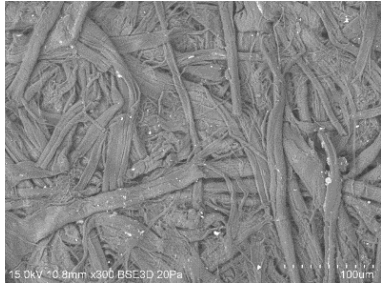




Figure 3.1. Areas of analysis selected for the SEM-EDS study; Legend: 1- area containing darker stains, 2- area from the whitish stains, 3-unfoxed area

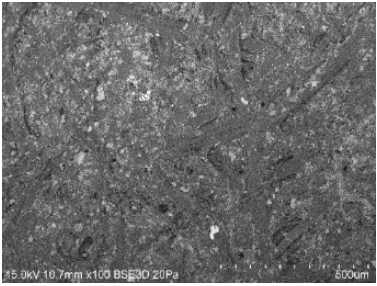
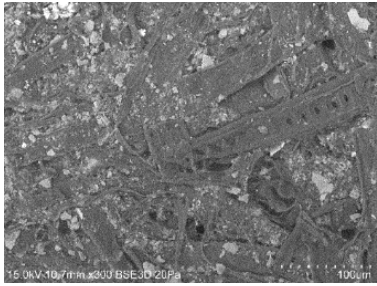
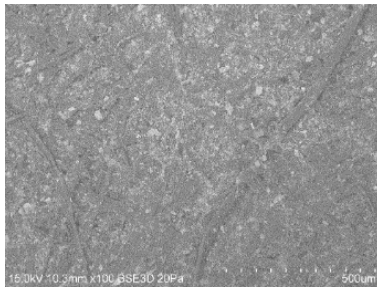
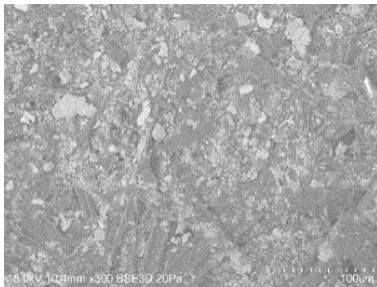
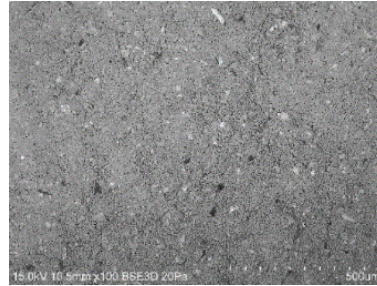
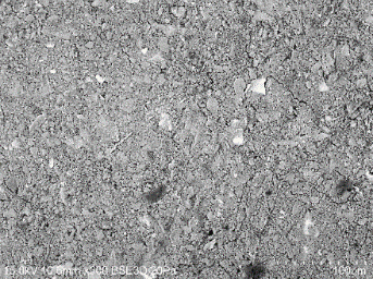
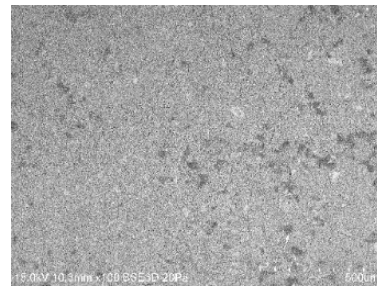
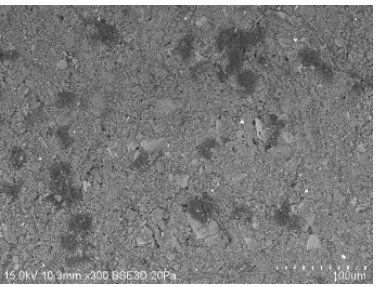
Images of unfoxed and foxed areas of paper *P* are presented in table 3.5. These results are representative of other analyses that were done but are not presented. The comparison of the images from three different regions showed no differences from a morphological point of view for the unfoxed and foxed areas. Contrary to what was observed with other samples (Relvas *et al.*, 2015), and namely with S2 and S3 samples (Relvas *et al.*, 2015). The unfoxed areas do not present disruption of the fibers or accumulation of particles. The samples' surface was structurally organized, paper fibers seem to be in good condition, without any visible disturbance. A similar behavior was observed by sample S1 (Relvas *et al.*, 2015). Sample *P* does not present a large amount of fillers contrary to samples *NB* and *OB*.



Images of the unfoxed and foxed areas of paper samples *NB* and *OB* are presented in table 3.5. Images of the unfoxed and foxed areas show accumulation of dirt, do not present disruption of fibers, without any visible damage. Samples *NB* and *OB* present large amount of fillers and do not show presence of fibers. The foxed areas in paper sample *NB* exhibit the presence of more particles than unfoxed area. Samples observed with SEM do not show substantial degradation of the cellulose fibers. Analyses in paper sample *OB* were performed in foxed and unfoxed areas that were invisible to the naked eye but visible under UV radiation. The chemical analysis gives the same information the difference is only in the physical view.

Filler materials and impurities of heavier elements were observed in the backscattered electron images for more detailed information.

<i>Table 3.5 Scanning electron microscopy micrographs of foxed and unfoxed areas in paper samples P, NB and OB</i>		
<i>Unfoxed area (sample P)</i>		
<i>Foxed area (sample P, darker stains)</i>		
<i>Foxed area (sample P, whitish stains)</i>		

<p><i>Unfoxed area</i> (sample NB)</p>		
<p><i>Foxed area</i> (sample NB)</p>		
<p><i>Unfoxed area</i> (sample OB)</p>		
<p><i>Foxed area</i> (sample OB)</p>		

EDS analysis was used to obtain information on the elemental composition of paper samples. Elemental mapping (Table 3.6) and point analysis (Figure 3.2) of unfoxed area in paper sample *P* revealed the presence of silicon (Si), aluminum (Al) and calcium (Ca), the paper is homogenous and elements are not spread. Particles rich in calcium indicate the presence of  $\text{CaCO}_3$  (Manso *et al.*, 2011; Manente *et al.*, 2012; Nunes *et al.*, 2015) that can be produced when lime easily reacts with atmospheric carbon dioxide (Dąbrowski *et al.*, 2003). Lime was used during the production of paper for the beating process of rag fibers (Dąbrowski *et al.*, 2003). The presence of aluminum (Al) and silicon (Si) was detected in this sample, suggesting the use of aluminum silicate as filler during the production of paper or more probably resulting from some type of contamination, like dust (Manso *et al.*, 2011). Point analysis also detected the presence of iron (Fe) that can be associated with the process of paper production (Manso *et al.*, 2015).

Table 3.6 EDS elemental mapping for the unfoxed area of paper sample *P*

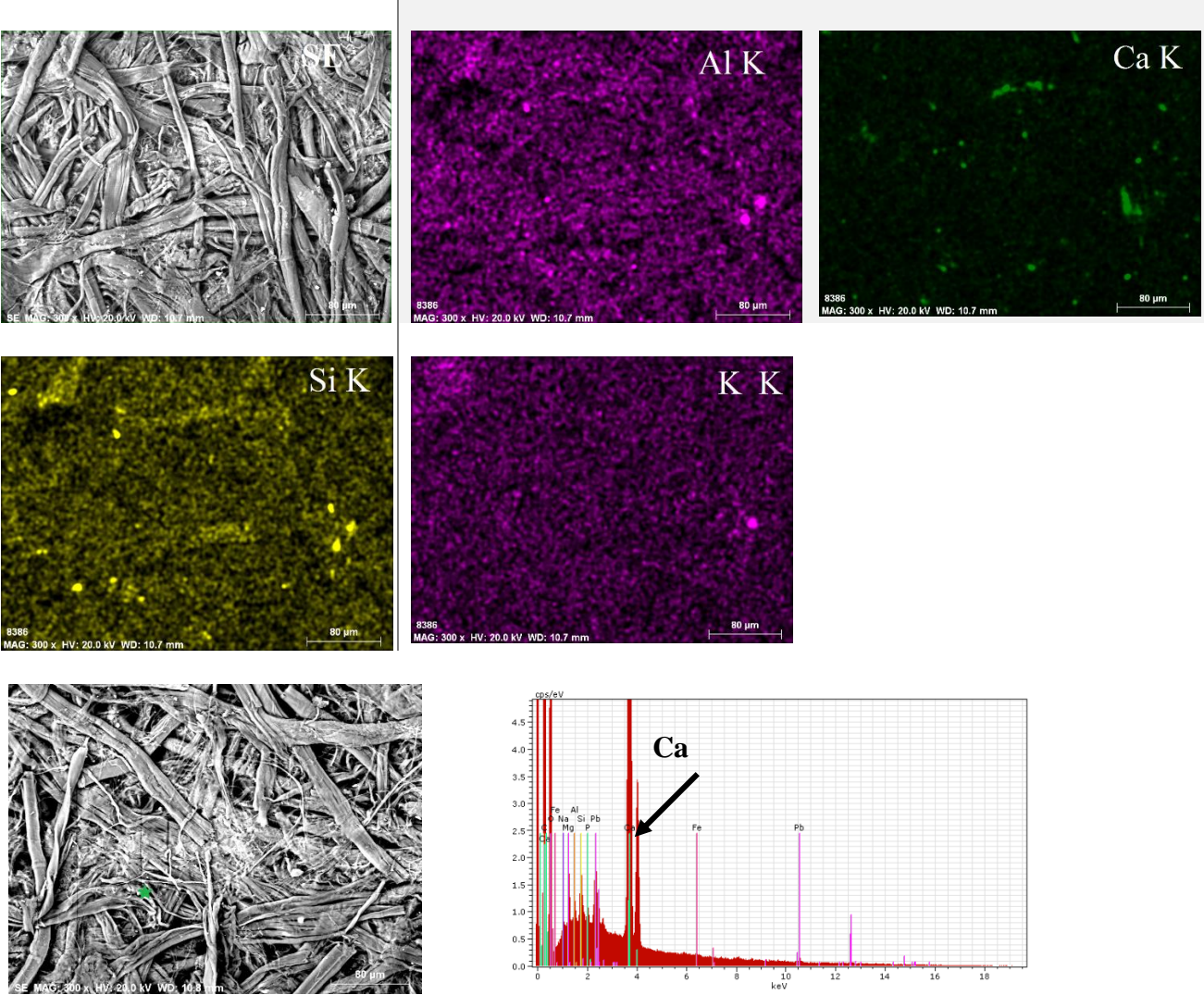


Figure 3.2. Point analysis of unfoxed area in paper sample *P*

EDS mapping (Table 3.7) of foxed area (darker stains, area 1) in paper *P* revealed the



presence of calcium (Ca), potassium (K), silicon (Si), and sulfur (S). These elements were detected also by point analysis (Figure 3.3) and elemental area analysis (Figure 3.4). Particles rich in calcium indicate the presence of  $\text{CaCO}_3$  (Manso *et al.*, 2011; Manente *et al.*, 2012; Nunes *et al.*, 2015).

Table 3.7. EDS elemental mapping for the foxed area (darker stains, area 1) in paper sample P

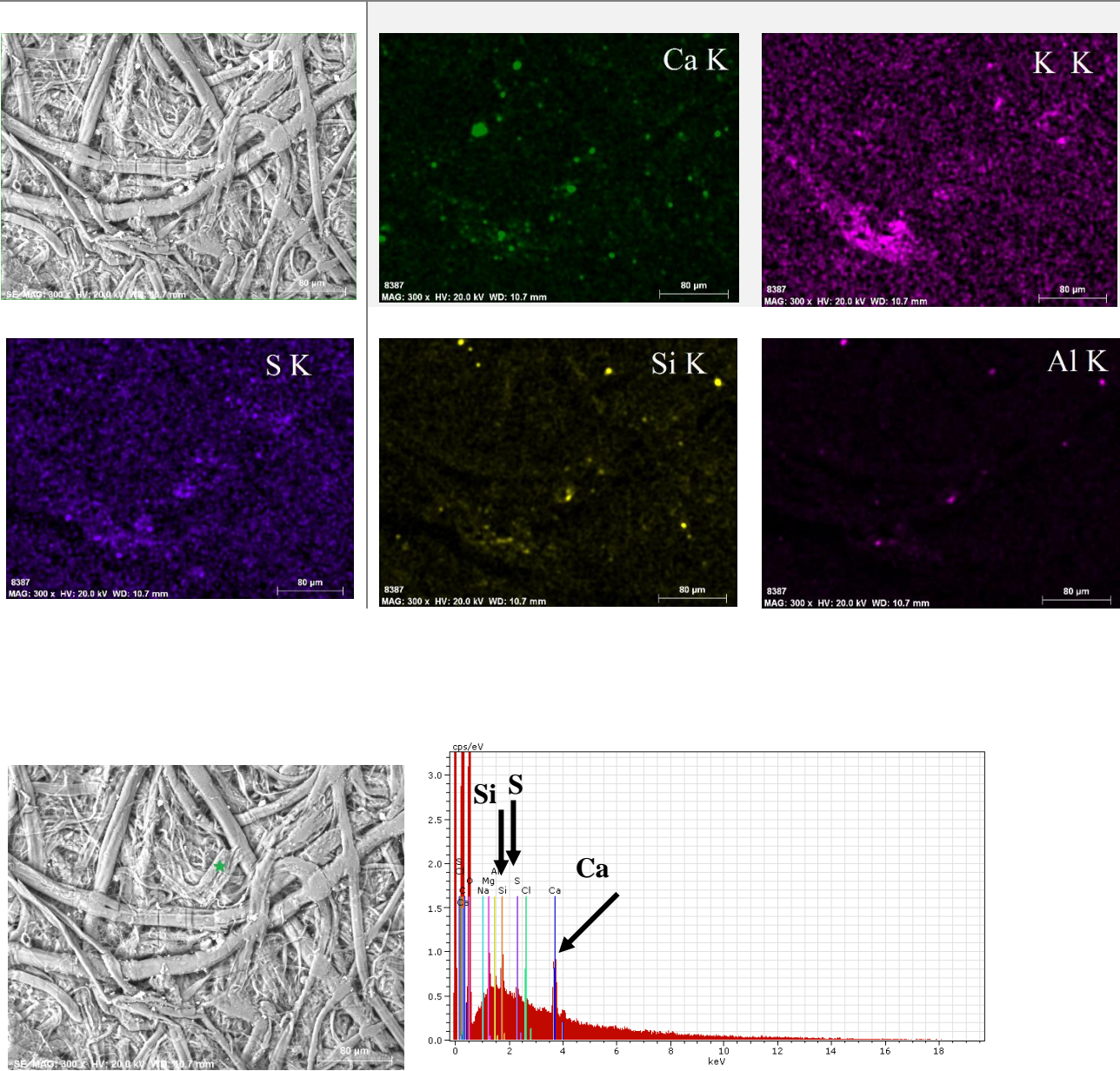


Figure 3.3 Point analyses of foxed area (darker stains, area 1) in paper sample P

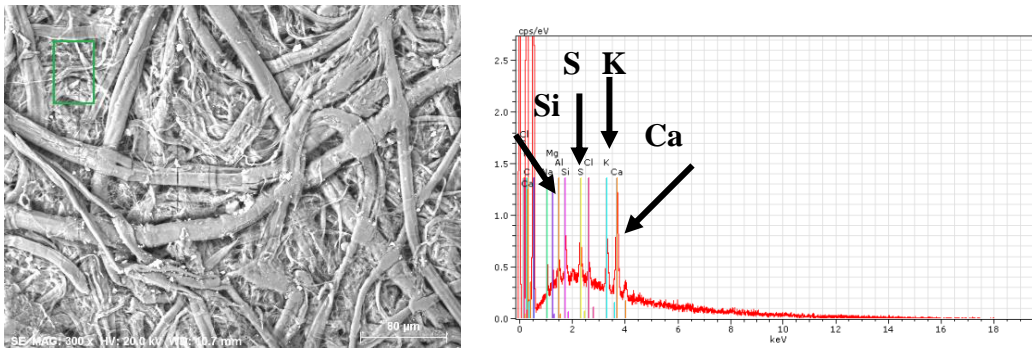
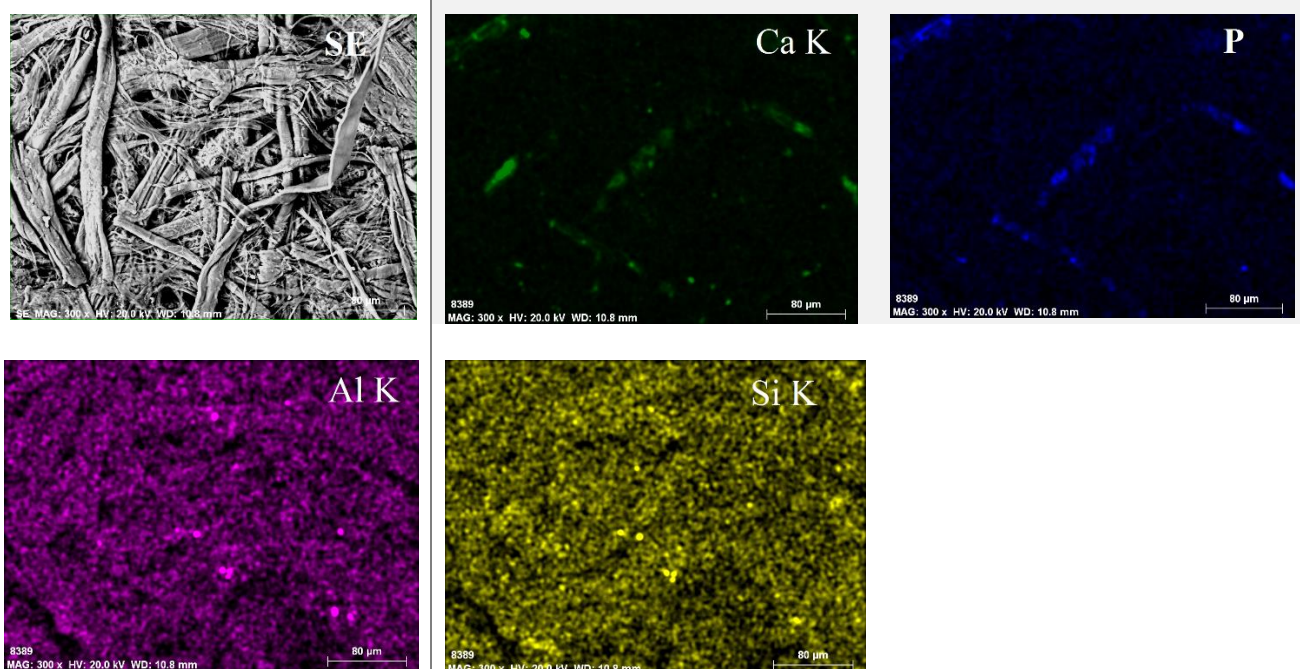


Figure 3.4 Area analyses of foxed area (darker stains, area 1) in paper sample P

EDS mapping of a foxed area (whitish stains, area 2) in sample P is presented in table 3.8. EDS analysis detected calcium (Ca) and phosphorus (P) as the main elements in particles, and small amounts of aluminum (Al) and silicon (Si). Particles rich in calcium indicate the presence of  $\text{CaCO}_3$  (Manso *et al.*, 2011; Manente *et al.*, 2012; Nunes *et al.*, 2015) which is the basic constituent of paper. The presence of silicon (Si) and aluminum (Al) was also detected in different particles but in small amounts, suggesting the use of aluminum silicate as filler.

The EDS analysis from the darker stains (area 1, figure 3.1) and whitish stains (area 2, figure 3.1) do not show differences between darker and whitish stains, they indicate the presence of the same elements, also the SEM analysis do not show differences between them.

Table 3.8. EDS elemental mapping for the foxed area (whitish stains, area2) in paper sample P





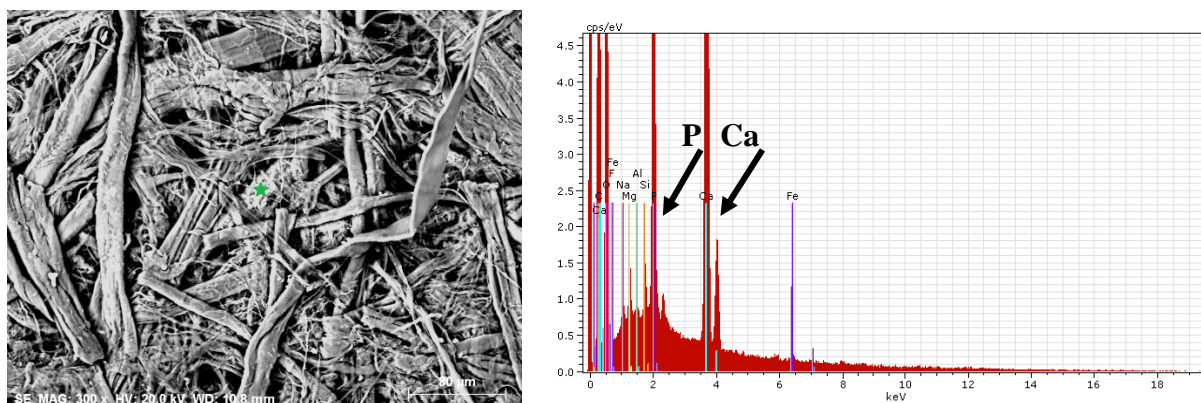
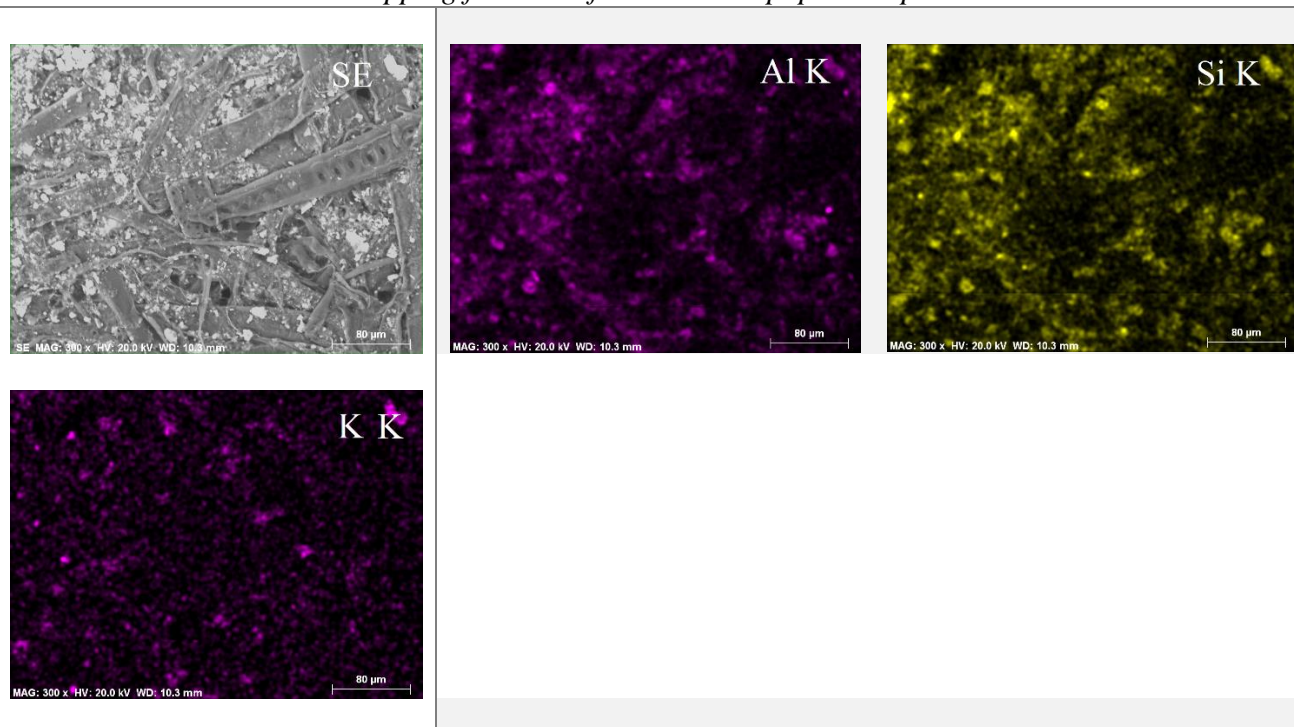


Figure 3.5 Point analysis of foxed area (whitish stains, area 2) in paper sample P

EDS mapping (Table 3.9) and point analysis (Figure 3.6) of unfoxed area in paper sample NB revealed the presence of silicon (Si), aluminum (Al) and potassium (K), and small amounts of iron (Fe), sulfur (S) and zinc (Zn). Elemental composition inferred that paper contain aluminum silicate as filler with potassium that can be from muscovite. The presence of kaolin was also observed, kaolin is most widely used filler in paper manufacture to improve paper performance, to increase opacity, brightness and paper gloss (Wilson *et al.*, 2006).

The presence of zinc and iron could be associated with contamination from the papermaking process (Nunes *et al.*, 2015).

Table 3.9. EDS elemental mapping for the unfoxed area in paper sample NB



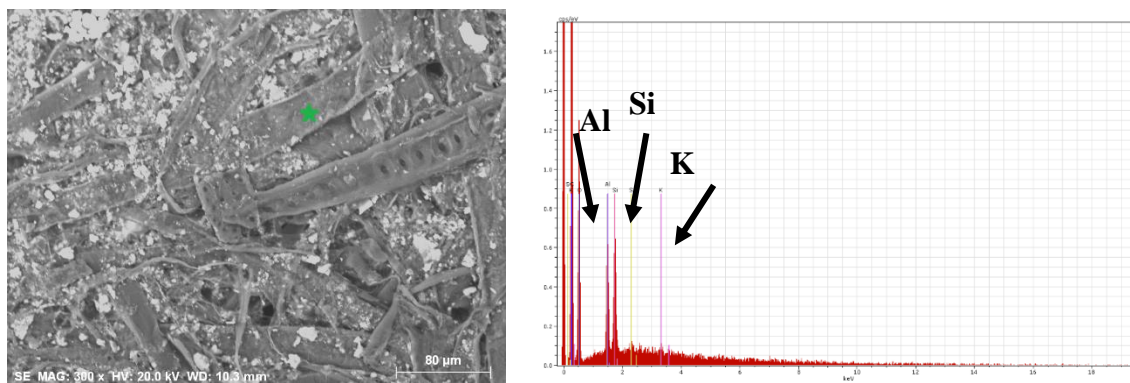
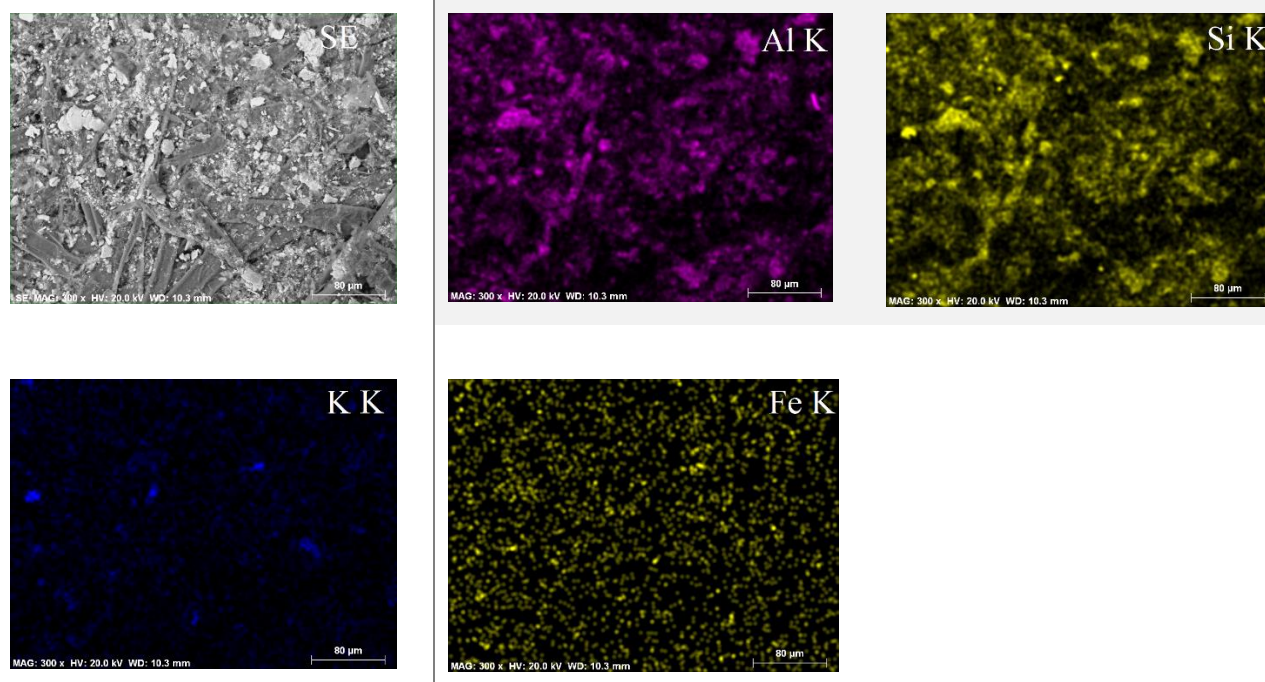


Figure 3.6 Point analysis of unfoxed area in sample NB

EDS mapping (Table 3.10) and point analysis (Figure 3.7) of foxed area in sample *NB* indicate the presence of aluminum (Al), silicon (Si) and potassium (K), and small amounts of iron (Fe) and magnesium (Mg). The elements were also identified by the elemental area analysis (Figure 3.7) indicates the presence of same elements. The chemical composition of unfoxed and foxed areas of sample *NB* are the same, foxed area also contain aluminum silicate with potassium that can be from muscovite.

Table 3.10. EDS elemental mapping for the foxed area in paper sample *NB*



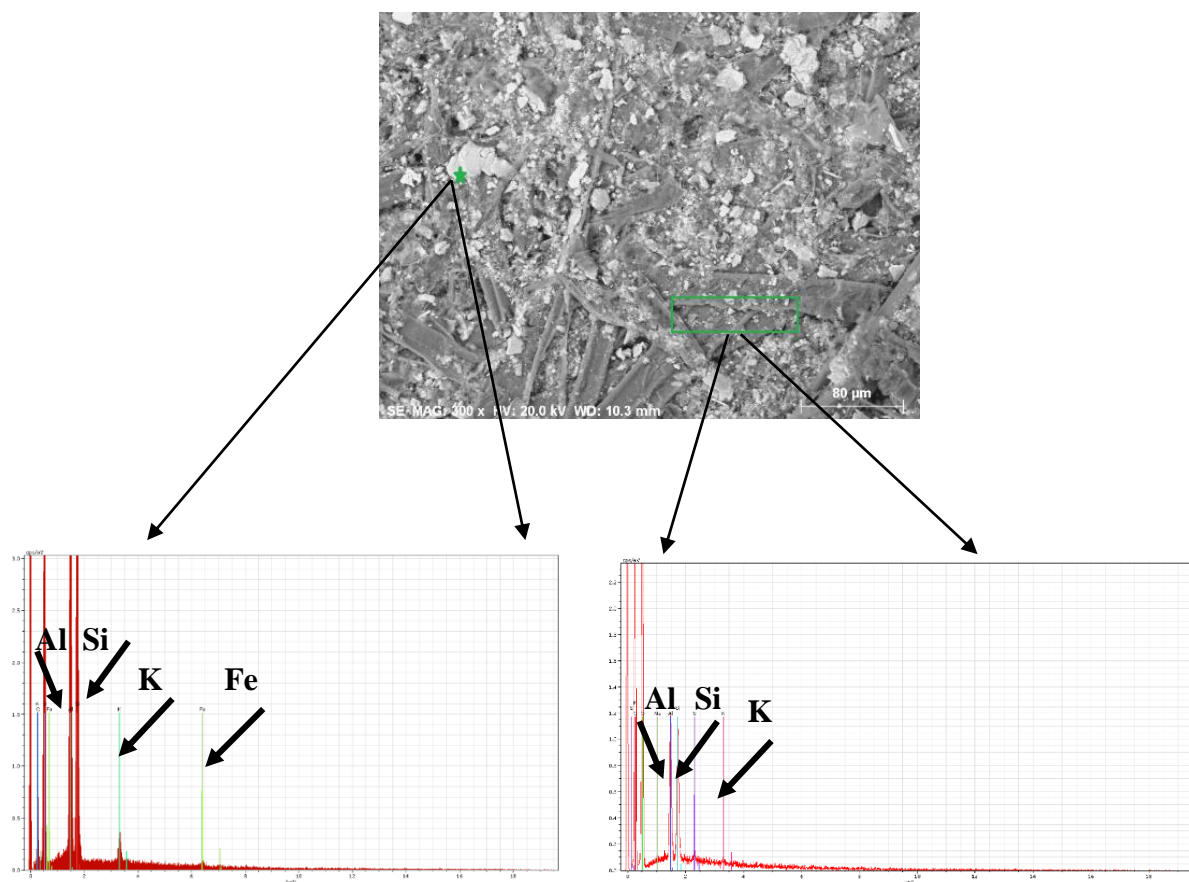
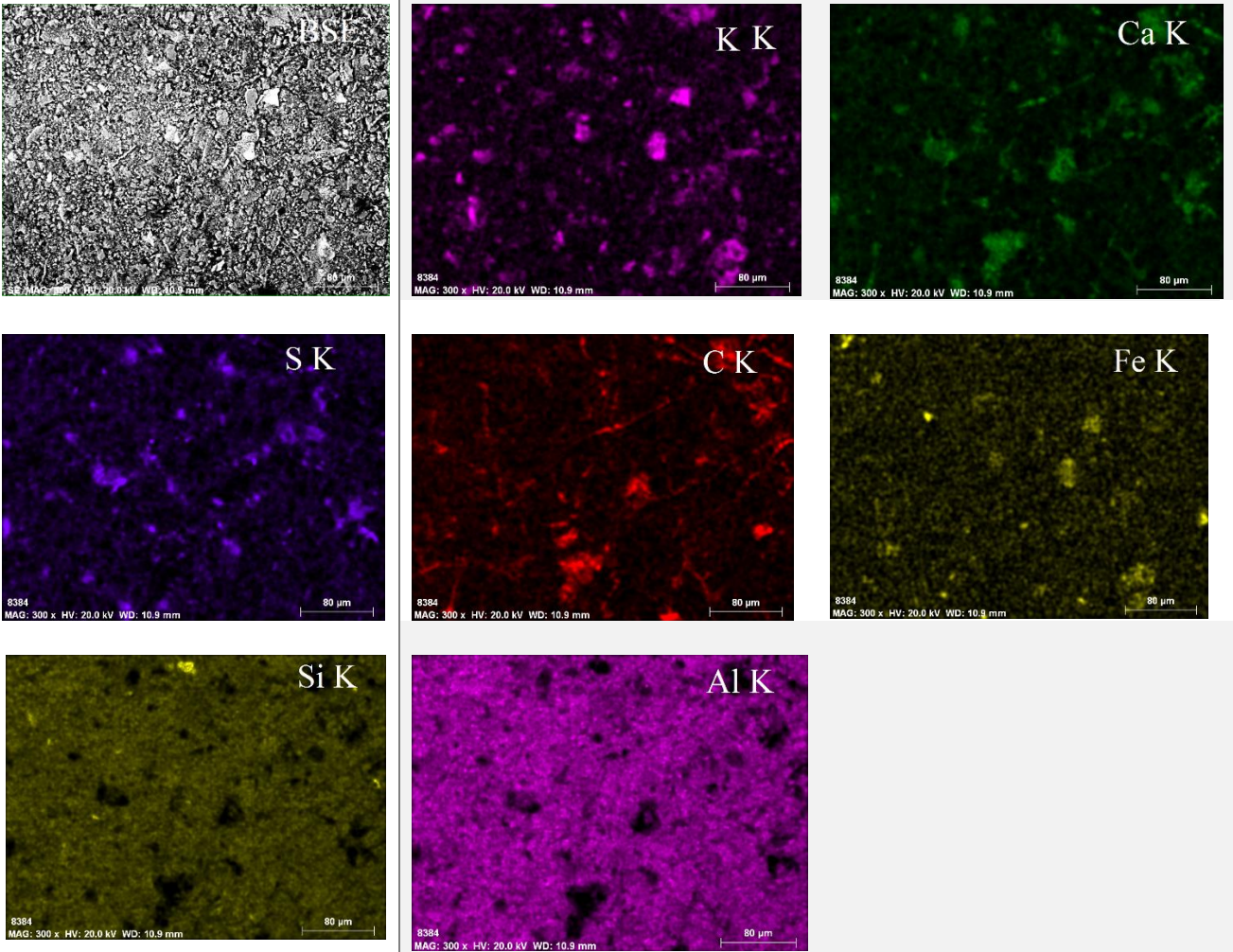


Figure 3.7 Point (top) and area (bottom) analysis of foxed area in sample NB

EDS mapping (Table 3.11) and point analysis (Figure 3.8) in the unfoxed area in paper sample *OB* indicate particles that contain aluminum (Al), silicon (Si), potassium (K), calcium (Ca) and sulfur (S) and small amounts of iron (Fe), magnesium (Mg), and phosphorus (P). The elements were also identified by area analysis (Figure 3.8). It can be inferred from the elemental composition that paper contain aluminum silicate with potassium that would probably be related to muscovite (Bazely *et al.*, 1991).



Table 3.11. EDS elemental mapping for the unfoxed area in paper sample OB



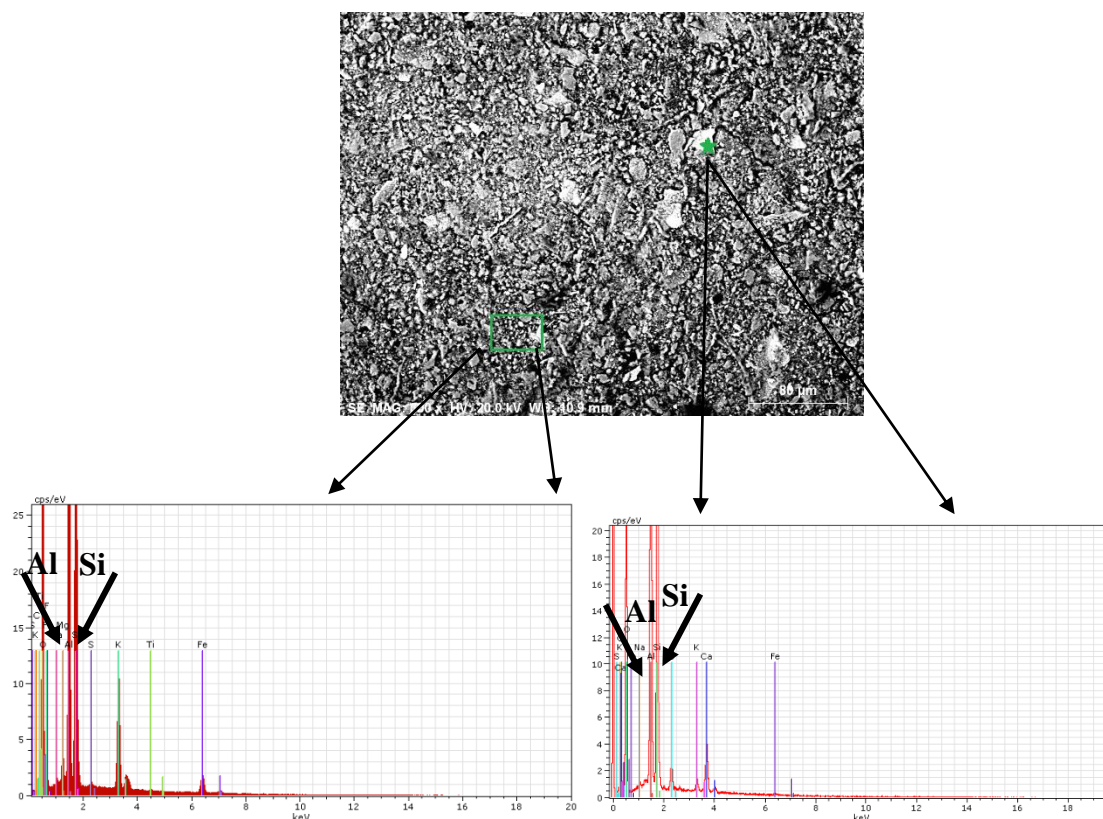


Figure 3.8 Point (top) and area (bottom) analysis for the unfoxed area in sample OB

EDS mapping analysis (Table 3.12) and point analysis (Figure 3.9) of foxed area in sample OB indicate the presence of aluminum (Al) and silicon (Si) as the main elements, and in small amounts calcium (Ca), magnesium (Mg), and iron (Fe). The area analysis (Figure 3.10) detected the same elements as the point analysis. Kaolin is one of the most versatile industrial mineral and is mostly used as filler for paper (Sengeputa 2008) and has platy morphology, is preferable for fiber coverage and paper gloss (Wilson 2006). Kaolin filler, a hydrated aluminum silicate ( $\text{Al}_2\text{O}_3 \cdot \text{SiO}_2 \cdot 2\text{H}_2\text{O}$ ), was very common and may be found in most grades of 19<sup>th</sup>-century papers (Beazley *et al.*, 1991; Nunes *et al.*, 2015).



Table 3.12. EDS elemental mapping for the foxed area in paper sample OB

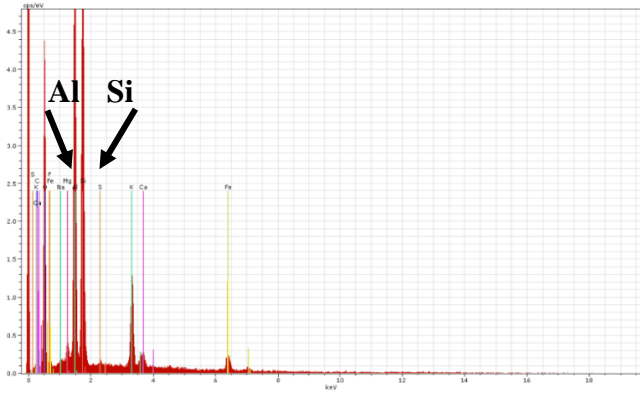
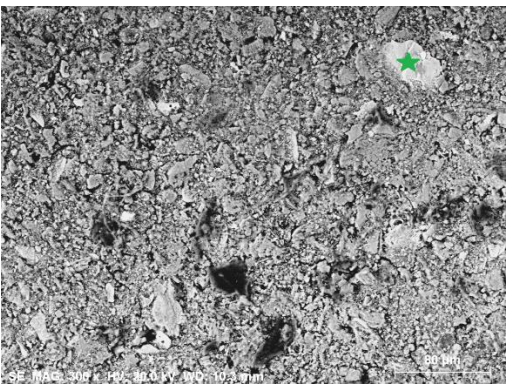
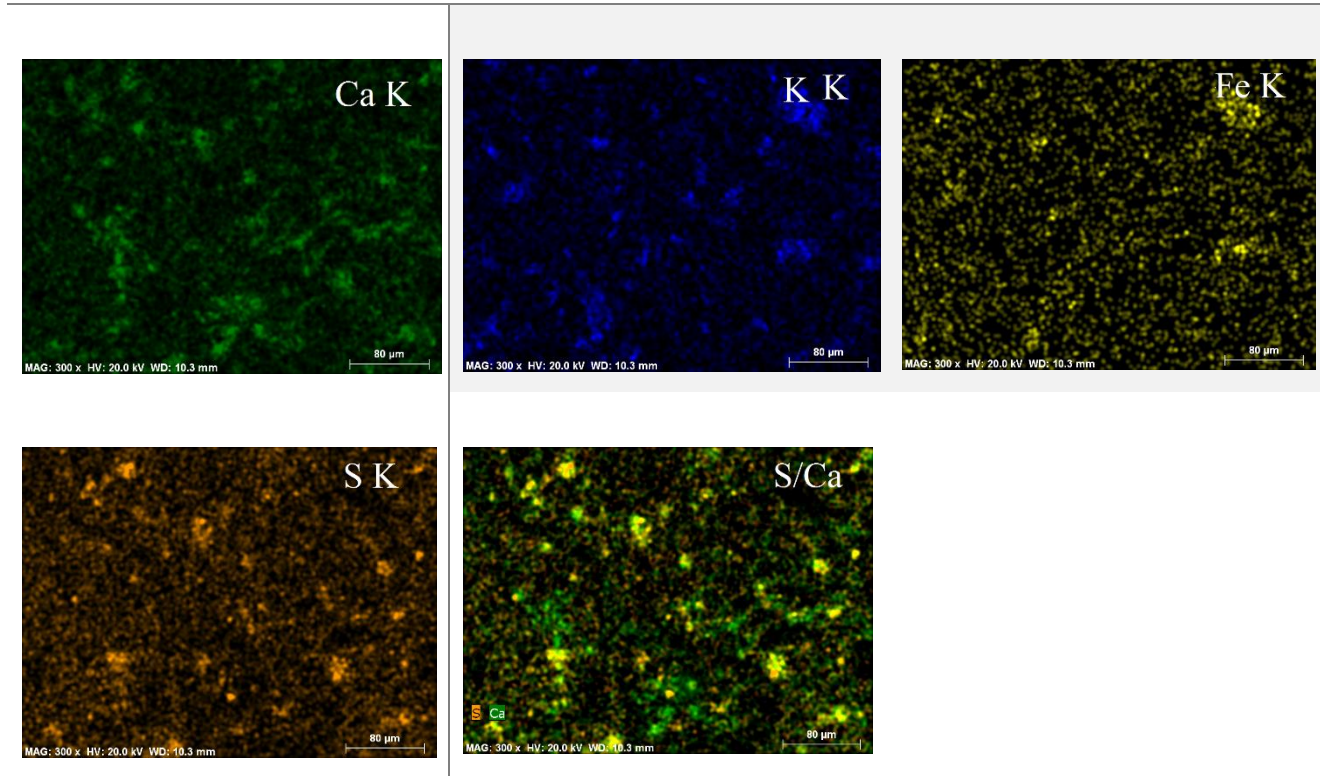


Figure 3.9 Point analysis of foxed area in sample OB

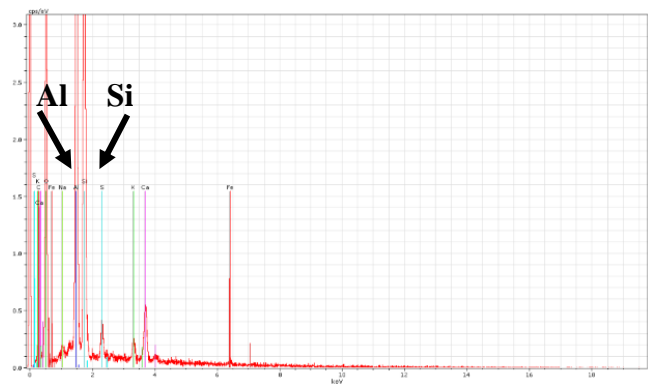
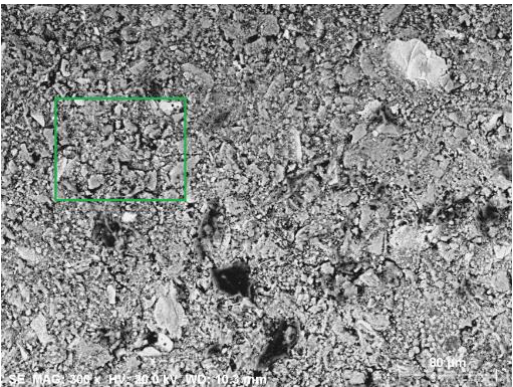


Figure 3.10 Area analysis of foxed area in sample OB

### 3.5 Fourier transform infrared spectroscopy (FT-IR)

ATR-FT-IR analysis is used to identify organic and inorganic constituent of the paper as organic coating and others materials of interest that are present on unfoxed and foxed areas of the paper samples.

ATR-FT-IR aspectra showed in all the samples the absorption bands of cellulose in the region between 1500-850  $\text{cm}^{-1}$ . Usually cellulose bands are recognized in the fingerprint region, being the vibrational pattern of cellulose very complex in this range (Manente *et al.*, 2012; Nunes *et al.*, 2015). Cellulose is a long chain polymer of glucose and the main component of paper materials (Udriștioiu *et.al.*, 2012). A band at about 3330  $\text{cm}^{-1}$  corresponds to the O–H stretching mode of cellulose/water molecules, while a band in the region of 3000-2900  $\text{cm}^{-1}$  corresponds to the C–H stretching vibrations of cellulose (Brandt *et al.*, 2009; Manente *et al.*, 2012; Derrick *et al.*, 1999). The range between 1200 and 900  $\text{cm}^{-1}$  covers the C-O and C-C stretching, anti-symmetric bridge C-O-C, as well as C-C-H and O-C-H deformation vibrations (Proniewicz *et al.*, 2002; Nunes *et al.*, 2015; Rakotonirainy *et al.*, 2015). C-O-H in-plane bendings, C-C-H, O-C-H, and C-C-H deformation stretching, as well as H-C-H bending and wagging are observed in range of 1500 and 1200  $\text{cm}^{-1}$  (Proniewicz *et al.*, 2001; Nunes *et al.*, 2015).

In figure 3.11 is presented the AT-FT-IR spectra of sample *P*. The spectra are representative of several analyses done in the non-foxed areas and in the foxing stains with darker color and not so dark (whitish) color. AT-FT-IR spectra for the foxing dark stains and whitish stains is presented in figure 3.3, the spectra of both stains are identical and do not show differences between the dark and whitish stains of the paper.

In the figure 3.12 is presented the AT-FT-IR spectra of the sample *P*. In sample *P* of unfoxed area were observed bands at 1427 and 900  $\text{cm}^{-1}$  which were due to calcium carbonate (Manete *et al.*, 2012; Nunes *et al.*, 2015). Two bands of unfoxed area in sample *P* can be assigned at around 1630  $\text{cm}^{-1}$  and 1561  $\text{cm}^{-1}$ , these bands are attributable to amide I and II of a proteinaceous material used in sizing (Manente *et al.*, 2012; Derrick *et al.*, 1999), but the bands increase more in the foxed areas that can be due to the presence of fungi in the paper sample.

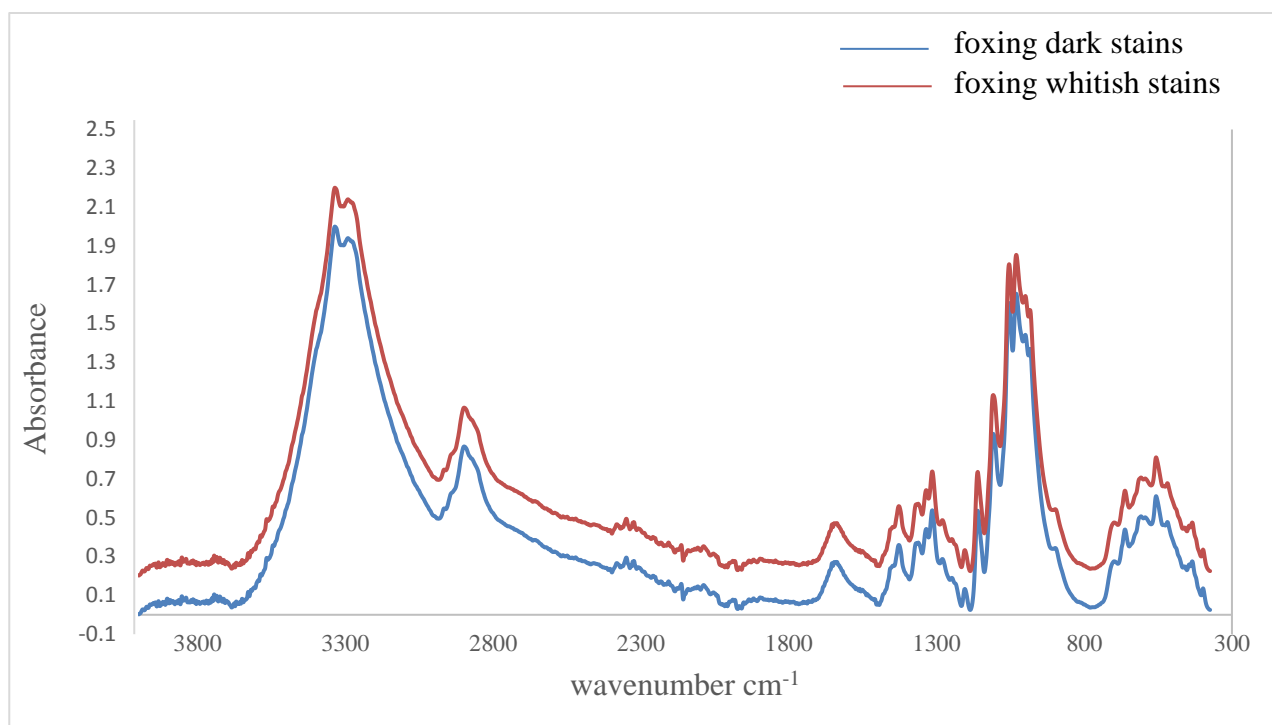


Figure 3.11. Attenuated total reflection Fourier transform infrared spectra of foxed dark stains (blue line) and foxed whitish stains (red line) of paper sample P

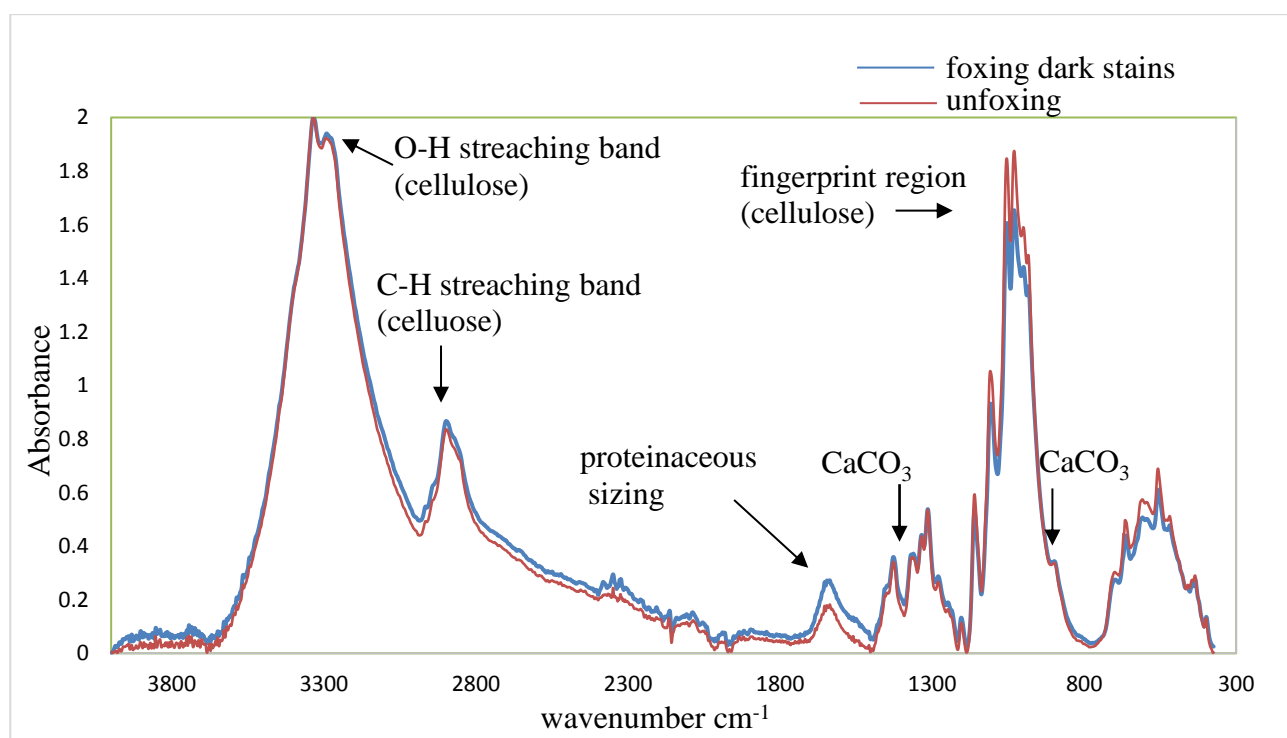


Figure 3.12. Attenuated total reflection Fourier transform infrared spectra of unfoxed (red line) and foxed darker areas (blue line) of paper sample P

Figure 3.13 show the spectra corresponding to paper sample *NB* obtained for the unfoxed and foxed areas. Two characteristic bands in the foxed area at  $3680\text{ cm}^{-1}$  and  $3618\text{ cm}^{-1}$  are due to the presence of kaolin, inorganic filler (Udriștioiu *et al.*, 2012; Saikia *et al.*, 2010).

Paper sample has in its composition lignin, visible by the characteristics bands at  $1504\text{ cm}^{-1}$ , and  $793\text{ cm}^{-1}$  (Manente *et al.*, 2012; Bordilau *et al.*, 2009; Nunes *et al.*, 2015, Derkacheva *et al.*, 2008), this suggest that paper is composed of mechanical wood.

In unfoxed area of sample *NB* was observed one band at  $1729\text{ cm}^{-1}$ , characteristic for resinaceous materials, as rosin (Manente *et al.*, 2012; Derrick *et al.*, 1999). Rosin was used as a sizing agent for many years, extracted from coniferous trees, as a soap or an emulsion was added to the fiber suspension and fixed to cellulose (Bazley *et al.*, 1991).

The characteristic bands of amide I and II, at  $1560$  and  $1648\text{ cm}^{-1}$  is notorious in the spectrum of the foxed area. These visible protein bands can be attributed to the presence of fungi (Nunes *et al.*, 2015). Decomposition of cellulosic material by fungi depends on the chemical composition of the materials (Manente *et al.*, 2012; Abdel-Maksoud *et al.*, 2011). The presence of fungi in the paper can cause discoloration of the paper and physical disruption (Manente *et al.*, 2012).

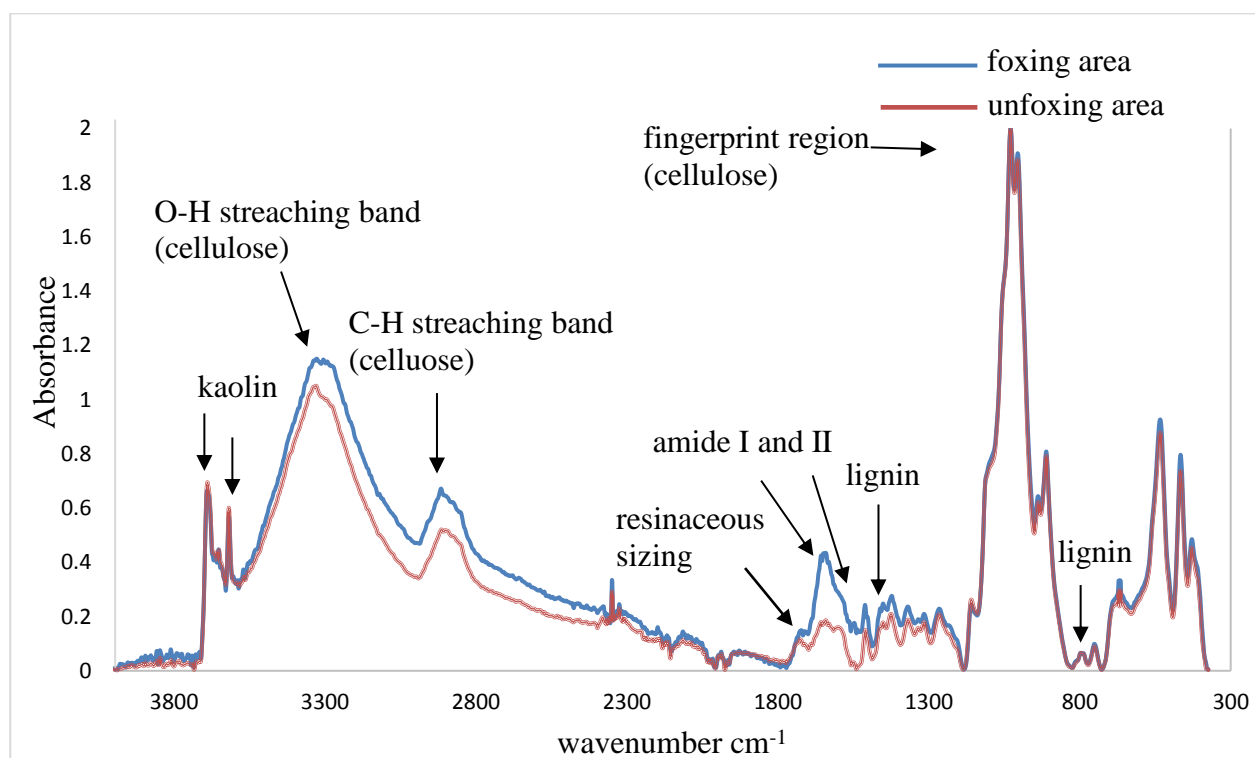


Figure 3.13. Attenuated total reflection Fourier transform infrared spectra of unfoxed (red line) and foxed areas (blue line) of paper sample *NB*

Figure 3.14 shows the spectra corresponding to paper sample *OB* obtained for foxed and unfoxed areas. The bands in the unfoxed area at  $3680\text{ cm}^{-1}$  and  $3618\text{ cm}^{-1}$  are due to the presence of kaolin, inorganic filler that was added to paper to confer good physical-mechanical properties, and one small band of kaolin was observed at  $1114\text{ cm}^{-1}$  (Udriștioiu *et al.*, 2012; Saikia *et al.*, 2010). The bands at range  $529$  and  $461\text{ cm}^{-1}$  indicate also the presence of kaolin (Proniewicz *et al.*, 2002; Nunes *et al.*, 2015). Kaolin filler, a hydrated aluminum silicate ( $\text{Al}_2\text{O}_3 \cdot 2\text{SiO}_2 \cdot 2\text{H}_2\text{O}$ ) and as a filler may be found in papers that are produced after 19<sup>th</sup> century. Primary clay of kaolin may contain some percent of muscovite that contain potassium (Beazley *et al.*, 1991). The presence of aluminum silicate with potassium was observed also by EDS analysis. In the range at  $1700$ - $1250\text{ cm}^{-1}$  were observed the main spectral differences of foxed and unfoxed areas. The bands at  $1621\text{ cm}^{-1}$  and  $1545\text{ cm}^{-1}$  on the paper *OB* are due to amide I and II of peptide groups, and were more intense in the foxed area (Manente *et al.*, 2012; Nunes *et al.*, 2015).

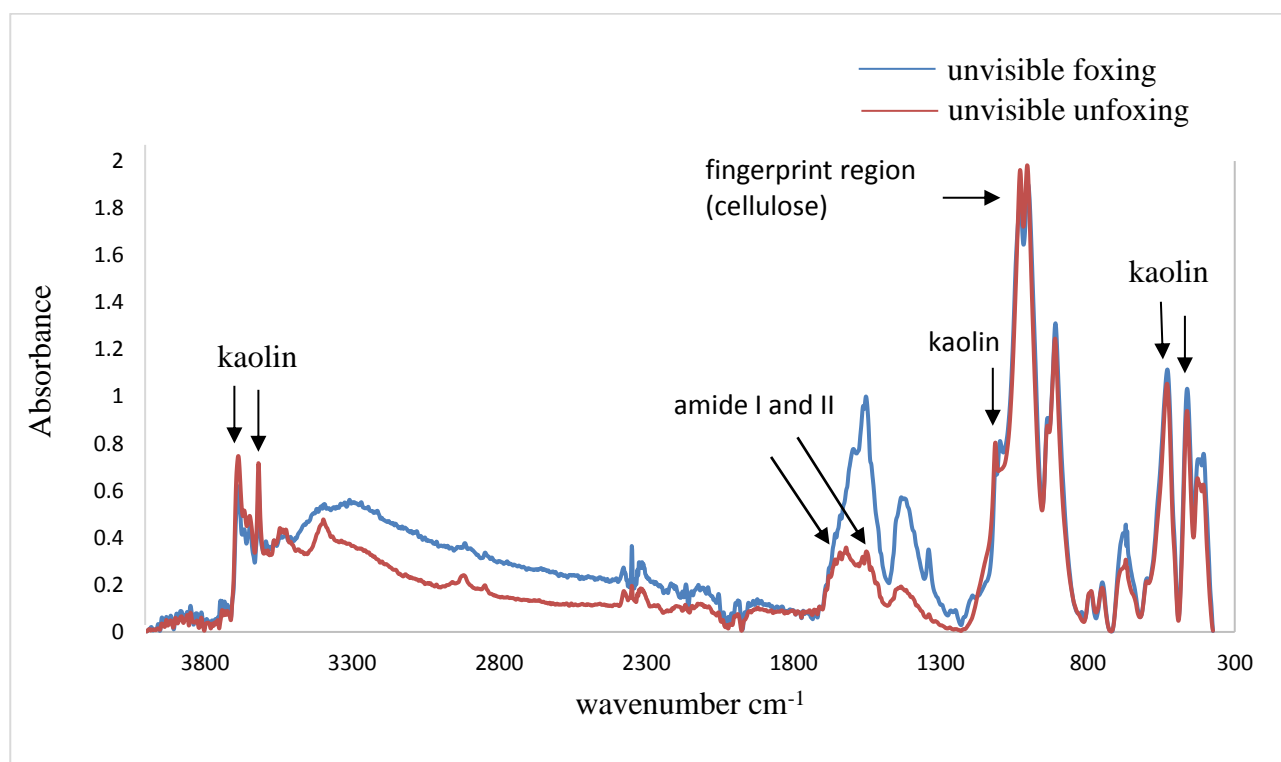


Figure 3.14. Attenuated total reflection Fourier transform infrared spectra of unfoxed (red line) and foxed areas (blue line) of paper sample *OB*

Differences in intensity and appearance of bands assigned to the vibration of C-H and O-H groups, and to the fingerprint region of cellulose, were due to the surface modification of the morphology of paper. The most important band wave numbers, possible assignment and interpretation of paper samples are presented in the table 3.13.

<i>Table 3.13 Band Wave numbers (cm<sup>-1</sup>), Tentative Assignment, and Interpretation of ATR-FTIR spectra of sample NB, P and OB</i>				
<i>Wavenumber (cm<sup>-1</sup>)</i>				
<i>Books</i>		<i>Print</i>		
<i>NB</i>	<i>OB</i>	<i>Pd</i>	<i>Tentative Assignment</i>	<i>Interpretation</i>
3,680	3,680		Si-O-Al stretching	Kaolin
3,618	3,618		Si-O-Al stretching	Kaolin
3,330	3,325	3,327	O-H stretching	Hydroxyl group of cellulose, water in cellulose
2,916	2,914	2,899	C-H stretching	Aliphatic hydrocarbons
1,729			C=O stretching	Resinaceous sizing
		1,630	C=O stretching	Amide I (proteinaceous sizing)
1648	1,621		C=O stretching	Amide I (presence of fungi)
1560	1,545		C-N stretching	Amide II (presence of fungi)
		1,561	C-N-H bending	Amide II (proteinaceous sizing)
1,504			C=O stretching	Lignin
1,431		1,427	CO <sub>3</sub> <sup>2-</sup> stretching	Calcium carbonate
	1,114		Si-O-Al stretching; C-O-C symmetric stretching	Kaolin; cellulose
900		900	O-C-O; skeletal vibrations	Calcium carbonate; cellulose
793			C-H deformation out of plane, aromatic ring	Lignin
	529		Si-O-Al stretching	Kaolin
	461		Si-O-Si bending	Kaolin

Rows in grey refer to the foxed area spectra. Other results were obtained from the unfoxed area spectra (Udriștioiu *et al.*, 2012; Manente *at al.*, 2012; Nunes *et al.*, 2015)

Attenuated total reflection Fourier transform infrared spectroscopy



### 3.6 Micro X-ray diffraction ( $\mu$ -XRD)

Micro XRD analysis on the paper samples *P*, *NB* and *OB* was carried out in order to evaluate crystalline fillers in the sample.

$\mu$ -XRD analysis of paper sample *P* showed the presence of type I cellulose with peak at  $14.98^\circ$ ,  $16.48^\circ$  and  $22.78^\circ$   $2\theta$ , (Figure 3.15). The X-ray diffraction patterns confirmed the SEM visualization of the amount of fillers: sample *P* almost does not present fillers while *NB* and *OB* contain huge amounts of them with less amounts of fibers. The presence of others minerals, kaolinite and among others muscovite was observed in paper samples *NB* and *OB*, the assignment has been made on the basis of results reported in figure 3.16 and 3.17. Muscovite was noticed in larger quantities in the paper sample *OB*. Kaolin minerals frequently include small amounts of K, Mg, Fe and Ti and are most common developed from muscovite., the presence of those elements was confirmed also by EDS analysis.

The presence of Aluminium magnesium hydroxide silicate ( $18.78^\circ$   $2\theta$ ) was observed in the paper sample *OB*. In the appendix 1 is presented table 1.1 for the diffraction peak list, identified for the paper samples *P*, *NB*, *OB*.

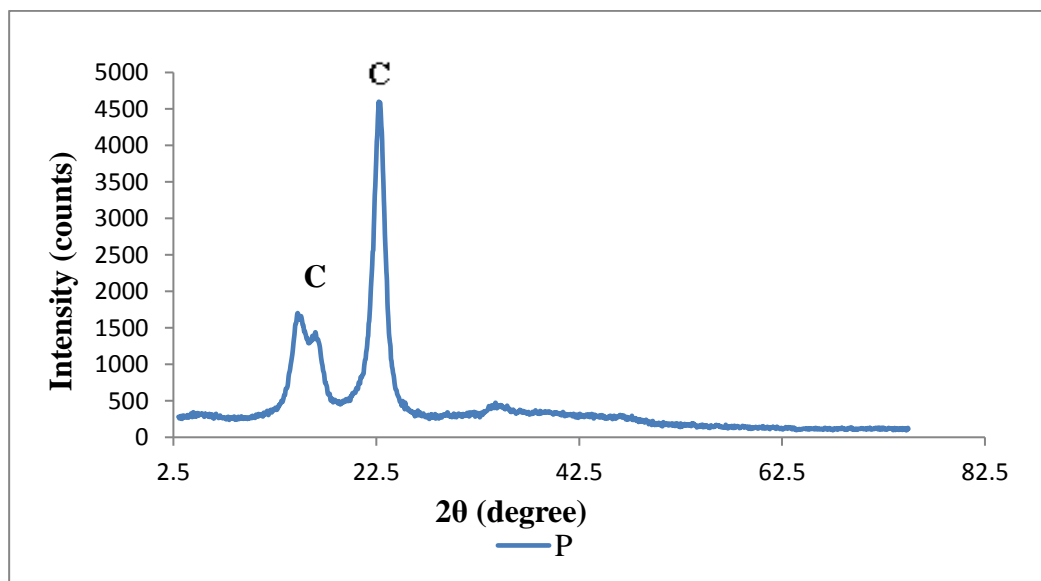


Figure 3.15 Micro-XRD diffractogram of paper sample *P*; C-cellulose

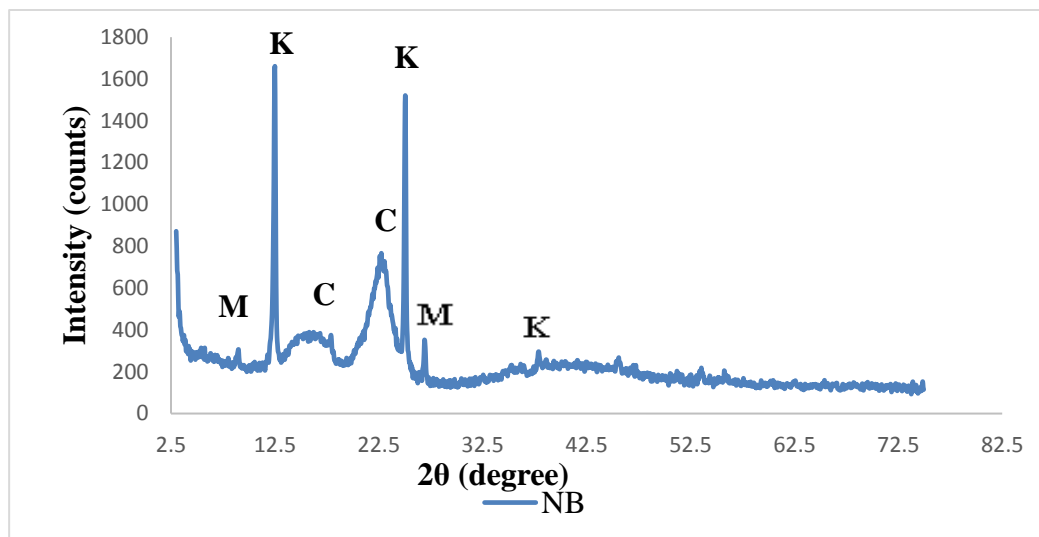


Figure 3.16 Micro-XRD diffractogram of paper sample NB; M-muscovite, K-kaolinite, C-cellulose

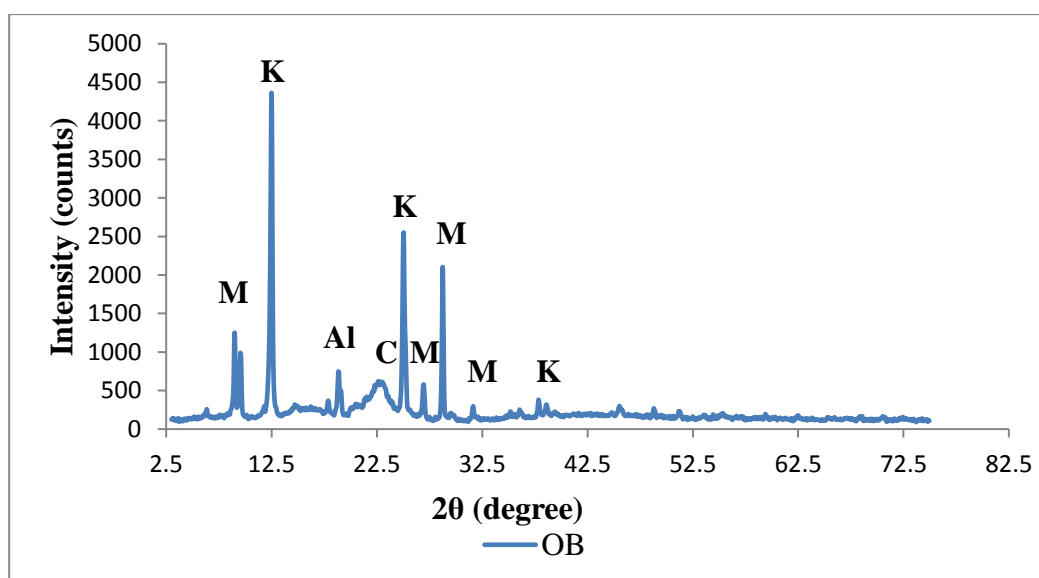


Figure 3.17 Micro-XRD diffractogram of paper sample OB; M-muscovite, K-kaolinite, Al-Aluminium Magnesium Hydroxide Silicate, C-cellulose

### 3.7 Pyrolysis-Gas Chromatography/Mass Spectrometry (Py-GC/MS)

#### 3.7.1 Evaluation of Py-GC/MS to access paper foxing

Py-GC/MS is an analytical technique widely used for characterization of paper (Odermatt *et al.*, 2003), and in this work it was used to study the different papers and investigate possible differences in the composition of the foxing stains and unfoxed areas.

Paper S1 and S2 were sampled in the foxed and unfoxed areas and figures 3.18 and 3.19 show representative pyrograms of these samples. A variety of products is released from the pyrolysis of the samples (compounds from sample S1 are listed in the table 3.13 and for the sample S2 in table 2.1, appendix 2), but there also no significant differences in terms of composition between foxed and unfoxed areas.

As the major difference observed between the samples was the peak area, the reproducibility of the pyrograms became a very important issue. If the peak areas are not reproducible, the observed differences became irrelevant for the purpose of comparing the chemical composition of foxed and unfoxed areas.

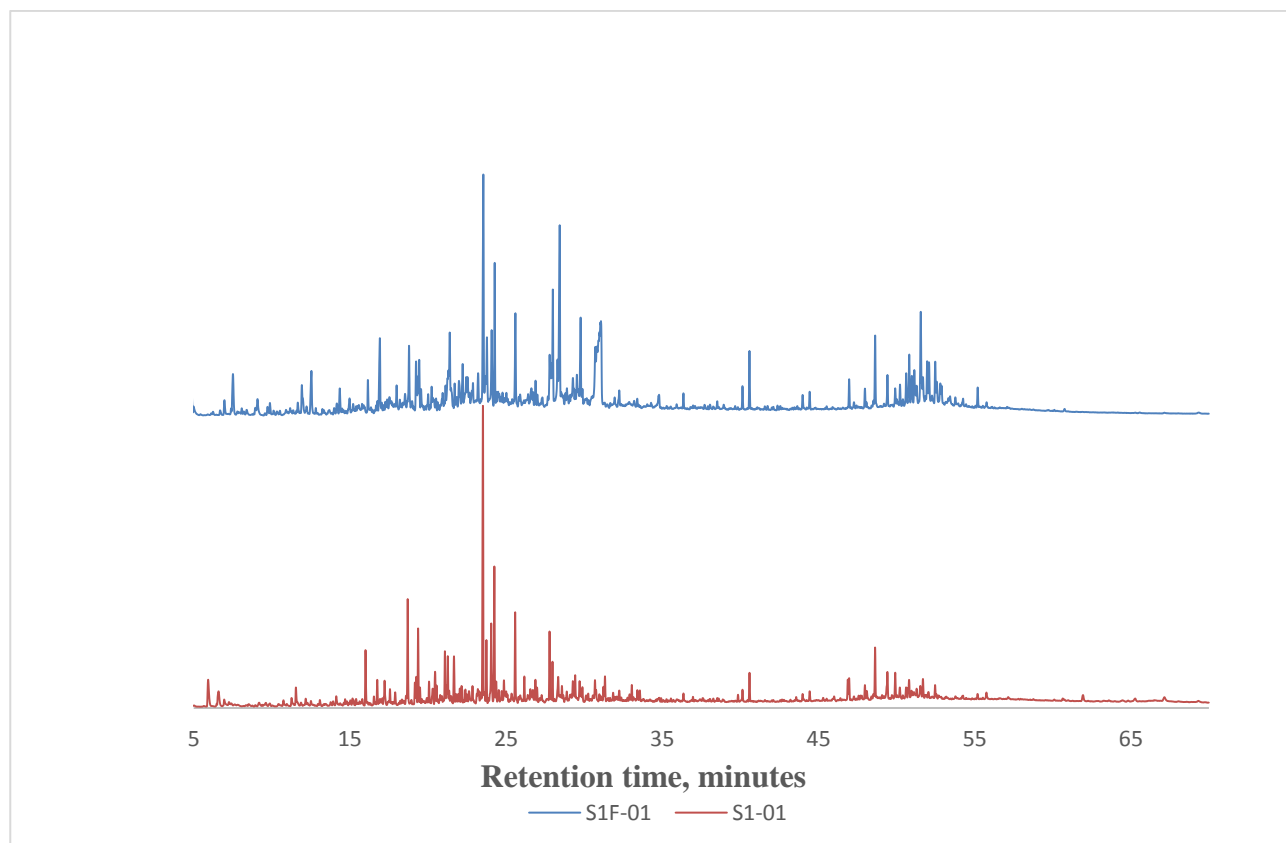
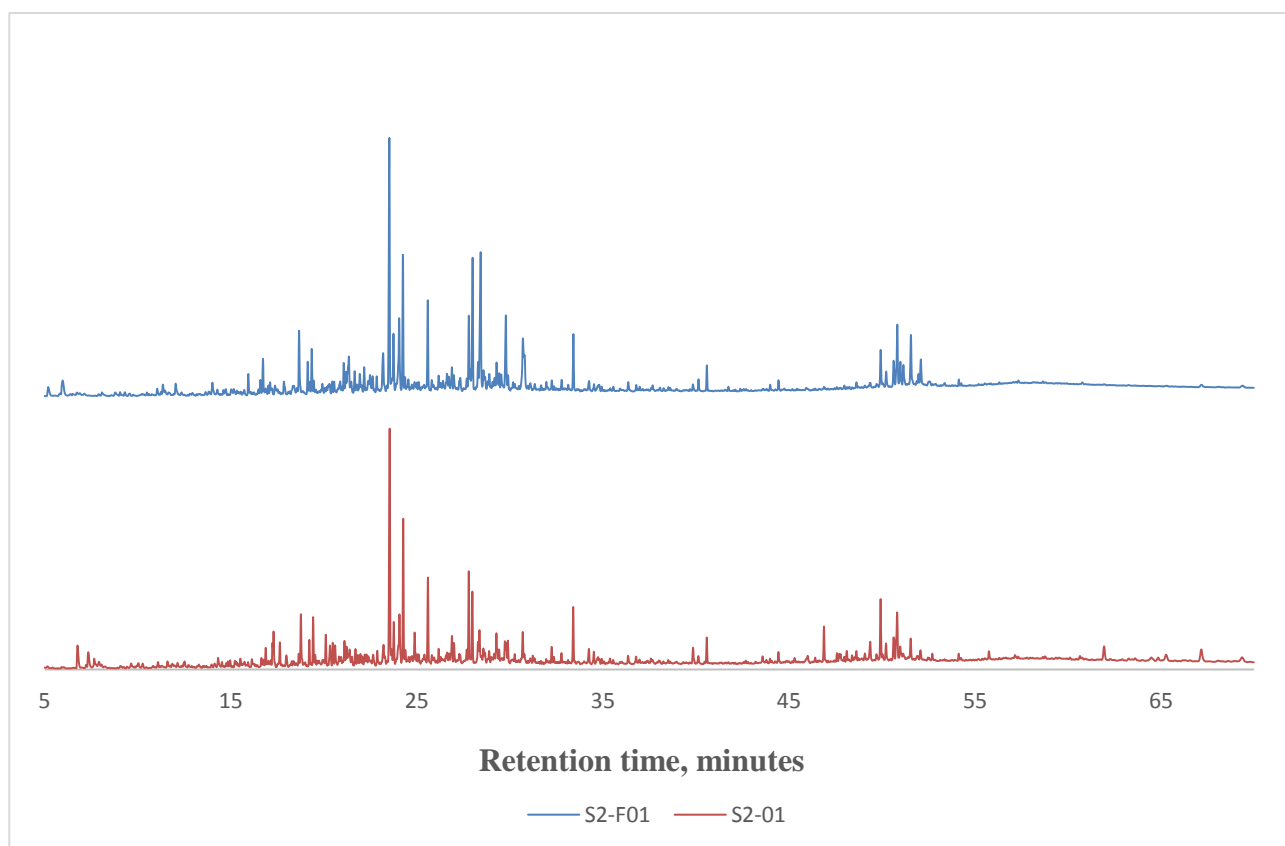
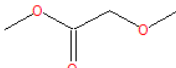
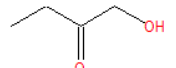
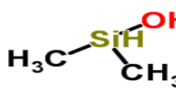
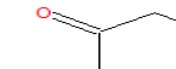
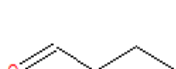
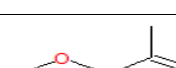

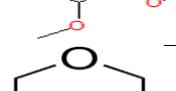

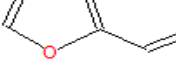

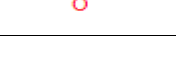
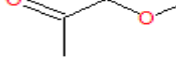
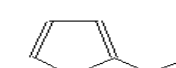


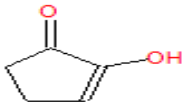
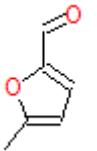
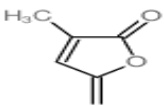
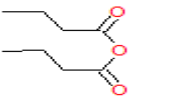
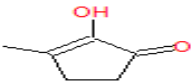
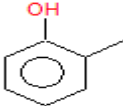
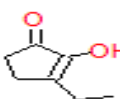
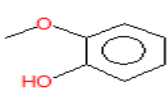
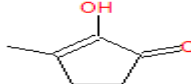
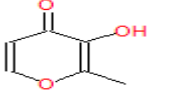
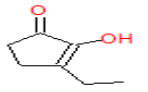
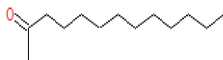
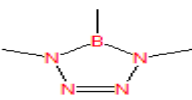
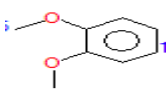
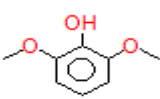
Figure 3.18. Py-GC/MS pyrogram of sample S1, Legend: S1F-01 sample from a foxing stain; S1-01, sample from the unfoxed area of the sample

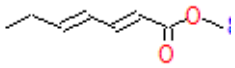
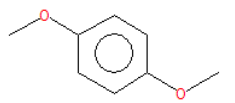
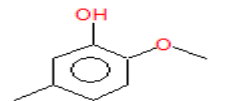

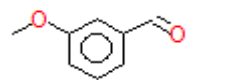

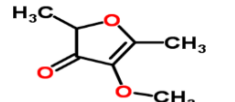
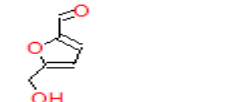
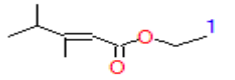
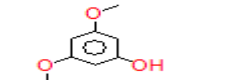
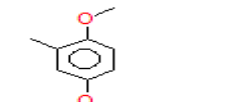
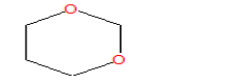

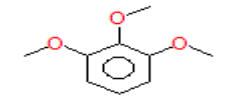
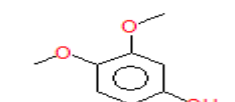
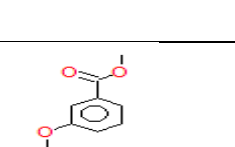


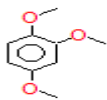
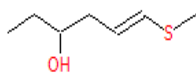
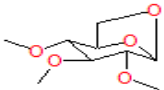
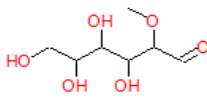
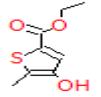
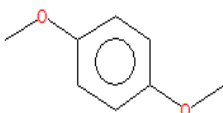
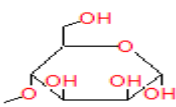
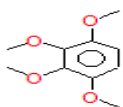
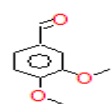
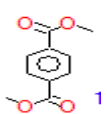
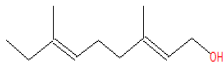
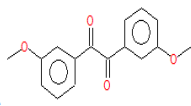
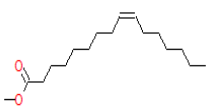
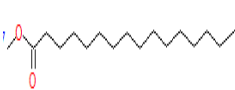
*Figure 3.19. Py-GC/MS pyrogram of sample S2, Legend: S2-F01, sample from a foxing stain; S2-01, sample from the unfoxed area of the sample*

Table 3.13. Compound obtained from the Py-GC/MS from the foxed and unfoxed area of the sample S1

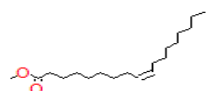
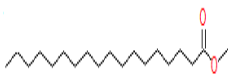
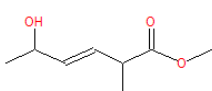
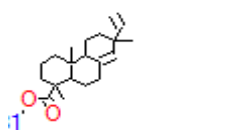
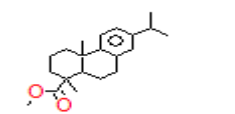
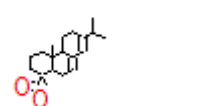
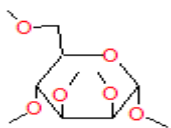
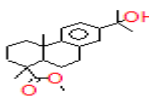
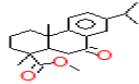
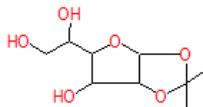
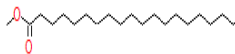
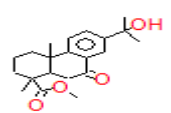
Rt (min)	Chemical name	Intensity	Structure	S1	S1F	Source
2.6867	Acetic acid, methoxy-, methyl ester	2		-	+	hemicellulose
2.8558	1-Hydroxy-2-butanone	1		-	+	cellulose
3.0500	Dimethylsilanol	2		-	+	unknown
3.1608	2-Propanone, 1-hydroxy-	1		-	+	cellulose
3.7250	Succindialdehyde	2		-	+	unknown
4.4892	Propanoic acid, 2-oxo-, methyl ester	1		-	+	sugar
4.7017	Propanoic acid, 2-methoxy-, methyl ester	1		-	+	sugar
5.0025	1,4-dioxadiene	1		-	+	unknown
7.5158	Furfural	2		-	+	cellulose
9.0933	2-Butanone	1		-	+	Carbon Selectvity (sugar)
9.8817	2-Propanone, 1-(acetyloxy)-	1		-	+	sugar
11.5350	Ethanone, 1-(2-furanyl)-	1		+	-	cellulose
11.6658	2-Cyclopenten-1-one, 2-methyl-	1		-	+	cellulose
11.9275	Butyrolactone	1		-	+	cellulose

Rt (min)	Chemical name	Intensity	Structure	S1	S1F	Source
12.5383	2-Cyclopenten-1-one, 2-hydroxy-	2		-	+	Cellulose
14.3442	5 METHYL FURFURAL	1		-	+	Cellulose
14.9825	3-Methyl-5-methyliden-2(5H)-furanone	1		-	+	hemicellulose
16.1533	Butanoic acid, anhydride	a)1 b)2		+	+	unknown
16.7533	2-Cyclopenten-1-one, 2-hydroxy-3-methyl-	1		+	-	cellulose
17.9975	Phenol, 2-methyl-	1		-	+	lignin
18.7033	2-Cyclopenten-1-one, 3-ethyl-2-hydroxy-	3		+	-	cellulose
19.2350	Phenol, 2-methoxy-	2		-	+	lignin
19.3683	2-Cyclopenten-1-one, 2-hydroxy-3-methyl-	3		+	-	cellulose
20.0133	Maltol	1		-	+	cellulose
20.2342	2-Cyclopenten-1-one, 3-ethyl-2-hydroxy-	1		-	+	cellulose
20.4517	2-Tridecanone	1		+	-	unknown
20.5517	1H-Tetrazaborole, 4,5-dihydro-1,4,5-trimethyl-	1		+	-	unknown
21.0842	Benzene, 1,2-dimethoxy-	2		+	-	lignin
21.2967	7-methyl-1,4-dioxaspiro[2.4]heptan-5-one	3		-	+	lignin

Rt (min)	Chemical name	Intensity	Structure	S1	S1F	Source
21.3933	Hepta-2,4-dienoic acid, methyl ester	3		-	+	unknown
21.6608	Benzene, 1,4-dimethoxy-	2		+	-	lignin
22.2208	2-Methoxy-5-methylphenol	2		-	+	lignin
22.5317	7-Tetradecene	1		-	+	unknown
22.8817	Benzaldehyde, 3-methoxy-	1		-	+	lignin
23.2017	1,4:3,6-Dianhydro-α-d-glucopyranose	1		-	+	cellulose
23.5450	4-methoxy-2,5-dimethyl-3(2H)-furanone	5		-	+	hemicellulose
23.6742	2-Furancarboxaldehyde, 5-(hydroxymethyl)-	1		-	+	cellulose
23.7725	2-Pentenoic acid, 3,4-dimethyl-, ethyl ester	2		-	+	unknown
24.2508	Phenol, 3,5-dimethoxy-	4 (74)		+	-	lignin
24.3850	2,5-Dimethoxytoluene	1		-	+	lignin
24.8625	1,3-Dioxane	1		+	-	unknown
25.5825	4-Hydroxy-3-methoxybenzyl alcohol	3 (70)		+	-	lignin
26.1725	1,2,3-Trimethoxybenzene	1		+	-	lignin
26.6158	Phenol, 3,4-dimethoxy-	a)1 b)1		+	+	lignin
26.9833	Benzoic acid, 3-methoxy-, methyl ester	1		+	-	lignin

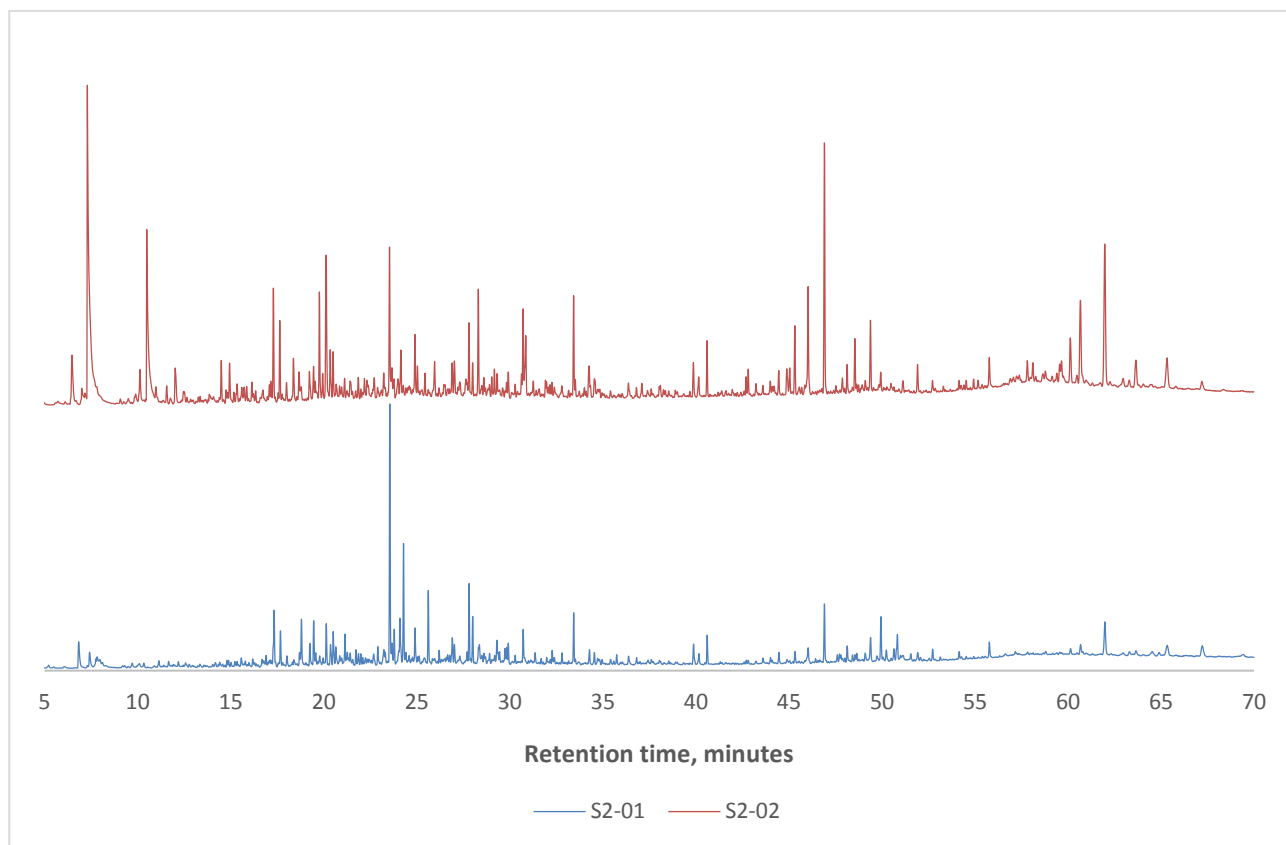
Rt (min)	Chemical name	Intensity	Structure	S1	S1F	Source
27.785	1,2,4-Trimethoxybenzene	a)3 b)2		+	+	lignin
27.8692	1,3-diaza-4-imino-cyclohexane-2,6-dione	2	C <sub>4</sub> H <sub>5</sub> N <sub>3</sub> O <sub>2</sub>	-	+	unknown
27.9717	6-(Methylthio)hex-5-en-3-ol	2		+	-	unknown
27.9933	Methyl 3-(cis-2,3-Epoxybutanoxy)propanoate	3	C <sub>8</sub> H <sub>14</sub> O <sub>4</sub>	-	+	unknown
28.2942	2,3,4-Trimethyllevoglucosan	2		-	+	cellulose
28.4325	2-O-Methyl-D-mannopyranosa	4		-	+	hemicellulose
29.2758	2-Thiophenecarboxylic acid, 4-hydroxy-5-methyl-, ethyl ester	1		+	-	unknown
29.4242	Benzene, 1,2,3-trimethoxy-5-methyl-	2		-	+	lignin
29.5317	4-O-Methylmannose	2		-	+	hemicellulose
29.8050	1,2,3,4-Tetramethoxybenzene	1		+	-	lignin
30.6867	Benzaldehyde, 3,4-dimethoxy-	a)1 b)3		+	+	lignin
31.2350	1,4-Benzenedicarboxylic acid, dimethyl ester	1		+	-	lignin
31.3325	3,7-Dimethyl-2,6-nonadien-1-ol	1		+	-	unknown
31.9525	3,3'-Dimethoxybenzil	1		-	+	lignin
40.1383	9-Hexadecenoic acid, methyl ester, (Z)-	a)1 b)1		+	+	unknown
40.5858	Hexadecanoic acid, methyl ester	1		+	-	unknown



Rt (min)	Chemical name	Intensity	Structure	S1	S1F	Source
43.9850	9-Octadecenoic acid (Z)-, methyl ester	a)1 b)1		+	+	unknown
44.4375	Octadecanoic acid, methyl ester	a)1 b)1		+	+	unknown
46.8783	3-Hexenoic acid, 5-hydroxy-2-methyl-, methyl ester, [r@,R@-(E)]-	1		+	-	unknown
46.9650	1-Phenanthrenecarboxylic acid, 7-ethenyl-1,2,3,4,4a,4b,5,6,7,9,10,10a-dodecahydro-1,4a,7-trimethyl-, methyl ester, [1R-(1à,4aà,4bà,7à,10aà)]-	a)1 b)1		+	+	resin
48.6275	Methyl dehydroabietate	a)2 b)2		+	+	resin
49.4175	Methyl abietate	1		-	+	resin
49.9158	$\alpha$ -Methyl tetramethyl-d-mannoside	1	C <sub>11</sub> H <sub>22</sub> O <sub>6</sub>	+	-	hemicellulose
50.8125	$\alpha$ -D-Mannopyranoside, methyl 2,3,4,6-tetra-O-methyl-	1		-	+	sugar
51.5475	$\alpha$ -Methyl 4-methylmannoside	3	C <sub>8</sub> H <sub>16</sub> O <sub>6</sub>	-	+	sugar
51.6883	15-Hydroxydehydroabietic acid, methyl ester	1		+	-	resin
52.4667	7-Oxodehydroabietic acid, methyl ester	1		+	-	resin
52.8017	$\alpha$ -D-Glucofuranose, 1,2-O-(1-methylethylidene)-	1		-	+	cellulose
54.2558	Tetracosanoic acid, methyl ester	1		+	-	unknown
55.1883	15-Hydroxy-7-oxodehydroabietic acid, methyl ester	a)1 b)1		+	+	resin

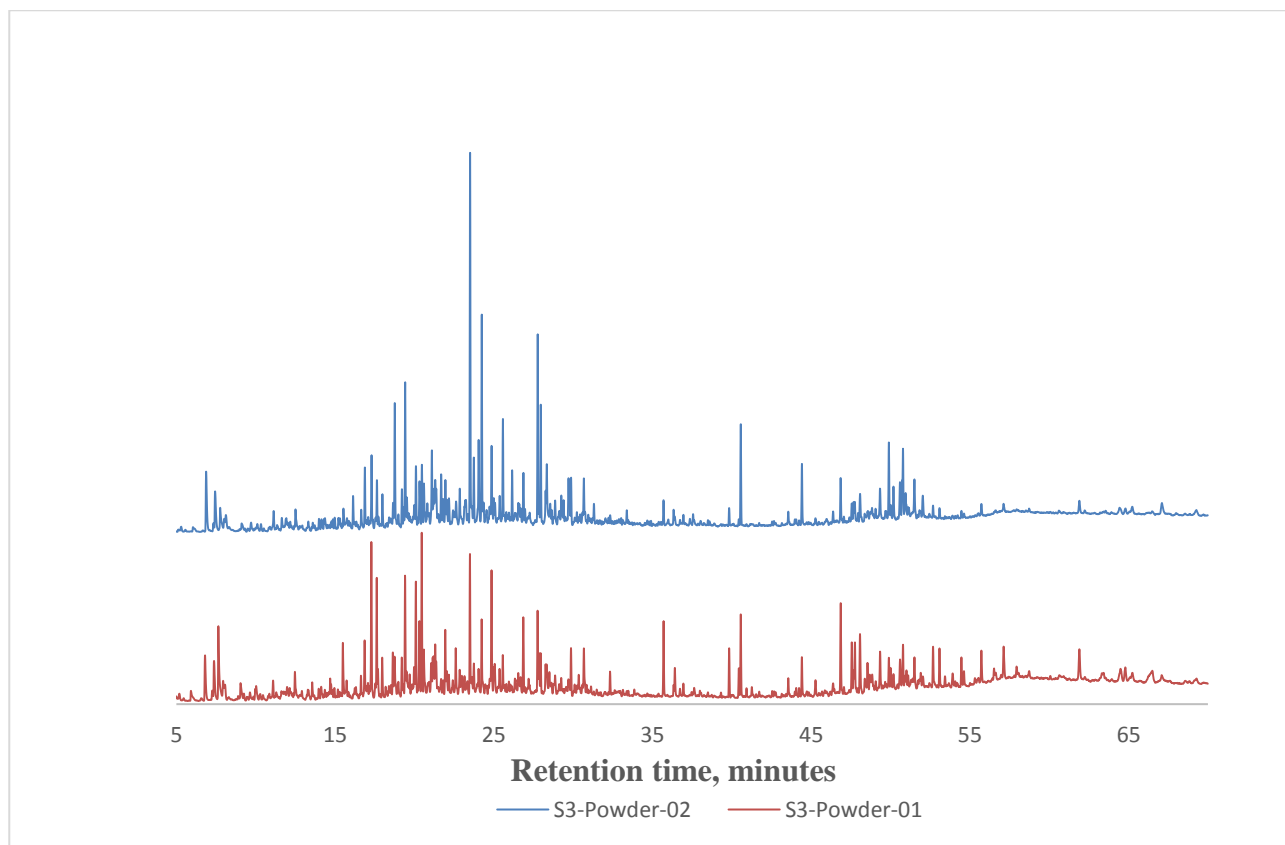
Notes: Intensity with *a* is for S1 and *b* is for S1F, the lowest intensity is with 1 and the highest is with 5; the sign + means that the compound is present in the sample and sign – means that the compound is absent from the sample.

In order to investigate the pyrograms' reproducibility, two samples of an unfoxed area of paper S2 were analyzed (figure 3.20). As it can be seen in the pyrograms the same compounds are released from the samples but the peak areas are different. The lack of reproducibility was initially attributed to heterogeneity of paper S2 and small amounts of sample pyrolyzed.



*Figure 3.20. Py-GC/MS pyrogram of sample S2, Legend: S2-01 and S2-02, sample from the unfoxed area from two different areas of the sample*

Paper S3, dating from 1862, was previously characterized, it was found to be rich in fibers, with a small amounts of paper furnishing materials (Relvas *et al.*, 2014). It is a more homogenous paper with less inorganic compounds, making it a more suitable sample to investigate organic composition and therefore more appropriate to access the reproducibility of the GC signals. Paper S3 was sampled in different foxed and unfoxed areas in order to increase sample size and representativeness. Liquid nitrogen was used to grind the foxed and unfoxed paper samples and, from these larger samples, several sub-samples were removed for pyrolysis in order to evaluate signal reproducibility. In figure 3.21, the pyrograms of two replicates from unfoxed areas are presented (compounds identified in table 3, appendix 3.1), and again we observe that the list of compounds eluting from the column is similar, but the peak areas of all the compounds are different in both chromatograms. The same behavior was found in the foxed area (data not shown).



*Figure 3.21. Py-GC/MS pyrogram of sample S3-powder, Legend: S3-Powder-01 and S3-Powder-02, samples from different unfoxed areas of the paper*

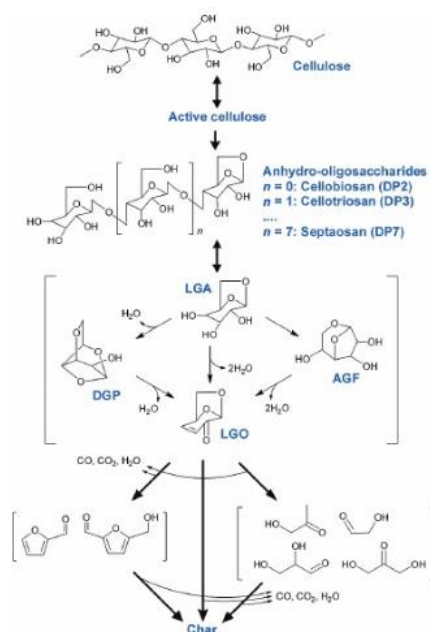
From the experiments done we concluded that we cannot use this analytical technique to evaluate any chemical differences between foxed and unfoxed areas of the papers studied. However, Py-GC/MS can be used to investigate paper composition.

### 3.7.2 Composition of papers using Py-GC/MS

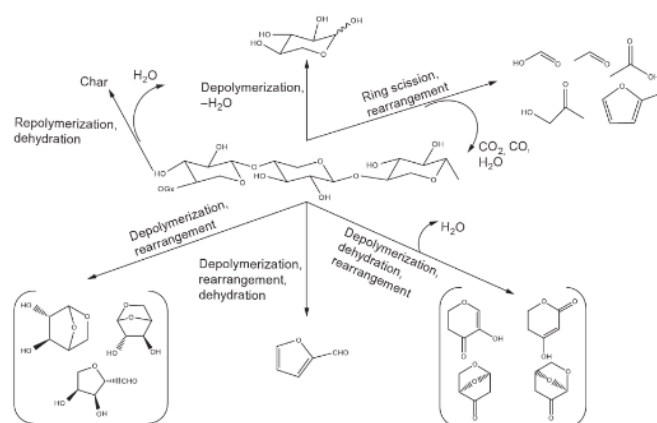
Paper samples, S1, S2, and S3 were already characterized using several analytical techniques (Relvas *et al.*, 2014). For this part of the study we intend to characterize the composition of paper with Py-GC/MS technique.

Pyrolysis of sample S1 originated several products, most of them originating from carbohydrates (table 3.11 in the section 3.7.1). Cellulose, hemicellulose and lignin are components of wood. Unprotected wood is degraded under several environmental conditions, being the presence of water the prerequisite for most degradation processes, due to the strong attraction by the hydrophilic hydroxyl and carboxyl groups (Schwarzingger *et al.*, 2010). The possible pathways of the pyrolysis mechanism of cellulose, hemicellulose and lignin are presented in figure 3.22.

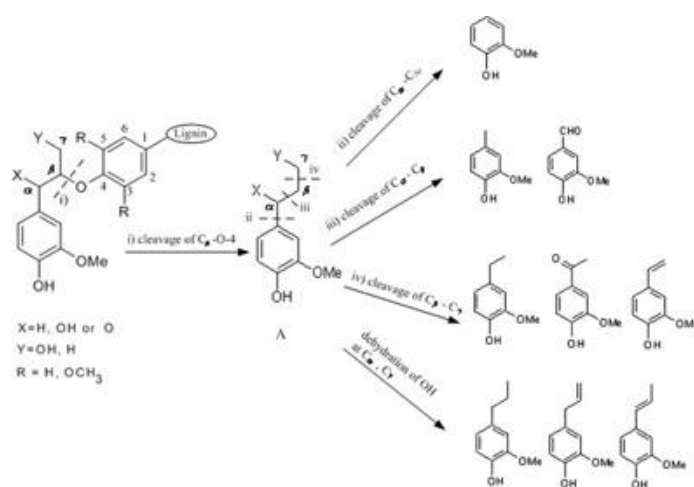
The analysis of the sample S1 also showed typical long chain hydrocarbons pyrolysis products. Pyrolysis products also included many other aromatic derivatives such as, 1,4-dimethoxybenzene, benzaldehyde, 3,4-dimethoxybenzene, 1,2,4-trimethoxybenzene and other aromatic products that are derived from lignin. This suggests that the paper sample consists of a mixture of rag fibers and mechanical wood (Relvas *et al.*, 2014). Several small, often superimposed, peaks of resin-derived compounds can be found, such as 15-hydroxydehydroabietic acid-, methyl ester-; 7-oxodehydroabietic acid-, methyl ester; 15-hydroxy-7-oxodehydroabietic acid-, methyl ester; methyl abietate, and methyl dehydroabietate. The presence of resin had already been identified with FT-IR analysis (Relvas *et al.*, 2014).



### a) Cellulose



### b) Hemicellulose



### c) Lignin

Figure 3.22. Possible pathways of pyrolysis mechanism of cellulose, hemicellulose and lignin (Lin *et al.*, 2009; Gu *et al.*, 2013; Triantafyllidis *et al.*, 2013)

Paper sample S2 was pyrolyzed and the Py-GC/MS analyses revealed the formation of large amounts of carbonyls, such as aldehydes, ketones and acids, furans, such as furfural, and phenols (table 2, appendix 2).

Phenolic compounds such as 3-methoxy- benzoic acid-, methyl ester, 1,2,3-trimethoxy- benzene, 3,5-dimethoxy- phenol-, and 1,2-dimethoxy- benzene were produced by lignin deconstruction.

Lignin is a renewable resource of aromatics in nature, from which high-value aromatic molecules can potentially be obtained. Lignin is a complex, heterogeneous, three-dimensional polymer consisting of an irregular array of differently bonded hydroxyl- and methoxy-substituted phenyl-propane units. (Gu *et al.*, 2013).

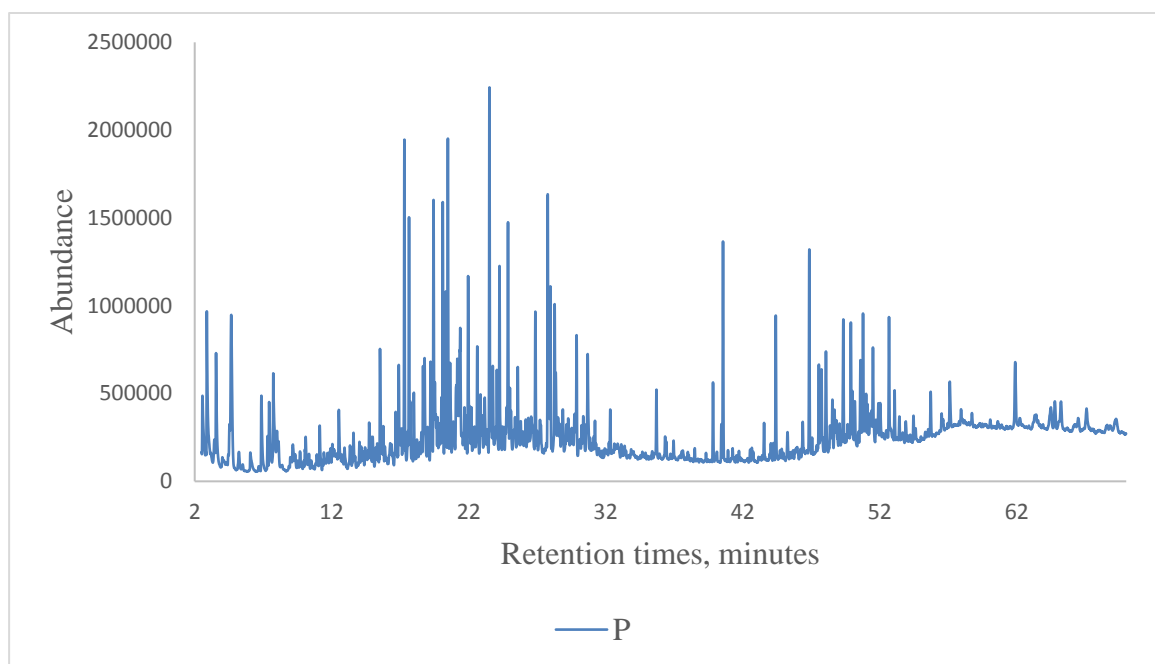
The compounds that were identified from the pyrolysis of the paper sample S3 show the presence of methoxy- acetic acid-, methyl ester, succindialdehyde, furfural and 1,2-cyclopentanedione. Acetic acid is formed in the pyrolysis of carbohydrates which are present in the wood (Schwarzinger *et al.*, 2010). The others products beside acetic acid are also derived from carbohydrates.

Breakdown of glucosidic bonds and rearrangement of cellulose monomer results in the formation of 1,4:3,6-Dianhydro- $\alpha$ -d-glucopyranose, a compound also identified in the sample S3 (Gao *et al.*, 2013).

Compounds such as 3,4-dimethoxy- benzaldehyde, 1,2,3-trimethoxybenzene, 3,5-dimethoxy- phenol, 2-methoxy- phenol and 1,2-dimethoxy- benzene, were formed by lignin deconstruction (table 3.1, appendix3).

Concerning paper sample *P* (figure 3.23), the identified compounds derived mainly from cellulose, such as 2-hydroxy-3-methyl-2-cyclopenten-1-one, 3,5-dimethoxy- cyclopentene, 3-methyl-1,2-cyclopentanedione, fructofuranose, 2,6-anhydro-1,3,4-tri-O-methyl-, 3,4,6-tri-O-methyl-d-glucose;  $\alpha$ -D-mannopyranoside and methyl 2,3,4,6-tetra-O-methyl-. These compound were formed by breaking the molecule bonds between C2 and C3 of glucose monomer and by opening the hemiacetal groups (Gao *et al.*, 2013).

Lignin related pyrolysis products include 2-methoxy- phenol, 1,4-dimethoxy- benzene, 3-methoxy- benzaldehyde, 3,5-dimethoxy- phenol, 2,6-dimethoxy- phenol and also long chain hydrocarbons (table 4.1, appendix 4).



*Figure 3.23. Py-GC/MS pyrogram of sample P*

The products that were identified in paper sample *NB* (figure 3.24) show the presence of carbohydrates such as 3,5-dimethoxy- cyclopentene, 3-ethyl-2-hydroxy-2-cyclopenten-1-one and lignin related pyrolysis products such as 2-methoxy- phenol, 3,5-dimethoxy-phenol, 1,2-dimethoxy- benzene, 1,4-dimethoxy- benzene, 2-methoxy-5-methylphenol, 3,4 dimethoxytoluene, 1,2,4-trimethoxybenzene, 3,4-dimethoxy- benzaldehyde and 1,2-dimethoxy-4-(2methoxyethenyl) benzene. Analysis of the sample also showed the presence of protein derived product, 1-propanamine, the presence of long-chain hydrocarbons and resin-related compounds derived from methyl dehydroabietate (table 5.1, appendix 5). The presence of proteins and resin was also identified during this study with the help of AT-FT-IR analysis.

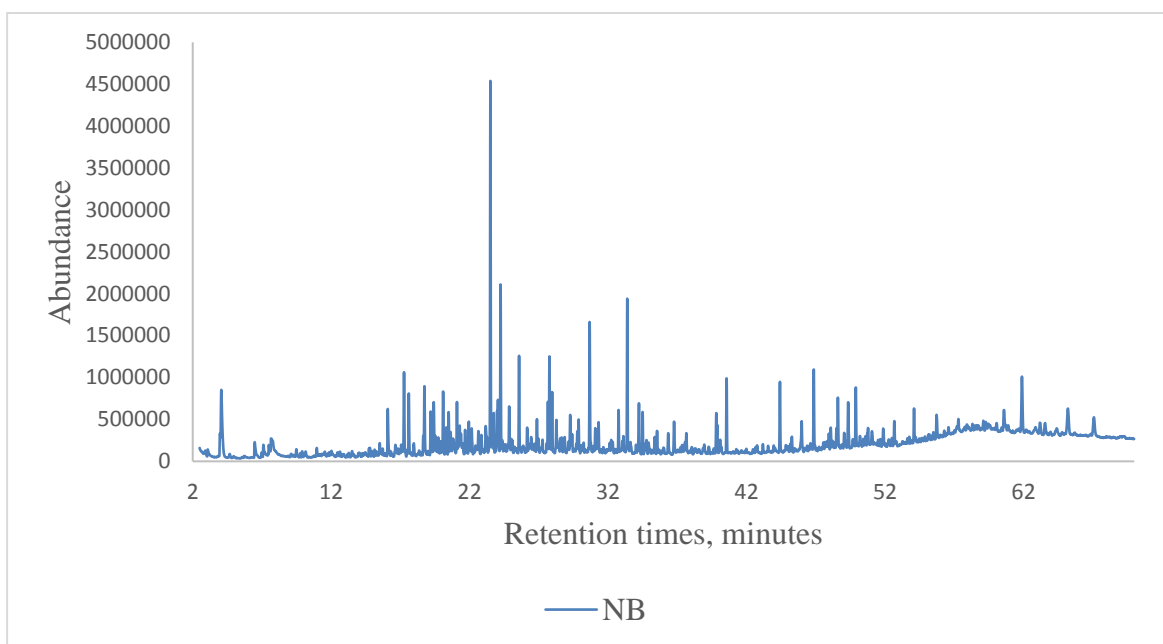


Figure 3.24. Py-GC/MS pyrogram of sample NB

Carbohydrate degradation products such as methyl 2,3,4-tri-O-methyl-  $\alpha$ -D-glucopyranoside and 3-ethyl-2-hydroxy-2-cyclopenten-1-one were identified after pyrolysis of paper sample *OB* (figure 3.25). Some lignin derived pyrolysis products were also identified, such 1,2-dimethoxybenzene, 3,5-dimethoxy- phenol, 2,6-dimethoxy- phenol, 1,2,4-trimethoxybenzene and 4-methoxybenzoic acid-methyl ester. The analysis of the sample also showed the presence of resin-related compounds methyl dehydroabietate, methyl abietate and long-chain hydrocarbons (table 6.1, appendix 6).

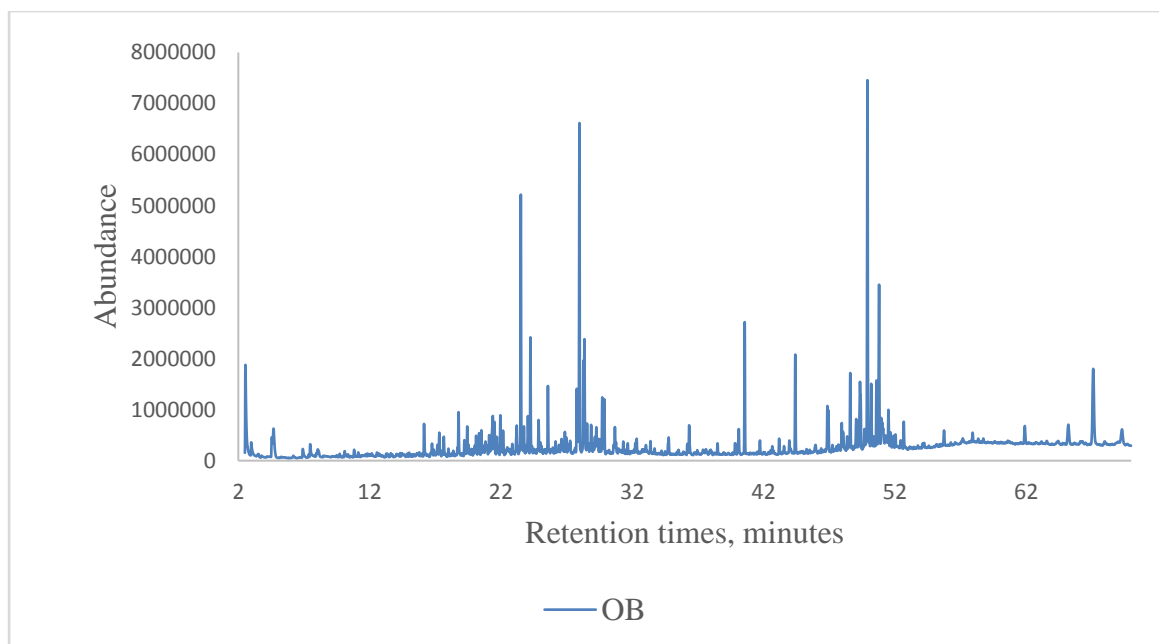


Figure 3.25. Py-GC/MS pyrogram of sample OB



## **4.CONCLUSIONS**

In this work two groups of samples were selected for the study: samples S1, S2 and S3 already characterized by non-destructive techniques in a previous work, and used in this study for development of a methodology to analyze organic compounds by Py-GC/MS used in paper production. The second group of samples, labeled *NB* (new book) dating from 1931, *OB* (old book) dating from 1951 and *P* (print), were collected from stationary shops in Lisbon, from different manufactures. Paper conservator selected the samples by visual observation, based on the color of the foxing stains, and morphology of the papers.

The materials used in production of paper and foxing stains, a type of degradation process, were evaluated for the second group of investigated samples. Detailed investigation of the composition of each paper sample was done based on a non-invasive approach described in the section of materials and methods. The first part focused on the visual and photographic description of paper samples, with the objective to characterize as much as possible. Texture and color of each sample as well as description of size and shape of foxing stains were evaluated by optical microscopy and photography under different illumination.

Images of the unfoxed and foxed areas of paper samples *P*, *NB* and *OB* showed no differences from a morphological point of view. The unfoxed areas do not present disruption of fibers or accumulation of particles. The sample' surface was structurally organized, paper fibers seem to be in good condition, without any visible disturbance. Sample *P* do not present a large amount of fillers contrary to samples *NB* and *OB*.

EDS analyses indicate the presence of different elements such as calcium, aluminum, silicon, potassium, iron, magnesium and phosphorus among others. Basically constituent of paper sample *P* was calcium carbonate and was produced when lime react with atmospheric carbon dioxide, while aluminum silicate is related with papermaking process and intended to assure a more stable physical structure.

AT-FT-IR spectra of the sample *P* showed the presence of amide I and II of a proteinaceous materials used in sizing. Paper sample *NB* has in its composition lignin this suggest that the paper is composed of mechanical wood. The presence of rosin of a resinaceous materials was also observed, rosin was used as a sizing agent for many years. AT-FT-IR analysis noticed the presence of kaolin in paper samples *NB* and *OB*, this was also confirmed by XRD analysis.

$\mu$ -XRD analysis of paper sample *P* showed the presence of cellulose. The presence of others minerals, kaolin and muscovite were observed in paper samples *NB* and *OB*, muscovite was in larger quantities in paper sample *OB*. In the paper sample *OB*, aluminium magnesium hydroxide silicate was also present.

Paper samples were analyzed also with Py-GC/MS, this technique is widely used for characterization of paper. The first group of samples S1 and S2 were pyrolysed in unfoxed and foxed area in order to investigate the difference in composition of foxing stains and unfoxed areas. The analysis shows a variety of products but no significant difference in terms of composition between the unfoxed and foxed area. Sample S2 was analyzed in two replicates from the unfoxed area, the results shown the same compounds but the peak areas are different.

Paper sample S3 is a more homogenous paper with less inorganic compounds, making it a more suitable sample to investigate organic composition. The obtained results show the presence of the same compounds but also in this paper sample as in the paper sample S2 the peak areas are different in both chromatograms.

From the studied papers we concluded that we cannot use this analytical technique to evaluate any chemical difference between foxed and unfoxed areas. However, Py-GC/MS was used to investigate paper composition.

The obtained results of paper sample S1 showed the presence of several products, most of the identified products were from carbohydrates. The presence of typical long chain hydrocarbons pyrolysis products was observed, also products that contain aromatic derivatives that can be from lignin.

Analysis of the paper sample S2 showed the presence of large amounts of carbonyls, such as aldehydes, ketones and acids, furans such as furfural and phenols, and phenolic compounds. Compounds that were identified from the pyrolysis of the paper sample S3 showed the presence of different compounds as acetic acid, methoxy-, methyl ester; succindialdehyde, furfural, 1,2-cyclopentanedione.

Concerning paper sample *P*, the identified compounds derived mainly from cellulose but also other compounds were present as lignin and hydrocarbons.

In the paper sample *NB* and *OB* were identified compounds from carbohydrates, lignin, hydrocarbons, protein and resin.

The combination of several non-destructive techniques allowed the characterization of paper composition and the evaluation of morphological aspects.

## **BIBLIOGRAPHY**

- Abdel-Maksoud, G., 2011. "Analytical techniques used for the evaluation of a 19th century quranic manuscript conditions." *Measurement* 1606–1617.
- Adams, J., 2011. "Analysis of printing and writing papers by using direct analysis." *International Journal of Mass Spectrometry* 301 109–126.
- Ali, M., Emsleyb, A.M., Hermanb, H., Heywooda R.J., 2001. "Spectroscopic studies of the ageing of cellulosic paper." *Polymer* 42 2893-2900.
- Bajpai, Pratima. 2005. *Emerging Technologies in Sizing*. UK: Pira International Ltd.
- Barth, A., 2007. "Infrared spectroscopy of proteins." *Biochimica et Biophysica Acta* 1767 1073–1101.
- Barth, A., Zscherp, Ch., 2002. "What vibrations tell us about proteins." *Quarterly Reviews of Biophysics* 369–430.
- Bazley, K. 1991. "Minerall fillers in paper." *Pap Conservator* 15 15-27.
- Beazley, K. 1991. "Mineral fillers in paper." *Paper Conservator: Journal of the Institute of Paper Conservation* 15(1) 17-27.
- Berns, R. S. 2005. "Color-Accurate Image Archives Using Spectral Imaging." *Scientific Examination of Art: Modern Techniques in Conservation and Analysis, National Academy of Sciences* 105-119.
- Bicchieri, M., Ronconi, S., Romanob, F.P., Pappalardoc, L, Corsid, M., Cristoforettid, G., Legnaiolid, S., Palleschid, V., Salvettid, A., Tognonid E. 2002. "Study of foxing stains on paper by chemical methods, infrared spectroscopy, micro-X-ray fluorescence spectrometry and laser induced breakdown spectroscopy." *Spectrochimica Acta Part B* 57 1235–1249.
- Blumich, B., Anferova, S., Sharma, S., Segre, A.L., and Federicid, C. 2003. "Degradation of historical paper: nondestructive analysis by the NMR-MOUSE." *Journal of Magnetic Resonance* 161 204–209.
- Boruvka, N. 2008. "The Development of Foxing Stains on Samples of Book Paper after Accelerated Ageing." *Canadian Association for Conservation* 33 38-45.
- Bronzato, M., Calvini, P., Federici, C., Bogialli, S., Favaro, G., Meneghetti, M., Mba, M., Brustolon, M., and Zoleo, A. 2013. "Degradation Products from Naturally Aged Paper Leaves of a 16th-Century-Printed Book: A Spectrochemical Study." *Chemistry a European journal* 1.
- Bussière, J.F., Green, R.E., Ruud, C.O. 1991. *Nondestructive Characterization of Materials IV*. New York: Plenum Press.
- Buzio, R., Calvini, P., Ferroni, A., Valbusa, U. 2004. "Surface analysis of paper documents damaged by foxing." *Applied Physics A, Materials Science & Processing* 79 383–387.
- Buzio, R., P. Calvini, A. Ferroni, U. Valbusa. 2004. "Surface analysis of paper documents damaged." *Applied Physics A* 383–387.
- Carr, D. P. 2012. *Assesment of alternative uses for lingocelluostic waste products*. PhD Thesis, Ireland: Nacional University of Ireland.
- Castro, K., Proietti, N., Princi, E., Pessanhad, S., Carvalhod, M.L., Vicini, S., Capitanib, D., Madariagaa, J.M. 2008. "Analysis of a coloured Dutch map from the eighteenth century: The need for a multi-analytical spectroscopic approach using portable instrumentation." *Analytica Chimica Acta* 623 187–194.

- Causin, V., Marega, C., Marigo, A., Casamassima, R., Peluso, G., Ripani, L. 2010. "Forensic differentiation of paper by X-ray diffraction and infrared spectroscopy." *Forensic Science International* 197 70–74.
- Celipa. 1993. *Association of the paper industry*. Accessed June 5, 2016. [www.celipa.pt](http://www.celipa.pt).
- Chamberlain, D. 2007. "Anion mediation of aluminium-catalysed degradation of paper." *Polymer Degradation and Stability* 1417-1420.
- Choi, S. 2007. "Foxing on Paper: A Literature Review." *Journal of the American Institute for Conservation* 64(2) 137-1 52.
- Chu, S., Subrahmanyam, A.V., Hubert, G.W. 2013. "The pyrolysis chemistry of a  $\beta$ -O-4 type oligometric lignin model compound." *Green chemistry* 125-136.
- Conte, A. M., Pulci, O., Knapik, A., Bagniuk, J., Sole, D.R., Lojewska, J., and Missori, M. 2012. "Role of Cellulose Oxidation in the Yellowing of Ancient Paper." *PHYSICAL REVIEW LETTERS* 108.
- Corsaro, C., Mallamace, D., Łojewska, J., Mallamace, F., Pietronero, L., & Missori, M. 2013. "Molecular degradation of ancient documents revealed by  $^1\text{H}$  HR-MAS NMR spectroscopy." *Scientific Reports* 1.
- Cristina, M.A., Cheradame, H. 2011. "Paper aging and degradation: recent findings and research methods." *BioResources* 6(4) 5307-5337.
- Dąbrowski, A., Jon S.G. Simmons. 2003. "Permanence of early European hand made papers." *Fibres and Textile in Western Europe*, 11, 1(40) 8-13.
- Dabrowski, J., Simmons, J. S. G. 2003. "Performance of early European hand-made papers." *Fibres and textile in Eastern Europe* 8-13.
- Daniels, V. D. 1996. "The Chemistry of Paper Conservation." *Chemical Society Reviews* 179-186.
- Derkacheva, O., Sukhov, D. 2008. "Investigation of Lignins by FTIR Spectroscopy." *Macromol. Symp.* 265 61–68.
- Derkacheva, O., Sukhov, D. 2008. "Investigation of Lignins by FTIR Spectroscopy." *Macromol. Symp.* 265 61–68.
- Dutrow, L. B., Clark, M. Ch. 2016. *Geochemical Instrumentation and Analysis*. August 24. Accessed August 30, 2016. [http://serc.carleton.edu/research\\_education/geochemsheets/techniques/XRD.html](http://serc.carleton.edu/research_education/geochemsheets/techniques/XRD.html).
- Enami, K., Sakamoto, S., Okada Y. 2010. "Paper History." *Journal of the International Association of Paper Historians* 14(2).
- Fan, M., Dai, D., and Huang, B. 2012. *Fourier Transform Infrared, Spectroscopy for Natural Fibres*. Rijeka, Croatia: InTech.
- Fellers, Ch. Iversen, T., Lindström, T., Nilsson, Th., Rigdahl, M. 1989. "Ageing/Degradation of papper." Stockholm, 6.
- Ferreira, A., Figueira, F., Pessanha, S., Nielsen, I., and Carvalho, M.L. 2010. "Study of Air-Induced Paper Discolorations by Infrared Spectroscopy, X-ray Fluorescence, and Scanning Electron Microscopy." *APPLIED SPECTROSCOPY* 64(2) 1-5.
- Ferreira, P. J., Gamelas, J. A., Moutinho, I. M., Ferreira, A. G., Go´mez, N., Molleda, C., and Figueiredo M. M. 2009. "Application of FT-IR-ATR Spectroscopy to Evaluate the Penetration of Surface Sizing Agents into the Paper Structure." *Ind. Eng. Chem. Res.* 48, 3867–3872.

- French, A.D. 2014. "Idealized powder diffraction patterns for cellulose." *Cellulose* 21 885–896.
- Gao, N., Li, A., Quan, C., Du, L., Duan, Y. 2013. "TG-FTIR and Py-GC/MS analysis on pyrolysis and combustion of pine sawdust." *Journal of Analytical and Applied pyrolysis* 26-32.
- Garlick, K. 2013. "A Brief Review of the History of Sizing and Resizing Practices." *The American Institute for Conservation, The Book and paper group, annual* 1-5.
- Goltz, D., Attas, M., Young, E.C., Bedynski, M. 2010. "Assessing stains on historical documents using hyperspectral imaging." *Journal of Cultural Heritage* 19–26.
- Gu, C., Ma, X., Li, L., Liu, Ch., Cheng, K., Li, Zh. 2013. "Pyrolysis of polar wood sawdust by TG-FTIR and Py-GC/MS." *Journal of Analytical and Applied Pyrolysis* 16-23.
- Heigenmoser, A., Liebner, F., Windeisen, E., Richter, K. 2013. "Investigation of thermally treated beech (*Fagus sylvatica*) and spruce (*Picea abies*) by means of multifunctional analytical pyrolysis-GC/MS." *Journal of Analytical and Applied Pyrolysis* 117-126.
- Heldt, H. 2005. *Plant Biochemistry*. 3<sup>rd</sup> ed. USA: Elsevier.
- Howell, C., Steenkjaer Hastrup, A.Ch., and Jellison, J. 2007. *The use of X-ray diffraction for analyzing biomodification of crystalline cellulose by wood decay fungi*. Paper prepared for the 38th Annual Meeting Jackson Lake Lodge, Wyoming, USA, Stockholm: IRG SECRETARIAT SE-100 44 Stockholm, Sweden.
- Hundhausen, U., Militz, H., Mai, C. 2009. "Use of alkyl ketene dimer (AKD) for surface modification of particleboard chips." *Eur. J. Wood Prod.* 37–45.
- Ioelovich, M. 2008. "Cellulose as a nanstructured polymer: A short review." *BioSources* 3(4) 1403-1418.
- Jasna, M., Drago K., Aneta B. Fabjan. 2012. "Stabilization of copper- and iron-containing papers in mildly alkaline environment." *Polymer Degradation and Stability* 118-123.
- Jeong, M.J., Dupont, A.L., René E. de la Rie. 2012. "Degradation of cellulose at the wet-dry interface: I- study of the depolymerization." *Cellulose* 19 1135–1147.
- Jeong, M.J., Dupont, A.L., René E. de la Rie. 2014. "Degradation of cellulose at the wet–dry interface. II. Study of oxidation reactions and effect of antioxidants." *Carbohydrate Polymers* 101 671– 683.
- Johansson, A., Lennholm, H. 2000. "Influences of SO and O on the ageing of paper investigated by 2 3." *Applied Surface Science* 161 163-169.
- Jose´ C. del Río, Gutie´rrez, A., Hernando, M., Landi´n, P. 2005. "Determining the influence of eucalypt lignin composition in paper pulp yield using Py-GC/MS." *Journal of Analytical and Applied Pyrolysis* 74 110–115.
- Kavkler, K., A. Desmar. 2012. "Application of FTIR and Raman Spectroscopy to Qualitative Analysis of Structural Changes in Cellulosic Fibres." *Application of FTIR and Raman Spectroscopy to Qualitative* 55 19-31.
- Keheyán, Y. 2008. "PY/GC/MS Analysis of historical papers." *BioResources* 829-837.
- Keheyán, Y., G. Eliazán, P. Engel, B. Rittmeier. 2009. "Py/GC/MS characterisation of naturally and artificially aged inks and papers." *Journal of Analytical and Applied Pyrolysis* 86 192-199.
- Kiuberis, J., Stasys Tautkus, Rolandas Kazlauskas, Irma Pakutinskiene, Aivaras Kareiva. 2005. "Protective coating for paper: new development." *Journal of Cultural Heritage* 6 245–251.

- Klemm, D., Brigitte Heublien, Hans-Peter Fink and Andreas Bohn. 2005. "Cellulose: Fascinating Biopolymer and Sustainable Raw Material." *Angewante Chemie* 44 3358-3393.
- Kolbe, G. 2004. "Gelatine in Historical Paper Production and as Inhibiting Agent for Iron-Gall Ink Corrosion on Paper." *Restaurator* 25(1) 26-39.
- Kong, J., Yu, Sh. 2007. "Fourier Transform Infrared Spectroscopic Analysis of Protein Secondary Structures." *Acta Biochimica et Biophysica Sinica* 39(8) 549–559.
- Laguardia, L., E. Vassallo, F. Cappitelli, E. Mesto. 2005. "Investigation of the effects of plasma treatments on biodetoried ancient paper." *Applied Surface Science* 252 1159–1166.
- Leng, Y. 2008. *Materials characterization: Introduction to microscopic and spectroscopic methods*. Singapore: John Wiley & Sons (Asia) Pte Ltd, 2 Clementi Loop.
- Lichtblau, D., M. Strlic, T. Trafela, J. Kolar, M. Anders. 2008. "Determination of mechanical properties of historical paper based on NIR spectroscopy and chemometrics – a new instrument." *Applied Physics A, Materials Science & Processing* 92 191–195.
- Lin, L.D., Ching-Min Hsieh, Been-Huang Chiang, Ming-Jer Tsai. 2006. "Modified atmosphere and humidity packages for conservation of paper antiques." *The Japan Wood Research Society* 121–126.
- Lin, Y.CH., Cho, J., Tompsett, A.G., Westmoreland, R.Ph., Huber, W.G. 2009. "Kinetics and mechanism of cellulose pyrolysis." *Journal Phys. Chem. C*, 113 (46) 20097-20107.
- Lindström, T., Larsson, T. 2008. "Alkyl Ketene Dimer (AKD) sizing – a review." *Pulp and Paper Research Journal* 202-209.
- Lisperguer, J., Patricio Perez, Silvio Urizar. 2009. "Structure and thermal properties of lignins: characterization by Infrared Spectroscopy and differential scanning calorimetry." *J. Chil. Chem. Soc.* 54(4) 460-464.
- Łojewska, J., P. Miśkowiec, T. Łojewski, L.M. Proniewicz. 2005. "Cellulose oxidative and hydrolytic degradation: In situ FTIR approach." *Polymer Degradation and Stability* 88 512-520.
- Malešič, J., D. Kočar, and A. Fabjan. 2012. *Polym. Degrad. Stab.* 97 118-123.
- Manso, M., Carvalho, M.L. 2009. "Application of spectroscopic techniques for the study of paper documents: A survey." *Spectrochimica Acta Part B* 64 482–490.
- Manso, M., Carvalho, M.L., Queralt, I., Vicini, S., and Princi, E. 2011. "Investigation of the Composition of Historical and Modern Italian Papers by Energy Dispersive X-ray Fluorescence (EDXRF), X-ray Diffraction (XRD), and Scanning Electron Microscopy Energy Dispersive Spectrometry (SEM-EDS)." *APPLIED SPECTROSCOPY* 65(1) 52-59.
- Manso, M., Costa, M., Carvalho, M.L. 2008. "Comparison of elemental content on modern and ancient papers by EDXRF." *Applied Physics A* 90, *Materials Science & Processing* 43–48.
- Manso, M., Pessanha, S., Carvalho, M.L. 2006. "Artificial aging processes in modern papers: X-ray spectrometry studies." *Spectrochimica Acta Part B* 61 922–928.
- Manso, M., Pessanha, S., Figueira, F., Valadas, S., Guilherme, A., Afonso, M., Rocha, A.C., Oliveira, J., Ribeiro, I., Carvalho, M.L. 2009. "Characterisation of foxing stains in eighteenth to nineteenth century drawings using non-destructive techniques." *Anal Bioanal Chem* 395 2029–2036.



- Manturovskaya, N.V., N.L. Rebikova. 2000. "Foxing, A New Approach to an Old Problem." *Restaurator* 85–100.
- Matija Strlič, Tanja Trafela, Dirk Lichtblau, Jana Kolar. 2008. *NIR SPECTROSCOPY AND CHEMOMETRICS FOR NON-DESTRUCTIVE CHARACTERISATION OF HISTORICAL PAPER*. Jerusalem Israel: 9th International Conference on NDT of Art.
- Mauro Missori, Marcofabio Righini, Anne-Laurence Dupont. 2006. "Gelatin sizing and discoloration: A comparative study of optical spectra obtained from ancient and artificially aged modern papers." *Optics Communications* 289–294.
- Missori, M. Righini, M.S. Storace, A. Congiu Castellano, S. Selci. 2005. "OPTICAL SPECTROSCOPY AS A TOOL FOR THE STUDY OF DEGRADATION PROCESSES IN ANCIENT AND MODERN PAPERS." *MIP meeting, Rome (Italy), February 17-20* 1-2.
- Missori, M., Righini, M., Selci, S. 2004. "Optical reflectance spectroscopy of ancient papers with discoloration or foxing." *Optics Communications* 231 99–106.
- Murphy, D., B. & Davidson, M., W. 2012. *Fundamentals of light microscopy and electron imaging, 2nd edition*. New Jersey: NJ: John Wiley & Sons.
- Odermatt, J., Meier, D., Leicht, K., Meyer, R., Runge, T. 2003. "Approaches to applying internal standards for quantification of paper additives by Py-GC/MS." *J.Anal.App. Pyrolysis* 269-285.
- Oh, S.Y., Yoo, Il D., Shin, Y., Kim, H. Ch., Kim, H.Y., Chung, Y. S., Parkd, W.H., and Youke, H.J. 2005. "Crystalline structure analysis of cellulose treated with sodium hydroxide and carbon dioxide by means of X-ray diffraction and FTIR spectroscopy." *Carbohydrate Research* 340 2376–2391.
- Ormsby, M, Barrett., T, Lang,, J.B, Mazurek., J, and Schilling., M. 2011. *ESTIMATION OF GELATIN CONTENT IN HISTORICAL PAPERS USING NIR SPECTROSCOPY*. Article, e-Preservation Science.
- Pandian, M. S. 2014. "X-ray Diffraction Analysis: Principle, Instrument and Applications." 2010, Volume 14, Issue 2. "Paper history." *Journal of the International Association of Paper Historians*.
- Park, S., Baker, J.O., Himmel, M.E., Parilla, Ph. A., and Johnson, D.K. 2010. "Cellulose crystallinity index: measurement techniques and their impact on interpreting cellulase performance." *Biotechnology for Biofuels* 1-10.
- Park, S., John O. Baker, Michael E. Himmel, Philip A. Parilla and David K. Johnson. 2010. "Ceseealrlcuh lose crystallinity index: measurement techniques and their impact on interpreting cellulase performance." *Park et al. Biotechnology for Biofuels* 2-10.
- Pe´rez, J., Mun˜oz-Dorado, J., Rubia, de la T., Martı´nez, J. 2002. "Biodegradation and biological treatments of cellulose, hemicellulose and lignin: an overview." *Int Microbiol* 5 53–63.
- Peters, D. 2000. "An alternative to foxing? Oxidative degradation as a cause of cellulosic discolouration." *Restaurierung* 801-806.
- Pinzari, F., G. Pasquariello, and A. Mico. 2006. "macromolecules in cultural heritage." *Macromol. Symp.* 238 57-66.
- Porck, H.J. 2000. *Rate of Paper Degradation, The Predictive Value of Artificial Aging Tests*. Amsterdam: European Commission on Preservation and Access.

- Proniewicz, L.M., Paluszkiewicz, C., Birczyńska, W. A., Majcherczyk, H., Barański, A., Konieczna, A. 2001. "FT-IR and FT-Raman study of hydrothermally degraded cellulose." *Journal of Molecular Structure* 596 163-169.
- Proniewicz, L.M., Paluszkiewicz, C., Birczyńska, W.A., Majcherczyk, H., Barański, A., Dutka, D. 2002. "FT-IR and FT-Raman study of hydrothermally degraded groundwood containing paper." *Journal of Molecular Structure* 614 345–353.
- Rakotonirainy, M.S., Benaud, O., Vilmont, L.B. 2015. "Contribution to the characterization of foxing stains on printed books using infrared spectroscopy and scanning electron microscopy energy dispersive spectrometry." *International Biodeterioration & Biodegradation* 101 1-7.
- Ratanakhanokchai, K., Waeonukul, R., Pason, P., Tachaapaikoon, Ch., Lay Kyu, K., Sakka, K., Kosugi, A., and Mori, Y. 2013. *Paenibacillus curdlanolyticus* Strain B-6 Multienzyme Complex: A Novel System for Biomass Utilization. Ratanakhanokchai.
- Reis, M. 2009. *The history of paper*. June 5. Accessed June 5, 2016. <http://naturlink.sapo.pt/Natureza-e-Ambiente/Interessante/content/A-historia-dopapel>.
- Relvas C., M. Nunes, M. Santo, P. Mourinha, A.T. Caldeira, T. Ferreira, F. Figueira. 2014. "Characterization of old paper samples exhibiting foxing." *Science, Technology and Cultural Heritage*. Sevilla, Spain: CRC Press, Taylor and Francis Group, London, UK. 243-249.
- Russa, M.F.L., Ruffolo, A.S., Barone, G., Crisci, M.G., Mazzoleni, P., and Pezzino, A. 2009. "The Use of FTIR and Micro-FTIR Spectroscopy: An Example of Application to Cultural Heritage." *International Journal of Spectroscopy* 1-5.
- Saikia, B.J., Parthasarathy, G. 2010. "Fourier Transform Infrared Spectroscopic Characterization of Kaolinite from Assam and Meghalaya, Northeastern India." *J. Mod. Phys.*, 1, 206-210.
- Schwarzinger, C., List M. 2010. "Identification of marker compound in pyrolysis-GC/MS of various acetylated wood types." *Journal of analytical and applied pyrolysis* 144-153.
- Šelih, V., M. Strlič, J. Kolar, and B. Pihlar. 2007. *Polym. Degrad. Stabil.* 92 1476-1481.
- Sengeputa, P. Borthakur, P.C. Saikia and P.C. 2008. "SEM-EDS characterization of an iron-rich kaolinite clay." *Journal of Scientific & Industrial Research* 67 812-818.
- Skoog, D. A., Holler, F. J. & Nieman, T. A. 1998. *Principles of Instrumental Analysis, 5th edition*. Philadelphia: Harcourt Brace & Company. pp. 420-421.
- Song, X., Chen, F., and Liu, F. 2012. "Study on the reaction of alkyl ketene dimer (AKD) and cellulose fibre." *Bioresources* 7(1) 652-662.
- Souguir, Z., Anne-Laurence Dupont, E. René de la Rie. 2008. "Formation of Brown Lines in Paper: Characterization of Cellulose Degradation at the Wet-Dry Interface." *Biomacromolecules* 9 2546–2552.
- Stewart, C.D. n.d. "PYROLYSIS-GC/MS AS A METHOD FOR QUALITY AND MANUFACTURING CONTROL." *Chemist III, Intertape Polymer Group, Marysville, MI*.
- Strlič, M., Cassar, M. 2008. "NIR/Chemometrics approach to characterisation of historical paper and surveying of paper-based collections." *ICOM COMMITTEE FOR CONSERVATION* 293-300.
- Strlič, M., Kolar, J., and Lichtblau, D. 2007. "The SurveNIR project- a dedicated near infrared instrument for paper characterization." *Museum Microclimates, National Museum of Denmark* 81-84.

- Strlič, M., Kolar, J., Scholten, S. 2005. "Paper and durability." In *Ageing and stabilisation of paper*, by Jana Kolar Matija Strlič, 3-8. Ljubljana: National and University Library Ljubljana.
- Stuart, B. H. 2007. *Analytical techniques in materials conservation*. John Wiley & Sons Ltd. The Atrium, Southern Gate, Chichester, West Sussex. pp. 91-94.
- Triantafyllidis, S.K., Lappas, A.A., Stöcker, M. 2013. *The role of catalysis for sustainable production of bio-fuels and bio-chemicals*. Oxford, UK: Elsevier B.V.
- Udriștioiu, F.M., Andrei A. BUNACIU, Hassan Y. ABOUL-ENEIN, I. Gh. 2012. "Application of Micro-Raman and FT - IR Spectroscopy in Forensic Analysis of Questioned Documents." *Gazi University Journal of Science* 25(2) 371-375.
- Valerio Causin, Carla Marega, Antonio Marigo, Rosario Casamassima, Giuseppe Peluso, Luigi Ripani. 2010. "Forensic differentiation of paper by X-ray diffraction and infrared spectroscopy." *Forensic Science International* 197 70–74.
- Vohrer, U., Tricka, I., Bernhardt, J., Oehra, C., Brunner, H. 2001. "Plasma treatment an increasing technology for paper restoration?" *Surface and Coatings Technology* 142-144 1069-1073.
- Watkins, D., Nuruddin, M., Hosur, M., Tcherbi-Narteh, A., Jeelani, Sh. 2015. "Extraction and characterization of lignin from different biomass resources." *Journal of Materials Research and Technology* 26–32.
- Weinstock, I.A., Atalla, R.H., Agarwal, U.P., and Minor, J.L. 1993. "Fourier transform Raman spectroscopic studies of a novel wood pulp bleaching system." *Spectrochimica Acta* 819-829.
- Williams, R. 2006. *The invention of the paper*. Accessed June 5, 2016.  
[http://www.ipst.gatech.edu/amp/collection/museum\\_invention\\_paper.htm](http://www.ipst.gatech.edu/amp/collection/museum_invention_paper.htm).
- Wilson, I. 2006. "Filler and Coating Pigments for Papermakers, Filler and extender uses." *Industrial and minerals* 1287-1300.
- Xiaoa, B., Suna, X.F., Sunb, R.C. 2001. "Chemical, structural, and thermal characterizations of alkali-soluble lignins and hemicelluloses, and cellulose from maize stems, rye straw, and rice straw." *Polymer Degradation and Stability* 74 307–319.
- Zou, X., Gurnagul, N., Uesaka, T., Bouchard, J. 1994. "Accelerated aging of papers of pure cellulose: mechanism of cellulose degradation and paper embrittlement." *Polymer Degradation and Stability* 393-402.

## **APPENDIX**

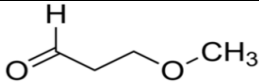

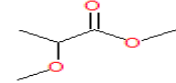
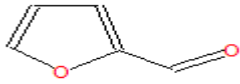
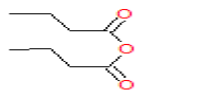
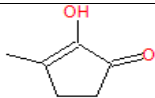
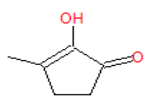
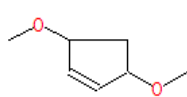
## Appendix 1. Micro-X-ray diffraction

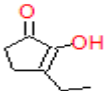
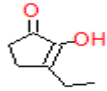
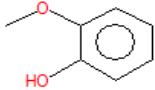
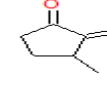
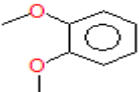
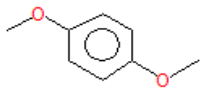
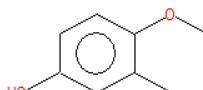
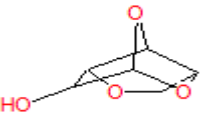
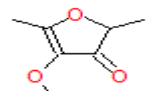
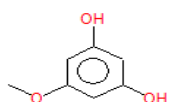
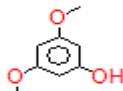
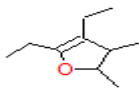
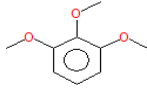
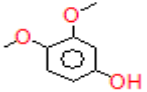
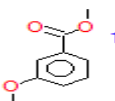
Table 1.1 Present the diffraction peak list identified for the paper samples P, NB, OB

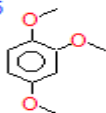
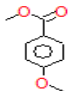
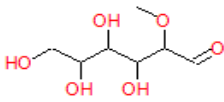
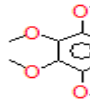
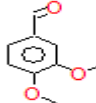
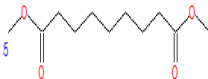
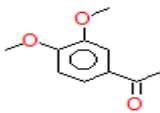
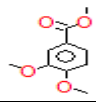
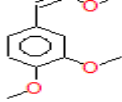
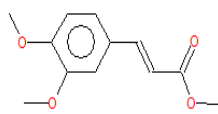
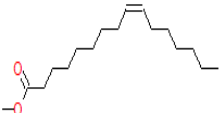
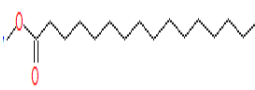
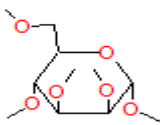
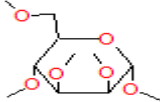
Diffraction peaks			
Compound name/ Sample	P	NB	OB
	Pos. (°2Th.)	Pos. (°2Th.)	Pos. (°2Th.)
Cellulose	14.988 16.487 22.782	14.988 16.487 22.782	22.782
Kaolinite		12.365 24.877 38.303	12.365 24.877 38.303
Muscovite		8.844 26.641	8.844 26.749 28.758 31.036
Aluminium Magnesium Hydroxide Silicate			18.784

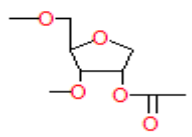
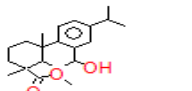
## Appendix 2. Py-GC/MS

Table 2.1 with the compounds that are present in foxing stains and unfoxed area of the sample S2

Rt (min)	Chemical name	Intensity	Structure	S2	S2F	Source
2.7533	>Methoxypropionaldehyde	1		+	-	unknown
3.4642	>Succindialdehyde	1		+	-	unknown
4.3992	>Propanoic acid, 2-methoxy-, methyl ester	1		+	-	sugar
5.9658	>Furfural	1		-	+	cellulose
15.9425	>Butanoic acid, anhydride	1		-	+	unknown
16.8775	>2-Cyclopenten-1-one, 2-hydroxy-3-methyl-	1		+	-	cellulose
16.7317	>2-Cyclopenten-1-one, 2-hydroxy-3-methyl-	1		-	+	cellulose
17.64	>Cyclopentene, 3,5-dimethoxy-	1		+	-	cellulose

Rt (min)	Chemical name	Intensity	Structure	S2	S2F	Source
18.6708	>2-Cyclopenten-1-one, 3-ethyl-2-hydroxy-	2		-	+	cellulose
18.7683	>2-Cyclopenten-1-one, 3-ethyl-2-hydroxy-	2		+	-	cellulose
19.1358	>Phenol, 2-methoxy-	2		-	+	lignin
19.4258	>2-Cyclopenten-1-one, 2-hydroxy-3-methyl-	a)2 b)2		+	+	cellulose
21.1117	>Benzene, 1,2-dimethoxy-	a)1 b)1		+	+	lignin
21.6675	>Benzene, 1,4-dimethoxy-	1		-	+	lignin
22.1808	>Creosol	1		-	+	lignin
23.1642	>1,4:3,6-Dianhydro-α-d-glucopyranose	1		-	+	cellulose
23.5325	3(2H)-Furanone, 4-methoxy-2,5-dimethyl-	4		+	-	cellulose
23.7592	Flamenol	2		-	+	lignin
24.2708	>Phenol, 3,5-dimethoxy-	a)3 (74) b)3 (74)		+	+	lignin
25.5975	Furan, 4,5-diethyl-2,3-dihydro-2,3-dimethyl-	3		+	-	cellulose
26.1733	>Benzene, 1,2,3-trimethoxy-	1		-	+	lignin
26.8892	>Phenol, 3,4-dimethoxy-	a)1 b)1		+	+	lignin
26.9883	>Benzoic acid, 3-methoxy-, methyl ester	1		+	-	lignin

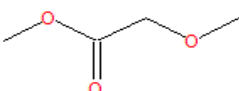

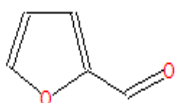
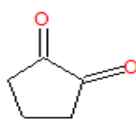
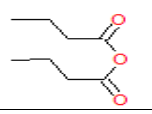
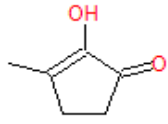
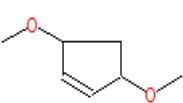
Rt (min)	Chemical name	Intensity	Structure	S2	S2F	Source
27.7917	>1,2,4-Trimethoxybenzene	a)3 b)3		+	+	lignin
27.98	>Benzoic acid, 2-methoxy-, methyl ester	3		-	+	lignin
28.4308	>2-O-Methyl-D-mannopyranosa	3		-	+	hemicellulose
29.805	>1,2,3,4-Tetramethoxybenzene	a)2 b)3		+	+	lignin
30.685	>Benzaldehyde, 3,4-dimethoxy-	a)2 b)3		+	+	lignin
32.2492	>Nonanedioic acid, dimethyl ester	1		+	-	unknown
32.7733	>Ethanone, 1-(3,4-dimethoxyphenyl)-	1		+	-	lignin
33.4067	>Benzoic acid, 3,4-dimethoxy-, methyl ester	a)2 b)3		+	+	lignin
34.2542	>1,2-Dimethoxy-4-(2-methoxyethenyl)benzene	1		+	-	lignin
34.515	>1,2-Dimethoxy-4-(2-methoxyethenyl)benzene	1		+	-	lignin
39.8325	>2-Propenoic acid, 3-(3,4-dimethoxyphenyl)-, methyl ester	1		+	-	lignin
40.1417	>9-Hexadecenoic acid, methyl ester, (Z)-	1		-	+	unknown
40.5892	>Hexadecanoic acid, methyl ester	1		-	+	unknown
49.9275	$\alpha$ -D-Mannopyranoside, methyl 2,3,4,6-tetra-O-methyl-	a)2 b)2		+	+	hemicellulose
50.8258	$\alpha$ -D-Mannopyranoside, methyl 2,3,4,6-tetra-O-methyl-	3		-	+	hemicellulose

51.2033	2-O-Acetyl-1,4-anhydro-3,5-di-O-methyl-D-ribitol	2		-	+	hemicellulose
51.5842	Methyl 7β-hydroxyabieta-8,11,13-trien-18-oate	2		-	+	resin

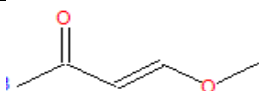
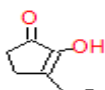
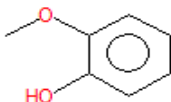
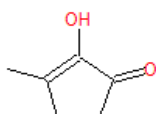
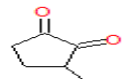
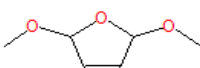
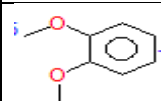
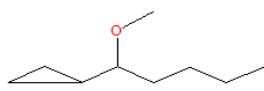
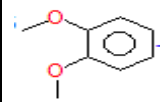
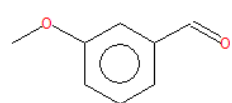
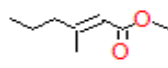
Note: Intensity with a is for S2 and b is for S2F, the lowest intensity is with 1 and the highest is with 3; the sign + means that the compound is present in the sample and sign – means that the compound is absent from the sample

### Appendix 3. Py-GC/MS

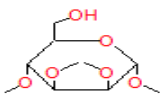
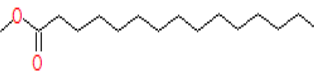
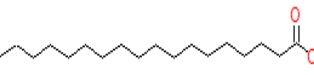
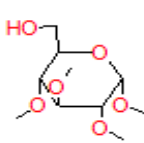
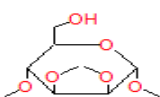
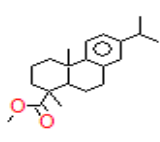
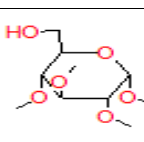
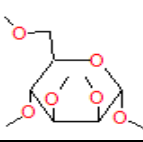
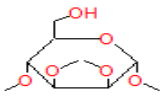
Table 3.1 with the compounds that are present in the unfoxed area of the powder sample S3

Table 3. Compounds that are present in the unfoxed area of the powder sample S3						
Rt (min)	Chemical name	Intensity	Structure	S3-Powder TMAH -01	S3-Powder TMAH -02	Source
2.5708	Acetic acid, methoxy-, methyl ester	2		-	+	sugar
2.8175	Methoxypropionaldehyde	1		+	-	sugar
3.4925	Succindialdehyde	1		+	-	unknown
3.6200	Succindialdehyde	2		-	+	unknown
7.3708	Furfural	1		+	-	cellulose
7.4408	Furfural	1		-	+	cellulose
12.4700	1,2-Cyclopentanedione	1		+	-	cellulose
16.1342	Butanoic acid, anhydride	1		-	+	unknown
16.8608	2-Cyclopenten-1-one, 2-hydroxy-3-methyl-	a)1 b)1		+	+	hemicellulose
17.2858	Cyclopentene, 3,5-dimethoxy-	a)5 b)1		+	+	cellulose
17.6242	Cyclopentene, 3,5-dimethoxy-	a)4(78) b)1(79)		+	+	cellulose



Rt (min)	Chemical name	Intensity	Structure	S3-Powder TMAH -01	S3-Powder TMAH -02	Source
18.6367	4-methoxy-3-buten-2-one	1		+	-	cellulose
18.7617	2-Cyclopenten-1-one, 3-ethyl-2-hydroxy-	2		-	+	cellulose
19.2042	Phenol, 2-methoxy-	1		+	-	lignin
19.4075	2-Cyclopenten-1-one, 2-hydroxy-3-methyl-	4		+	-	cellulose
19.4158	1,2-Cyclopentanedione, 3-methyl-	2		-	+	cellulose
20.0833	5-Methoxy-pent-4-enoic acid, methyl ester	4(72)		+	-	unknown
20.3133	5-Methoxy-pent-4-enoic acid, methyl ester	3(71)		+	-	unknown
21.0492	Furan, 2,5-dihydro-2,5-dimethoxy-	1		+	-	cellulose
21.0983	Benzene, 1,2-dimethoxy-	1		-	+	lignin
21.1508	3-METHOXY-2(5H)-FURANONE	1		+	-	cellulose
21.2083	1-Methoxy-1-cyclopropylpentane	1		+	-	unknown
21.6933	Benzene, 1,4-dimethoxy-	1		-	+	lignin
21.9417	4-Methoxy-methyl-hex-2-yn-1-ol	3		+	-	unknown
22.6017	(S)-4-Hexanolide	2		+	-	unknown
22.8525	Benzaldehyde, 3-methoxy-	a)1 b)1		+	+	lignin
23.4950	2-Hexenoic acid, 3-methyl-, methyl ester	4		+	-	unknown

Rt (min)	Chemical name	Intensity	Structure	S3-Powder TMAH -01	S3-Powder TMAH -02	Source
23.5083	3(2H)-Furanone, 4-methoxy-2,5-dimethyl-	4		-	+	hemicellulose
24.2350	Phenol, 3,5-dimethoxy-	a)3 b)3		+	+	lignin
24.8575	1,3-Dioxane	a)4 b)2		+	+	unknown
25.5742	Phenol, 2,6-dimethoxy-	2		-	+	lignin
26.1575	1,2,3-Trimethoxybenzene	1		-	+	lignin
26.8642	Phenol, 2,6-dimethoxy-	3		+	-	lignin
26.8675	Phenol, 3,4-dimethoxy-	1		-	+	lignin
27.7600	1,2,4-Trimethoxybenzene	a)3 b)3		+	+	lignin
27.8392	1,3-diaza-4-imino-cyclohexane-2,6-dione	1		+	-	unknown
29.7833	1,2,3,4-Tetramethoxybenzene	1		-	+	lignin
30.6658	Benzaldehyde, 3,4-dimethoxy-	1		-	+	lignin
30.6800	2,4-Hexadienedioic acid, dimethyl ester, (E,E)-	1		+	-	unknown
35.6983	$\alpha$ -D-Mannopyranoside, methyl 2,3,4,6-tetra-O-methyl-	3		+	-	cellulose
36.4092	Methyl-2-O-methyl- $\alpha$ -D-glucopyranoside	1		+	-	cellulose

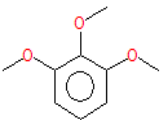
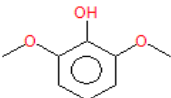
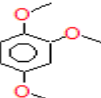
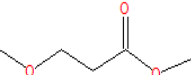
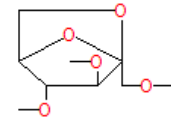
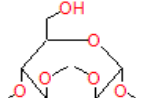
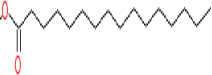
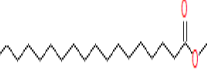
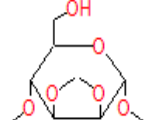


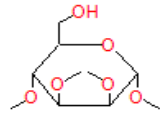
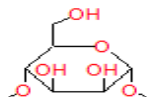
Rt (min)	Chemical name	Intensity	Structure	S3-Powder TMAH -01	S3-Powder TMAH -02	Source
39.8317	1,2,3,4-Tetramethylmannose	2		+	-	cellulose
40.5608	Hexadecanoic acid, methyl ester	a)3 b)2		+	+	unknown
44.4117	Methyl stearate	a)2 b)2		+	+	unknown
46.8608	$\alpha$ -D-Glucopyranoside, methyl 2,3,4-tri-O-methyl-	a)3 b)2		+	+	cellulose
47.7567	1,2,3,4-Tetramethylmannose	2		+	-	cellulose
48.5992	1-Phenanthrenecarboxylic acid, 1,2,3,4,4a,9,10,10a-octahydro-1,4-dimethyl-7-(1-methylethyl)-, methyl ester, [1R-(1 $\alpha$ ,4 $\alpha$ ,10 $\alpha$ )]-	1		+	-	resin
49.8950	$\alpha$ -D-Glucopyranoside, methyl 2,3,4-tri-O-methyl-	a)2 b)2		+	+	cellulose
50.1867	$\alpha$ -D-Mannopyranoside, methyl 2,3,4,6-tetra-O-methyl-	1		-	+	cellulose
50.5933	$\alpha$ -D-Mannopyranoside, methyl 2,3,4,6-tetra-O-methyl-	2		+	-	cellulose
50.7850	$\alpha$ -D-Mannopyranoside, methyl 2,3,4,6-tetra-O-methyl-	a)3 b)2		+	+	cellulose
53.0842	$\alpha$ -D-Mannopyranoside, methyl 2,3,4,6-tetra-O-methyl-	2		+	-	cellulose
54.4650	1,2,3,4-Tetramethylmannose	2		+	-	cellulose

Note: Intensity with a is for S3-P-TMAH-01 and b is for S3-P-TMAH-02, the lowest intensity is with 1 and the highest is with 5; the sign + means that the compound is present in the sample and sign – means that the compound is absent from the sample

#### Appendix 4. Py-GC/MS

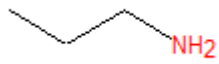
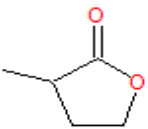
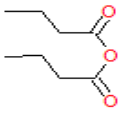
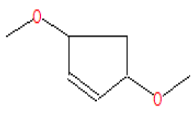
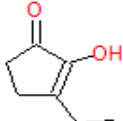
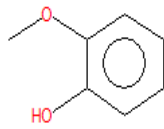
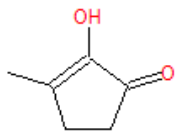
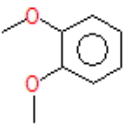
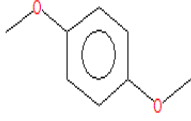
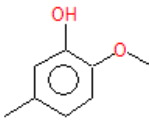
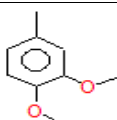
Table 4.1 with the compounds that are present in the paper sample P

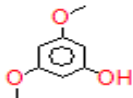
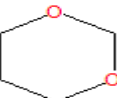
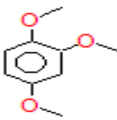
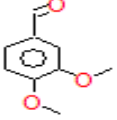
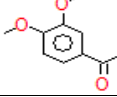
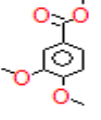
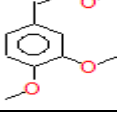
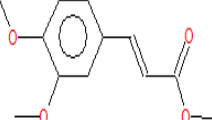
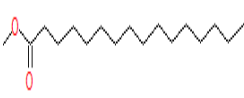
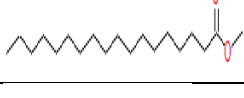
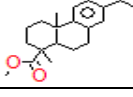
Rt(time)	Chemical name	Intensity	Structure	Source
2.5633	Acetic acid, methoxy-, methyl ester	1		sugar
2.8842	Methoxypropionaldehyde	2		
3.5567	Succindialdehyde	2		unknown
16.8958	2-Cyclopenten-1-one, 2-hydroxy-3-methyl-	1		cellulose
17.3067	Cyclopentene, 3,5-dimethoxy-	4		cellulose
17.6450	Cyclopentene, 3,5-dimethoxy-	3		cellulose
19.2167	Phenol, 2-methoxy-	2		lignin
19.4308	1,2-Cyclopentanedione, 3-methyl-	3		cellulose
21.6983	Benzene, 1,4-dimethoxy-	1		lignin
22.6258	(S)-4-Hexanolide	1		
22.8617	Benzaldehyde, 3-methoxy-	1		lignin
23.5133	3(2H)-Furanone, 4-methoxy-2,5-dimethyl-	5		cellulose
24.2492	Phenol, 3,5-dimethoxy-	3 (72)		lignin
24.8700	1,3-Dioxane	3		unknown

Rt(time)	Chemical name	Intensity	Structure	Source
26.1625	1,2,3-Trimethoxybenzene	1		lignin
26.8733	Phenol, 2,6-dimethoxy-	2		lignin
27.7700	1,2,4-Trimethoxybenzene	3		lignin
27.9658	Propanoic acid, 3-methoxy-, methyl ester	2		sugar
28.2742	Fructofuranose, 2,6-anhydro-1,3,4-tri-O-methyl-,	2		cellulose
32.3358	3,4,6-Tri-O-methyl-d-glucose	1	C <sub>9</sub> H <sub>18</sub> O <sub>6</sub>	cellulose
39.8375	1,2,3,4-Tetramethylmannose	1		cellulose
40.5658	Hexadecanoic acid, methyl ester	3		unknown
44.4183	Methyl stearate	3		unknown
46.8633	1,2,3,4-Tetramethylmannose	3		cellulose
47.7567	α-D-Mannopyranoside, methyl 2,3,4,6-tetra-O-methyl-	2		cellulose
49.8983	α-D-Mannopyranoside, methyl 2,3,4,6-tetra-O-methyl-	2		cellulose
50.7875	1,2,3,4-Tetramethylmannose	2		cellulose
51.5133	α-Methyl 4-O-methyl-D-mannoside	2		cellulose

## Appendix 5. Py-GC/MS

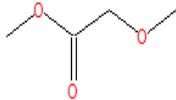
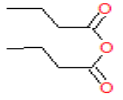
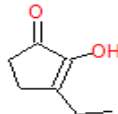
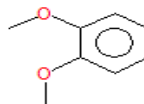
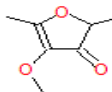
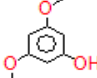
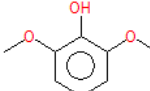
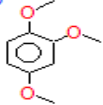
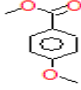
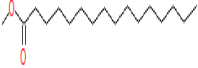
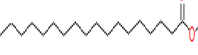
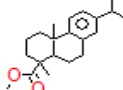
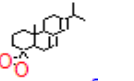

Table 5.1 with the compounds that are present in paper sample NB

Rt(min)	Chemical name	Intensity	Structure	Source
3.9708	1-Propanamine	1		protein
4.0667	2(3H)-Furanone, dihydro-3-methyl-	1(70)		cellulose
16.0850	Butanoic acid, anhydride	1		unknown
17.2642	Cyclopentene, 3,5-dimethoxy-	1(78)		cellulose
17.6058	Cyclopentene, 3,5-dimethoxy-	1		cellulose
18.7383	2-Cyclopenten-1-one, 3-ethyl-2-hydroxy-	1		cellulose
19.1850	Phenol, 2-methoxy-	1		lignin
19.4050	2-Cyclopenten-1-one, 2-hydroxy-3-methyl-	1		cellulose
20.0808	1-methoxycarbonyl-2-methylaminoethene	1	C <sub>5</sub> H <sub>9</sub> NO <sub>2</sub>	
21.0850	Benzene, 1,2-dimethoxy-	1		lignin
21.6792	Benzene, 1,4-dimethoxy-	1		lignin
22.1942	2-Methoxy-5-methylphenol	1		lignin
23.9867	3,4-Dimethoxytoluene	1		lignin

Rt(min)	Chemical name	Intensity	Structure	Source
24.2350	Phenol, 3,5-dimethoxy-	3(75)		lignin
24.8567	1,3-Dioxane	1		unknown
27.7650	1,2,4-Trimethoxybenzene	2		lignin
30.6675	Benzaldehyde, 3,4-dimethoxy-	3		lignin
32.7575	Ethanone, 1-(3,4-dimethoxyphenyl)-	1		lignin
33.3875	Benzoic acid, 3,4-dimethoxy-, methyl ester	3		lignin
34.2325	1,2-Dimethoxy-4-(2-methoxyethenyl)benzene	1		lignin
34.4942	1,2-Dimethoxy-4-(2-methoxyethenyl)benzene	1		lignin
39.8167	2-Propenoic acid, 3-(3,4-dimethoxyphenyl)-, methyl ester	1		lignin
40.5608	Hexadecanoic acid, methyl ester	1		unknown
44.4133	Methyl stearate	1		unknown
48.5975	Methyl dehydroabietate	1		resin

## Appendix 6. Py-GC/MS

Table 6.1 with the compounds that are present in the paper sample OB

Rt (min)	Chemical name	Intensity	Structure	Source
2.5425	Acetic acid, methoxy-, methyl ester	2		sugar
16.1450	Butanoic acid, anhydride	1		unknown
18.7742	2-Cyclopenten-1-one, 3-ethyl-2-hydroxy-	1		cellulose
21.1058	Benzene, 1,2-dimethoxy-	1		lignin
23.5167	3(2H)-Furanone, 4-methoxy-2,5-dimethyl-	3		hemicellulose
24.2475	Phenol, 3,5-dimethoxy-	2 (73)		lignin
25.5808	Phenol, 2,6-dimethoxy-	1 (72)		lignin
27.7767	1,2,4-Trimethoxybenzene	1		lignin
27.9717	Benzoic acid, 4-methoxy-, methyl ester	4		lignin
40.5675	Hexadecanoic acid, methyl ester	2		unknown
44.4192	Methyl stearate	2		unknown
48.6075	Methyl dehydroabietate	1		resin
49.3975	Methyl abietate	1		resin
49.9175	$\alpha$ -D-Glucopyranoside, methyl 2,3,4-tri-O-methyl-	5		Cellulose